Interpreting Macrophage Transcripts In Human T Cell-Mediated Rejection

by

Dina El Sayed Feisal Amin Badr

A thesis submitted in partial fulfillment of the requirements for the degree of

Doctor of Philosophy

in
Experimental Medicine

Department of Medicine
University of Alberta

ABSTRACT

The two types of rejection identified in the Banff histopathologic diagnosis are T cell-mediated rejection (TCMR) and antibody-mediated rejection (ABMR). TCMR is most common early post-transplant while ABMR is the main cause of late graft loss. Kidney transplant TCMR is diagnosed histologically by interstitial inflammation and tubulitis, dominated by T cells and cells of the monocyte-macrophage-dendritic cell (MMDC) lineage. TCMR is mediated by cognate T cell recognition of donor antigen in the allograft. We hypothesized that the transcripts preferentially increased in kidney allografts with TCMR compared to ABMR will reflect MMDC interaction with activated effector T cells. We used gene expression analysis to define the top transcripts preferentially increased in TCMR versus ABMR in 703 clinically-indicated human kidney transplant biopsies. Transcripts for the metalloprotease ADAMDEC1 and chemokines CXCL13 and CCL18 were the top three preferentially increased in TCMR versus ABMR, their expression was also higher when compared to non specific acute kidney injury and non TCMR biopsies, and correlated with the histologic lesions diagnostic for TCMR and with the inflammatory burden in biopsies.. Further analyses identified the chemokine CCL19 as the most strongly increased in TCMR after CXCL13 and CCL18. CCL19 transcript showed similar associations as CXCL13 and CCL18 but to a lesser degree. *In vitro* studies identified heterogeneous effects on ADAMDEC1, CXCL13, and CCL18 expression in response to macrophage differentiation, and activation following interaction with activated effector T cells but not IFNG alone. Our study suggests that ADAMDEC1, CXCL13, CCL18 are macrophage transcripts capable of differentiating TCMR from ABMR and reflect monocyte to macrophage differentiation, and macrophage interaction with effector T cells.

DEDICATION

To my parents Laila Zada and Feisal Badr,

my daughter and my son, Sara and Mostafa Rizk

ACKNOWLEDGEMENTS

I would like to express my deepest respect, appreciation and gratitude to my supervisor Dr. Philip Halloran for giving me the opportunity to participate in this project and to work with his distinguished research team at Alberta Transplant Applied Genomics Centre (ATAGC).

I would like to thank Dr. Banu Sis and Dr. Harissios Vliagoftis, members of my graduate committee, who have given time and support for the success of this project and helped my overall scientific progress.

The members of ATAGC and Halloran Lab Team, current and previous members: Konrad Famulski, Luis Hidalgo, Anna Hutton, Jeff Reeve, Robert Polakowski, Jeff Venner, Jessica Chang, Pam Publicover, Vido Ramassar, Kara Allanach, Michelle Ryan, Danielle Stewart, Gunilla Einecke, Michael Mengel, Joana Sellares, Gui Rennesto, Sujatha Kamma, Zija Jacaj, Lisa Billesberger, Sakarn Bunnag, Declan De Freitas, Nathalie and Danielle Kaiser, Chatchai Kreepala. They have provided technical and scientific help and have enriched my graduate experience at Halloran Lab.

The Department of Medicine particularly graduate program coordinators and advisors, current and previous members, Dr. Sean McMurtry, Dr. Karen Madsen, and Dr. Ross Tsuyuki, Sharon Campbell, Barb Thomson, Eleni Dimos, Aileen Leskow, Maggie Hill for their continuous help, support, and encouragement throughout my graduate program.

The Egyptian Ministry of Higher Education for sponsoring my scholarship and giving me such great opportunity to pursue my graduate studies in Canada.

The Egyptian Bureau of Cultural and Educational Affairs in Canada for their continuous help and support throughout my graduate studies in Canada.

The president of University of Mansoura, Egypt, the Dean of Mansoura Faculty of Medicine, the Chairman of the Department of Microbiology and Medical Immunology,

University of Mansoura, Egypt, for their patience, understanding, cooperation and the opportunity for extending my stay in Canada to complete my PhD degree.

TABLE OF CONTENTS

LIST OF TABLES

LIST OF FIGURES

ABBREVIATIONS

ABMR	Antibody mediated rejection
ADAM	A disintegrin and metalloprotease
ADAMDEC1	ADAM-like decysin 1
ADAMTS	ADAM with thrombospondin domain
ADCC	Antibody-dependent cell mediated cytotoxicity
AKI	Acute kidney injury
AMACtb	Alternative macrophage transcript burden
APC	Antigen presenting cell
ATAGC	Alberta Transplant Applied Genomics Centre
AUC	Area under the curve
BCA-1	B cell- attracting chemokine 1
BK	BK polyoma virus nephropathy
CD40L	CD40 ligand
cDNA	complementary deoxyribonucleic acid
cRNA	complementary ribonucleic acid
CTL	Cytotoxic T lymphocyte
CMACtb	Classical macrophage transcript burden
DC-CK1	Dendritic cell chemokine 1
DC-SIGN	Dendritic cell-specific ICAM-3 grabbing non integrin
DSA	Donor-specific HLA antibodies
DTH	Delayed type hypersensitivity
ELISA	Enzyme-linked immunosorbent assay
ECM	Extracellular matrix
EGF	Epidermal growth factor
FBS	Fetal bovine serum
FDR	False discovery rate
GM-CSF	Granulocyte macrophage colony stimulating factor
GN	Glomerulonephritis
HLA	Human leukocyte antigen

HUVEC	Human umbilical vein endothelial cells
IFNG	Interferon gamma
IFTA	Interstitial fibrosis and tubular atrophy
IL-2	Interleukin 2
IL-4	Interleukin 4
IQR	Interquartile range
LPS	Lipopolysaccharide
MHC	Major histocompatibility complex
M-CSF	Macrophage colony stimulating factor
MIP-3β	Macrophage inflammatory protein-3β
MIP-4	Macrophage inflammatory protein 4
MMDC	Cells of the monocyte macrophage dendritic cell lineage
MMP	Matrix metalloproteinase
MT-MMP	Membrane-tethered matrix metalloproteinase
NOMOA	No major molecular abnormalities
PARC	Pulmonary and activation-regulated chemokine
PBMC	Peripheral blood mononuclear cells
PBS	Phosphate buffered saline
PBT	Pathogenesis-based transcript set
PMA	Phorbol-12-myristate-13-acetate
PPARγ	Peroxisome proliferator-activated receptor-gamma
rIFNg	Recombinant Interferon gamma
RPTECs	Renal proximal tubular epithelial cells
RT-PCR	Reverse transcriptase polymerase chain reaction
SLO	Secondary lymphoid organs
TACE	TNF-alpha converting enzyme
TCMR	T cell mediated rejection
TCR	T cell receptor
TCtb	T cell transcript burden
TG	Transplant glomerulopathy
TIMP	Tissue inhibitor of metalloproteinase

TNF	Tumor necrosis factor
TLR	Toll-Like Receptor
WT	Wild type

All gene name abbreviations use Entrez Gene nomenclature: www.ncbi.nlm.nih.gov/entrez

CHAPTER 1

INTRODUCTION

INTRODUCTION

1.1. KIDNEY TRANSPLANT REJECTION

Kidney transplantation is the ultimate treatment for patients with end stage renal disease. Major technical advances, novel immunosuppressive drugs and improvements in management of transplant patients have improved the outcome of transplant rejection. However, the recipient's immune response to transplanted organ (i.e. allograft rejection) remains one of the major limitations to successful transplantation. The immune system has the ability to discriminate between self tissues and tissues of other members of the same species, and this ability is referred to as "allorecognition"(1). The immune response to alloantigens is initiated by innate immune receptors leading to activation of the antigen presenting cells (APCs) of donor and recipient origin. These activated APCs in turn leave the allograft and migrate to secondary lymphoid organs (SLO), the site where the alloimmune response is initiated (2;3). At least two distinct types of alloantigen recognition pathways have been described; direct alloreconition and indirect allorecognition. In direct allorecognition, the recipient T cells are activated by recognition of "intact" donor major histocompatibility complex (MHC) molecules on passenger "donor APCs" from the graft. In the indirect allorecognition, the recipient T cells are activated by recognition of processed donor "allogenic peptides" displayed by self MHC on "recipient APCs" (4).

1.2. GENERATION OF ALLOIMMUNE RESPONSE DURING REJECTION

Innate immune allorecognition of donor antigens by APCs (donor or recipient) trigger the alloimmune response. These activated APCs travel from the allograft to SLO. Alloimmune responses are triggered following activation of APCs in the graft tissues. Once activated, antigen-bearing dendritic cells leave the graft and migrate to the SLO where they encounter rare antigen-specific naive T cells and central memory T cells, leading to generation of effector T cells. Although naive T cells are optimally triggered by dendritic cells in SLO

(2;5), previously stimulated memory cells may be activated by other cell types, such as graft endothelium (6). These antigen experienced memory cells may have been activated previously by alloantigenic stimuli or more commonly by viral antigens that cross react with alloantigens. This type of immune response is referred to as "heterologous immunity" (7). These central memory T cells recirculate between lymphoid tissues but cannot enter peripheral tissues (8).

In SLO, antigen-bearing activated dendritic cells engage alloreactive naive T cells to deliver three types of signals required for priming of naive T cells with subsequent proliferation and differentiation into effector cells. Signal 1 is delivered by engagement of T cell receptor (TCR) complex with donor antigen on dendritic cells. Signal 2 is delivered by T cell costimulatory receptor CD28 binding to its B7 costimulatory molecules (B7.1/CD80 and B7.2/CD86) on dendritic cells. The costimulatory signal is required for survival and expansion of the T cells and induces the expression of many molecules including interleukin-2 and CD25 (9;10). Blocking the CD28-B7 T cell costimulation prolonged graft survival and induced long term graft acceptance of skin and cardiac allografts in murine transplant models (11). Signal 3 is mediated through different cytokines that directs T cell differentiation and clonal expansion into the different subsets of effector T cells (8;12). Primed antigen-specific T helper cells in SLO activate naive B cells and induce its proliferation and differentiation into alloantibody secreting plasma cells.

1.3. EFFECTOR MECHANISMS IN ALLOGRAFT REJECTION

The alloimmune response triggers the generation of many effector mechanisms that can mediate graft injury resulting in functional deterioration and graft rejection. Two types of allograft rejection have been described in Banff histologic classification (13): T cell-mediated rejection (TCMR) and antibody-mediated rejection (ABMR). TCMR is the most common cause of early rejection while ABMR is the main cause of late graft loss (14-16).

a) Antibody-mediated rejection

In ABMR, alloantibody response is the major effector mechanism operating and mediating graft injury and rejection. Naive B cells in SLO are activated by alloantigen-specific primed T helper cells, via the costimulatory CD40-CD40 Ligand (CD40L) pathway (17). Activation promotes clonal expansion and maturation of B cells into antibody-secreting plasma cells, leading to production of donor-specific HLA antibodies (DSA). Posttransplant DSA were identified as a risk factor for late graft loss (18). The DSA bind to microvascular endothelium in the graft and mediate microcirculation damage (19). Cells that express Fc receptors such as NK cells (Natural Killer) can be directly activated by DSA and can mediate endothelial injury via antibody-dependent cell mediated cytotoxicity (ADCC). The release of many inflammatory mediators may also contribute to endothelial damage (20;21). The DSA also trigger complement fixation and activation resulting in recruitment and activation of inflammatory cells and graft injury. C4d is one of the split products of complement, it binds to capillary endothelium and C4d deposition can be detected in peritubular capillaries in biopsies and is considered evidence of ABMR (22-25).

b) T cell-mediated rejection

Effector T cells that are generated in SLO, following encounter with mature donor antigen-bearing dendritic cells, migrate to the graft and perpetuate inflammation through the release of proinflammatory cytokines and chemokines. Leukocyte recruitment from circulation and subsequent transendothelial migration into the graft is mediated by adhesion molecules and chemokines expressed on the graft endothelium, epithelium and interstitium as well as on the infiltrating leukocytes. The proinflammatory cytokines in the inflamed graft stimulate the expression of adhesion molecules and chemokines (26). The inflammatory response in the graft during TCMR is characterized by interstitial mononuclear cell infiltration and tubulitis (invasion of the epithelium by mononuclear cells) (13). The interstitial mononuclear infiltrate in renal allografts with TCMR is dominantly T cells and MMDCs, forming up to 42% and 60% of interstitial cells, respectively. Other cells such as B cells may occur (27). The T cells infiltrating the graft are CD4 and CD8 T cells, but CD8 T cells are more common than CD4, and many of them are effector cytotoxic T lymphocytes

(CTL). In TCMR, the presence of tubulitis serves as an indicator that tissue injury is occurring and thus tubulitis constitutes the principle lesion for histologic diagnosis of TCMR. Tubulitis is dependent on host T cells: it is absent in allografts transplanted into T cell deficient mice, but can develop in mouse host lacking B cells and alloantibody (28). Consequently, T cells have been presumed to be the dominant mediator of tissue injury in allografts undergoing TCMR. However, little is known about the mechanisms by which T cells mediate epithelial deterioration in TCMR. Cytotoxic mechanisms are not required for TCMR: epithelial deterioration and histologic lesion indicative of TCMR (tubulitis) developed in mouse hosts lacking perforin and granzymes (A and B) (29;30) and in donor tissue lacking Fas (31). Interactions between alloantigen-specific effector T cells and APCs of the MMDC series infiltrating the interstitium could mediate effector functions analogous to delayed type hypersensitivity (DTH) (32). T cell activation following interaction with APC triggers an influx of MMDCs and lymphocytes to the graft, leading to production of proinflammatory cytokines including interferon gamma (IFNG) and tumor necrosis factor (TNF). These cytokines can activate MMDCs including macrophages, a prominent component of inflammatory infiltrate in TCMR, which may play a role as effector mediators of tissue damage (33-35). Soluble mediators of the DTH response act in an antigen-independent fashion to promote chemotaxis and further activation of immune cells (36;37).

Macrophages may contribute to allograft rejection via different mechanisms including antigen presentation and priming of immune response, inflammation, phagocytosis, cytotoxicity, tissue injury, and tissue remodeling and scarring (34;38). Macrophage accumulation within allograft is likely the result of monocyte recruitment and *in situ* proliferation (39). *In vitro*, monocytes can be differentiated into macrophages or dendritic cells depending on the cytokine environment. *In vivo*, however, this process is more complex and not well characterized, and MMDC and their myeloid precursors are integrated into a more puzzling system; the mononuclear phagocyte system (40;41). MMDC show marked phenotypic heterogeneity as a result of cellular differentiation, different tissue distribution and response to microenvironmental factors including tissue injury and inflammatory signals that are abundant within a rejecting allograft. The

phenotypic changes in MMDC are also associated with significant functional and molecular changes (42-44).

1.4. MACROPHAGES AS PART OF THE MONONUCLEAR PHAGOCYTE SYSTEM

Macrophages are part of the cell population forming the mononuclear phagocyte system, which includes bone marrow progenitors, blood monocytes and tissue macrophages. Macrophages occur in most tissues in the body in large numbers, and their numbers markedly increase during inflammation. Myeloid bone marrow progenitors differentiate into monocytes which leave the bone marrow to circulate in blood, and when enter tissues they differentiate to form tissue macrophages. Circulating blood monocytes can also differentiate to form dendritic cells (45). Under normal conditions, macrophages as phagocytes are involved in various homeostatic clearance processes including clearance of erythrocytes as well as apoptotic cells and cellular debris generated during tissue remodeling. This clearance process is mediated via various receptors e.g. scavenger receptors, is independent of other immune cells, and produce little or no immune mediators by the macrophages. Macrophages are also involved in clearance of necrotic cell debris that results from exposure of tissues to trauma or stress. The necrotic cells generate danger signals that are detected by macrophages via receptors such as Toll-like receptors (TLRs) (46), that results in major changes in stimulated macrophages including changes in expression of surface proteins and production of cytokines and inflammatory mediators (47;48).

Macrophages and dendritic cells, part of the mononuclear phagocyte system, are important APCs characterized by a high degree of heterogeneity and plasticity. They play major roles in many renal diseases, including allograft rejection (34;38;49), such that they are considered promising therapeutic targets (49;50)

1.5. MACROPHAGE CLASSIFICATION AND HETEROGENEITY

Macrophages can be classified by different schemes according to their activation or their function. Macrophage activation can be classified into classically activated (M1) macrophages and alternatively activated (M2) macrophages. Classical activation of macrophages is primarily induced by interferon-gamma (IFNG), which triggers a severe proinflammatory response against intracellular pathogens. Classical activation of macrophages can be induced by IFNG alone or together with other inflammatory cytokines (e.g. TNF) or microbial stimuli (e.g. LPS) (51;52). Alternative macrophage activation is induced by interleukin-4 (IL-4) and IL-13 among other signals, which trigger a different immune response to eliminate extracellular pathogens such as helminthes and promote tissue repair. The alternatively activated M2 macrophages include different macrophage populations/phenotypes that can be further subdivided into M2a, M2b, and M2c macrophages. M2a macrophages are induced by IL-4 or IL-13, M2b macrophages are generated upon exposure to immune complexes together with IL-1β or LPS, while M2c macrophages are induced by IL-10, TGF-β or glucocorticoids (53).

Different types of macrophage activation are associated with changes in macrophage function and distinctive gene signatures. Macrophages change their phenotype by encountering inflamed tissue e.g. a rejecting allograft (49). Therefore recent reviews propose that the activation phenotypes of macrophages present a broad spectrum, not really fitting the previous rigid dichotomous classification of M1 and M2 phenotypes. In other words, it is better to define the M1 and M2 as a continuum of a differential pathway and not as two separate entities (47).

According to their function, macrophages are divided into three major types: host defense macrophages, wound healing macrophages or immune regulatory macrophages (54). As macrophages play an important role during an inflammatory response and can drive tissue destruction as well as tissue repair and remodeling, macrophages can undergo bidirectional transformation between different activation phenotypes (43;48;55).

1.6. DENDRITIC CELLS

Dendritic cells are professional antigen presenting cells that are critical for initiation of primary immune response through their ability to stimulate naive T cells in SLO. Two types of dendritic cells have been described; plasmacytoid dendritic cells and conventional (myeloid) dendritic cells. Conventional dendritic cells are an important component of the mononuclear phagocyte system, together with macrophages, monocytes and bone marrow progenitors (56). Under normal conditions, conventional dendritic cells are present in peripheral tissues of most organs. They are continuously circulating between peripheral tissues and secondary lymphoid organs and acting as immunological sensors that detect various pathogens and danger signals. Once encountering antigen in peripheral tissues, immature dendritic cells are stimulated to mature and migrate to SLO to initiate adaptive immune response. Dendritic cell maturation results in upregulation of expression of MHC class II and induction of expression of costimulatory molecules (57). Once in SLO, naive T cells scan antigens on the surface of dendritic cells until rare antigen specific T cells recognize their specific antigen on surface of dendritic cells. Then dendritic cells induce priming of naive antigen specific T cells by providing signals through TCR complex engagement and costimulatory signals, followed by proliferation and differentiation of antigen-specific effector T cells (10).

Our knowledge about dendritic cells and their role in peripheral tissues, including kidney, is limited. This knowledge was even further challenged by the many reports demonstrating a considerable degree of overlap of surface markers between dendritic cells and macrophages in tissues.

1.7. OVERLAP BETWEEN MACROPHAGES AND DENDRITIC CELLS

The mononuclear phagocyte system and its cell populations, mainly macrophages and myeloid dendritic cells, have long been an active area of research. Distinguishing between macrophages and dendritic cells mainly relied on differences in expression of markers and in function between the two cell populations. Macrophages and dendritic cells are well characterized in the lymphoid tissues. However in non lymphoid tissues, these cells are still

poorly characterized. The initial studies of macrophages and dendritic cells in non-lymphoid tissues were based on the assumption that the markers typically used to characterize these cells in lymphoid tissues can also be used in non-lymphoid tissues (41). That assumption was later proved to be inaccurate, and recent studies showed that what applies to macrophages and dendritic cells in lymphoid tissues cannot be extended to non lymphoid tissues. This recent finding led to confusion in the field of study and raised the need for re-assessment and interpretation of the data from previous studies in the light of this recent finding (51;58).

A major challenge that faces researchers while studying the major members of the mononuclear phagocyte system, macrophages and dendritic cells, is related to nomenclature and differentiating between these cells, particularly *in vivo*. This challenge was raised following the growing body of evidence that demonstrates the overlap between many macrophage and dendritic cell markers that were typically used to distinguish between these cells, and were previously thought to be specific for each cell type (41). For example, studies of the renal mononuclear phagocytic cells showed that the typical human macrophage marker CD68 (macrosialin) was expressed on both macrophages and dendritic cells in the renal tubulointerstitial tissues (59). Similar data was reported in murine studies, the murine macrophage marker F4/80 was expressed on macrophages and dendritic cells in the mouse kidney. Thus the cell markers CD68 (human) and F4/80 (mouse) cannot differentiate between macrophages and dendritic cells (60). Moreover, expression of CD68 has been reported in non myeloid cells in tumors such as carcinomas and melanomas and in tumor cell lines. Also, expression of CD68 mRNA and protein has been reported in fibroblasts and endothelial cells (61).

The marked heterogeneity and plasticity among these cell populations, in addition to the finding that macrophages and dendritic cells occupy overlapping anatomical sites in the peripheral tissues have also contributed to the challenge (40). Even the functional distinction between dendritic cells and macrophages based on the ability of dendritic cells to stimulate naive T cells has recently been challenged. Published data demonstrated the ability of CD11c negative macrophages to prime naive T cells *in vivo*, a function that was

previously thought to be only restricted to dendritic cells, suggesting a potential overlap of function between macrophages and dendritic cells (62). Thus with the reported overlap in surface markers, function and anatomical sites between macrophages and dendritic cells in peripheral tissues together with their marked heterogeneity and plasticity, distinguishing between these cells, especially *in vivo*, and consequently their nomenclature system has been further complicated (56;62).

1.8. CHEMOKINES

Local expression of chemokines at sites of inflammation contributes to the recruitment of inflammatory cells. Accumulation of inflammatory cells in the interstitial tissue of kidney allograft resulting in tubulitis is a characteristic feature of TCMR. The inflammatory cells are continuously recruited from circulation and migrate across the vascular endothelium into the allograft (13). Locally produced chemokines and adhesion molecules are key players in directing the transendothelial migration of monocytes and other immune effector cells from the circulation into the allograft. Within the graft, chemokines bind to their respective chemokine receptors expressed on the inflammatory cells and guide them along a chemokine gradient within the interstitial tissue. In addition, chemokines play a role in activation of different types of cells including immune effector cells and renal parenchymal cells (63).

Chemokines are members of a family of small chemoattractant proteins that play a central role in orchestrating leukocyte migration and homing. They are related in their amino acid sequence but can be structurally divided into four subfamilies: CC-, CXC-, C-, and CX3C- based on the number and spacing of the conserved cysteine residues. Chemokines can also be functionally divided into homeostatic chemokines and inflammatory chemokines (64). The chemokine receptors are G-protein-coupled receptors and upon binding to their respective chemokines, they stimulate changes in cell adhesiveness and cytoskeleton that result in directed migration of the stimulated cells. Chemokines are produced by many types of cells in response to different stimuli including infection and tissue injury (9).

During the initial steps of cell recruitment, chemokines trigger conformational changes in adhesion molecules (integrins) on the recruited cells to facilitate their strong binding to their corresponding ligands on the vascular endothelium at the sites of inflammation (26). Then after transendothelial migration of cells, the chemokines guide the directional migration of the recruited cells along a concentration gradient towards the site of inflammation. During cell recruitment, chemokines act in concert with other cytokines (e.g. proinflammatory cytokines such as TNF) that induce activation of endothelial cells of the local blood vessels and expression of adhesion molecules that, together with chemokines, help orchestrate cell recruitment to sites of inflammation (65;66).

1.9. MATRIX METALLOPROTEINASES

Matrix metalloproteinases (MMPs) are a family of zinc-containing proteins that have proteolytic activity on different components of the extracellular matrix. They are secreted in an inactive form then undergo extracellular activation. Some MMPs are not secreted but remain anchored to cell membrane, thus referred to as membrane-tethered MMPs (MT-MMs) (67). Although MMPs were first known for their role in degradation of extracellular matrix (ECM) proteins to maintain ECM homeostasis, it is now known that they can also act on a broad spectrum of substrates including cell surface receptors, adhesion molecules, cytokines and growth factors. Thus MMPs play a critical role in tissue repair and remodeling as well as regulation of many aspects of cell behaviors such as cell proliferation, differentiation, migration and angiogenesis (68;69).

In general, MMPs are composed of multiple domains: a prodomain, a catalytic domain, a hinge region, and a hemopexin-like domain. In addition, secreted MMPs are synthesized with a signal peptide required for secretion out of the cell, while MT-MMPs have a transmembrane domain and cytoplasmic domain that keep them tethered to the cell. MMPs are classified into groups and subgroups according to their domain structure, i.e. the presence or absence of the structural domains, along with their substrate specificity. These include the secreted MMPs collagenases, gelatinases, stromelysins and matrilysins and the membrane-tethered MT-MMPs. The proteolytic activity of MMPs is inhibited by a family

of naturally occurring inhibitors known as tissue inhibitors of metalloproteinases (TIMPs) (67;69).

MMPs play an important role in regulation of the inflammatory response via their roles in inflammatory cell recruitment and chemotaxis. MMPs can promote inflammation by facilitating the release of cytokines from different inflammatory cells, e.g. MMP-7 facilitate the release of TNF from macrophage by its action on membrane bound TNF. Also, MMPs can promote local propagation and augmentation of inflammatory response via cleavage of ECM components, thus help creating a chemotaxis gradient and stimulating leukocyte migration (67;68).

In contrast, some MMPs may have an anti-inflammatory effect mediated by their proteolytic action on adhesion molecules promoting leukocyte transendothelial migration into the graft e.g. ICAM-1 cleavage by MMP-13. MMPs are now suggested to play a role in many forms of renal pathology such as diabetic nephropathy and acute kidney injury, although their exact mechanistic roles are not completely understood (67-69).

1.10. THE ADAM FAMILY OF METALLOPROTEASES

The ADAM (A disintegrin and metalloprotease) family is a family of zinc-binding transmembrane proteins with adhesion and/or protease/endopeptidase activity. The function of most of the members of the ADAM family is still unknown, however the ADAM members with known functions are involved in a many biological processes including immune/inflammatory response, fertilization, neurogenesis, and muscle development (69). The ADAM metalloproteases are composed of multiple domains: a pro-domain, a metalloprotease domain, a disintegrin domain, a cysteine-rich domain, epidermal growth factor (EGF) - like domain, a transmembrane domain and a cytoplasmic tail domain. Some members of ADAM family can be produced in a secreted form when they lack the transmembrane domain. The functions of these structural domains are: blocking protease activity (pro-domain), protease activity (metalloprotease domain), adhesion activity (disintegrin domain), stimulation of membrane fusion (EGF-like domain), phosporylation and regulation of other ADAM activities (cytoplasmic tail) (70).

Similar to MMPs, ADAM members play a role in the inflammatory response via their protease activity. They act on the extracellular domain of a large number of membrane-bound growth factors, cytokines, receptors, adhesion molecules and enzymes, to help their cleavage and release from the cell membrane (68). The best studied example of this function is the release of the cytokine TNF that plays an important role during the inflammatory response. TNF is initially synthesized as a membrane bound protein (inactive form of TNF) from which the active soluble extracellular domain is released by the proteolytic activity of TNF-alpha converting enzyme (TACE/ADAM17) (69).

1.11. REJECTION PATHOLOGY AND MOLECULAR CLASSIFICATION

a) Pathological classification of rejection: The Banff classification

Histologic assessment of renal allograft biopsies is currently the global standard for diagnosis of TCMR and ABMR. The Banff classification of renal allograft pathology is the international reference standard for histologic assessment and interpretation of renal allograft biopsies (13). The classification outlines a semi-quantitative scoring system for key histopathologic lesions in different kidney compartments. The lesions scored are interstitial (i-score and ci-score), tubular (t-score and ct-score), glomerular (g-score, cg-score and mm-score), and vascular (v-score, cv-score, ah-score, ptc-score, C4d). Two types of rejection are defined in the Banff classification, TCMR and ABMR (13;23;25;71) each displaying characteristic histologic lesions that are used for diagnosis. Both TCMR and ABMR cases are either acute or chronic (13;23;72).

The pathology of ABMR is predominantly microvascular. Acute ABMR is diagnosed by the presence of histologic evidence of acute tissue injury, current or recent antibody interaction with vascular endothelium in biopsies, and the presence of DSA in patient's serum (72;73). The histologic lesions in ABMR may include microvascular inflammation, intimal or transmural arteritis, acute thrombotic microangiopathy, and acute tubular injury that is not associated with other causes. Evidence of antibody interaction with vascular endothelium is defined as any one of the following: evidence of moderate microvascular inflammation or positive immunostaining of peritubular capillaries for complement

component C4d (23;25;71) (these ABMR biopsies are diagnosed as C4d positive ABMR, but C4d negative ABMR is also common) (72-74). The presence of DSA in patient's serum (i.e. DSA positive) is detected by crossmatching assays that test the reactivity of recipient antibodies against donor HLA (human leukocyte antigen) molecules. Chronic ABMR is diagnosed by fulfilling all the aforementioned criteria, in addition to histologic evidence of a more advanced form of injury such as transplant glomerulopathy in absence of thrombotic microangiopathy, severe multilayering of peritubular capillary basement membrane, or arterial intimal fibrosis.

The pathology of TCMR is characterized by interstitial and tubular changes in the form of rapid development of an inflammatory infiltrate, followed by damage to the parenchyma and arteries. The histologic lesions in TCMR described in the Banff classification (13) are interstitial inflammation (i-score) and tubulitis (t-score = invasion of tubular epithelium by lymphocytes) and intimal arteritis (v-score = invasion of inflammatory cells beneath the endothelium). The increase in lesion score reflects more severe rejection. Notably, intimal arteritis may also be characteristic of ABMR and is currently identified as non-diagnostic for TCMR (75;76).

b) <u>Molecular classification of rejection</u>

Despite continuing advances to Banff histologic classification, the assessment and classification of kidney transplant biopsies by conventional histology have several weaknesses including poor reproducibility due to variability in the subjective interpretation of rules by individual pathologists and the use of different classification systems in different centers (77;78). Also, the histologic diagnosis relies on lesions that are not specific. For example, the TCMR lesions tubulitis and arteritis (v lesions) can occur in other disease states: tubulitis occurs in some primary renal diseases and arteritis occurs in ABMR. Histological assessment is further limited by the lack of ability to determine the cause, activity and severity of tissue injury. The late stages of graft injury (interstitial fibrosis and tubular atrophy) are common to many forms of allograft damage (e.g. alloimmune, ischemic and inflammatory stimuli), thereby complicating the diagnosis of the underlying disease. The histology is only relevant when the disease has progressed to the

point of visible tissue injury, and thus cannot accurately reflect the true nature of progression to graft failure. In many transplant patients, rejection can be rapid or drawn out, and the developing histologic lesions of diseases lag their causative molecular mechanisms. For example, some biopsies may be classified as “borderline” (biopsies do not show the t2 threshold tubulitis lesion diagnostic for TCMR) but may in fact be undergoing TCMR at the molecular level (79-81).

The limitations in the conventional histologic classification have been addressed by the recent introduction of molecular classification (79;81). The molecular classification of rejection relies on characterization of gene expression changes in kidney transplant biopsies. Using gene expression microarray analysis, our group has focused on studying kidney transplant biopsies and defining sets of transcripts (82) that are differentially expressed in TCMR (80;81;83;84) or ABMR (85-87). These transcripts were later used to develop the recent molecular classification of rejection. The molecular classification, together with histology, will help improve the biopsy interpretation by adding new estimates of diagnosis, activity, stage, and prognosis (80;81;88;89).

1.12. RATIONALE

The phenotype of cells infiltrating the allograft during TCMR is not officially taken into consideration in the Banff classification during histological assessment of TCMR. However, studying the characteristics of the inflammatory compartment in allograft is critical for understanding the effector mechanisms and graft injury during TCMR. As we previously mentioned, TCMR is diagnosed histologically by interstitial inflammation and tubulitis, and is characterized by mononuclear cell interstitial infiltration dominated by T cells and MMDCs. CD8+ T cells are more common than CD4+ T cells, and most of them display the cytotoxic effector T cells characteristics. MMDCs can be recruited to graft in response to non-alloimmune injury following ischemia reperfusion injury and transplantation procedure as well as in response to alloimmune injury during TCMR. MMDCs are present in all TCMR and are associated with poor graft function. However, the functional significance of MMDCs is unclear and the effector role of these cells and extent of their contribution to the rejection and graft injury is not completely understood.

Our knowledge of the extent and contribution of MMDCs in shaping the phenotype of rejection has been hindered by many factors; the lack of robust MMDCs deficient animal model, the lack of specificity of the methods used to deplete a target population of MMDCs, the marked degree of plasticity and heterogeneity of MMDCs and the distinct characters and developmental origin for MMDC populations in different tissues. For decades, CTL cytotoxicity mechanisms mediated by perforin, granzymes and Fas have been adopted as the effector mechanism in TCMR. However, it has been demonstrated that other effector mechanisms, including DTH-like response and soluble mediators released during interaction of macrophages and effector T cells, may also contribute to alloimmune injury in TCMR.

Microarray analysis of transcriptional changes provides a valuable tool to understand the pathogenesis and improve diagnosis of various human diseases including allograft rejection. Profound changes in transcript expression are observed in rejecting allografts with a promising potential to distinguish rejection from other processes (89-91). Many transcripts have been suggested as potential diagnostic markers or promising therapeutic targets for rejection (92). We have previously demonstrated that transcript expression is altered in rejecting allografts and we defined a number of "pathogenesis-based transcript sets" that reflect transcriptome changes related to certain biological events occurring in kidney allograft biopsies during rejection (82). Our laboratory has previously dedicated a great deal of work in defining gene expression changes unique to ABMR (20;87;93-95). However, the reverse comparison has not yet been addressed. In this study, we focused on studying TCMR compared to ABMR. Defining the gene expression changes that differentiate TCMR from ABMR may have implications for treatment strategies, treatment response and graft outcome. Understanding the molecular correlates of immune events and effector mechanisms in TCMR and their relationship to histopathology is central to developing a mechanistic and biology based approach to transplant rejection that can be translated into novel therapeutic targets as well as to sensitive and specific diagnostic tests.

1.13. HYPOTHESIS

We hypothesized that the transcripts preferentially increased in kidney allografts with TCMR when compared to ABMR will reflect MMDC interaction with activated effector T cells.

1.14. AIMS OF THE STUDY

To define the transcripts preferentially increased in TCMR compared to ABMR, to study their relationship to histologic parameters in human kidney allografts, and attempt to attribute their expression to specific cells

To study expression of the transcripts defined above in primary human cells, in response to stimulation, and during interactions between effector T cells and macrophages.

1.15. RESEARCH QUESTIONS

1. What are the transcripts most increased in TCMR compared to ABMR and what cells are they expressed in?

2. How are transcripts defined above regulated in the cells they are primarily expressed in and what type of activation are they most likely to reflect in TCMR?

CHAPTER 2

MATERIALS AND METHODS

MATERIALS AND METHODS

2.1. HUMAN KIDNEY TRANSPLANTS

a) Human patient population and specimens

The study included 703 kidney transplant biopsy for clinical indication collected from 579 patients at six kidney transplant centres. Normal kidney tissue obtained from obtained from histopathologically unaffected areas of the cortex of native nephrectomies performed for renal carcinoma was used as controls. After obtaining a written informed consent, biopsy cores for conventional assessment were collected under ultrasound guidance by spring-loaded needles. In addition, one 18-gauge biopsy core was obtained for gene expression analysis and was placed immediately in RNALater at 4°C for 4-24 hours, then stored at -20°C. Biopsy collection for the current study was approved by the institutional review boards of participating transplant centres. Some biopsies were collected as part of the INTERCOM study (ClinicalTrials.gov NCT01299168).

b) Assessment of human allograft biopsies

All biopsies were assessed using the Alberta Transplant Applied Genomics Centre (ATAGC) Reference Standard (80) that include C4d-negative ABMR and the changes outlined in the Banff 2013 report (73). Paraffin sections were prepared and graded for Banff lesion scores and frozen sections were used for C4d staining. According to the Banff criteria, histologic diagnoses included biopsies with rejection (T cell mediated, antibody-mediated, mixed), or borderline changes, or non rejection including all other biopsies. Biopsies showing BK virus by *in situ* hybridization and/or electron microscopy were designated BK nephritis regardless of whether they also had evidence of TCMR. Definitions of histologic diagnoses are summarized in Table 2.1

2.2. HUMAN CELL ISOLATION AND CELL CULTURES

a) Human cell panel

Monocytes and macrophages: PBMCs were isolated from whole blood of healthy volunteers with Ficoll® (GE Healthcare Life Sciences, Baie d'Urfe, Quebec, Canada) density gradient centrifugation. Monocytes were purified from PBMCs by EasySep® Human CD14 Positive Selection (StemCell Technologies, Vancouver, BC, Canada). Purity of CD14+ monocytes was more than 97% by flow cytometry. Monocytes resuspended in complete RPMI-10 (RPMI 1640 supplemented with 10% FBS (Invitrogen Life Technologies, Burlington, ON, Canada), 2 mM L-glutamine, β-mercaptoethanol, 1% non-essential amino acids, 1% sodium pyruvate, and 1% antibiotic-antimycotic) were allowed to adhere on 100 mm plates (BD Falcon, Missassauga, Ontario, Canada) and incubated for 24 hours in 5% CO_2 at 37°C for 24 hours to generate macrophages (96).

Effector T cells: CD4+ and CD8+ T cells were generated from PBMCs by allostimulation at a ratio of 3:1 with mitomycin C –treated (Sigma, St. Louis, MO) myelogenous leukemia B cells (RPMI8866, ATCC). The cell cultures were maintained in complete RPMI-10 in 5% CO_2 at 37°C. Recombinant human IL-2 (e-Bioscience, San Diego, CA) was added to cultures. After four rounds (5 days per round) of stimulation, viable cells were collected with Ficoll® by density gradient centrifugation. CD4+ and CD8+ T cells were purified by immunomagnetic beads using EasySep® negative selection kits (StemCell Technologies, Vancouver, BC, Canada) according to manufacturer instructions. Cell purity was assessed by flow cytometry and varied between 92% to 98% . The leukocyte cell cultures were maintained in complete RPMI-10 in 5% CO_2 at 37°C. The effector phenotype was confirmed by intracellular staining for IFNG.

B cells: Following PBMCs isolation from whole blood of healthy volunteers with Ficoll® density gradient centrifugation, enrichment for CD19+ B cells was performed by EasySep® Human B Cell Enrichment Kit (StemCell Technologies, Vancouver, BC, Canada). Purity of CD19+ cells was more than 97% by flow cytometry. Cells were cultured in complete RPMI-10 in 5% CO2 at 37ºC.

NK cells: Following isolation of PBMCs from whole blood of healthy volunteers with Ficoll® density gradient centrifugation, NK cells were purified using EasySep® Human NK Cell Enrichment Kit (StemCell Technologies, Vancouver, BC, Canada). Purity of CD56+ cells ranged between 90 and 98% by flow cytometry. Cell cultures were maintained in complete RPMI-10 in 5% CO2 at 37°C.

Endothelial and epithelial cells: Human umbilical vein endothelial cells (HUVEC; ATCC, Manassas, VA) and renal proximal tubular epithelial cells (RPTEC; Lonza Inc., Allendale, NJ) were maintained in tissue culture media as recommended by the supplier.

Interferon gamma treatment: Cultures of macrophages, RPTEC and HUVEC were incubated in culture media only or with 500 U/ml recombinant human IFNG (rIFNG; eBioscience). After 24 hours, cells were harvested for TRIzol total RNA extraction and microarrays. The cell isolation and cultures for human cell panel were performed by Dr. Luis Hidalgo, Halloran Laboratory (84;96).

b) <u>THP-1 cell culture and stimulation</u>

THP-1 cell culture: THP-1 cells were acquired from ATCC and were plated into 6-well plates (Becton Dickinson, NJ, USA) at a cell density of 1x106/ml in complete RPMI-10. Plates were incubated at 37ºC in an atmosphere of 5% CO2. After 24 hours incubation, cells were harvested for TRIzol total RNA extraction and RT-PCR.

THP-1 cell stimulation: THP-1 cells were plated into 6-well plates at $1x10^6$/ml in complete RPMI-10 medium only (unstimulated controls) or they were stimulated with anti-CD40 antibodies, TNF or LPS (Figure 2.1). For TNF stimulation, 100 U/ml or 500 U/ml recombinant human TNF (eBioscience) was added to THP-1 cultures for 24 hours. For LPS stimulation, 100 ng/ml LPS (Clone; E.coli O111: B4, Sigma) was added to THP-1 cultures for 6 hours prior to harvesting. For anti- CD40 stimulation, THP-1 cells were stimulated for 24 hours by 5µg/ml anti human-CD40 antibodies (Clone; 5C3, eBioscience) immobilized to 6-well plate. The 6 well plate was coated with anti-human CD40 antibodies one day before performing the THP-1 culture by adding 1.5 ml/ well of 5µg/ml anti-CD40

antibodies to 2 wells. The covered plate was sealed and incubated overnight at 4 ºC. Next day, anti-CD40 antibody suspension was aspirated from wells, and 4 ml/well complete RPMI-10 was added to anti-CD40 coated wells and the plate was incubated at 37 ºC for 2 hours to block non specific binding of antibodies. After 2 hours, complete RPMI-10 medium was aspirated and THP-1 cells in fresh complete RPMI-10 were plated into the anti-CD40 coated wells. After 24 hours incubation, cells were harvested for TRIzol total RNA extraction and RT-PCR.

c) Monocyte-derived macrophage culture

Monocyte isolation: PBMCs were isolated from whole blood of healthy volunteers with Ficoll® by density gradient centrifugation. Monocytes were purified from PBMCs by negative selection using the EasySep® Human Monocyte Enrichment Kit (StemCell Technologies, Vancouver, BC, Canada). The kit utilizes enrichment cocktail containing antibodies against cell surface antigens on undesired cell populations including: CD2, CD3, CD19, CD20, CD56, CD66b, CD 123, and glycophorin A. An additional two rounds of magnetic separation were performed at the end of the monocyte enrichment protocol to increase the purity of isolated monocytes. CD14+ monocyte purity was assessed by flow cytometry and was more than 92%. We used two methods for *in vitro* differentiation of macrophages as described below.

Monocyte-derived macrophage differentiation: Monocytes were incubated in 6-well plates (BD Biosciences, Mississauga, ON, Canada) at 1 x 10^6 cells/ml in complete RPMI-10 and allowed to adhere for 24 hours in 5% CO2 at 37°C. After incubation, cells were harvested for TRIzol total RNA extraction and RT-PCR.

Monocyte-derived M-CSF macrophage differentiation: Monocytes were plated into 6 well plates at 2 x 10^5 cells/ml in complete RPMI-10 with 50 ng/ml recombinant human macrophage-colony stimulating factor (M-CSF; R&D Systems, Minneapolis, MN) to induce monocyte differentiation into M-CSF-macrophages. Cell cultures were replenished with fresh medium and 50 ng/ml-M-CSF on day 3 and day 5 and incubated in 5% CO_2 at

37°C. After for 6 days incubation, cells were harvested for TRIzol total RNA extraction and RT-PCR.

Macrophage stimulation: Freshly isolated monocytes were incubated in 6-well plates in complete RPMI-10 medium alone for 24 hours (unstimulated controls) or with recombinant human CD40L (R&D Systems, Minneapolis, MN, USA) or TNF or LPS added to cultures. TNF 500 U/ml (eBioscience) or LPS 100 ng/ml Lipopolysaccharide (LPS; Escherichia coli 0111:B4, Sigma) were added to cell culture for 24 hours and 6 hours, respectively prior to harvesting (Figure 2.2). CD40L stimulation for 24 hours prior to harvesting was performed as follows: 100 ng/ml CD40L was added to cultures and incubated at 37ºC. Cells were washed in 10x volume complete RPMI-10, and cells were plated in 6-well plate in complete RPMI-10 at $1x10^6$ /ml. Cross linking monoclonal-polyhistidine antibody 10 μg/ml was added to cell cultures and the plate was incubated in 5% CO_2 at 37ºC for 24 hours.

M-CSF macrophage stimulation: M-CSF macrophages were stimulated by incubating monocytes for 6 days with 50 ng/ml M-CSF in complete RPMI-10 medium alone (unstimulated controls) or with CD40L (100 ng/ml) or TNF (500 U/ml) for 24 hours or LPS (100 ng/ml) for 6 hours, prior to harvesting. After incubation, cells were harvested for TRIzol total RNA extraction and RT-PCR, and supernatants were collected for cytokine assay (Figure 2.3). CD40L stimulation for 24 hours prior to harvesting was performed as previously described in macrophage stimulation using crosslinking monoclonal-polyhistidine antibody 10 μg/ml.

M-CSF- macrophage time course: Monocytes isolated by negative selection from PBMCs from healthy volunteers were differentiated into macrophages by culture in complete RPMI-10 in presence of 50 ng/ml M-CSF as previously described for 1, 3, 5 and 7 days. Cultures were replenished with fresh medium and M-CSF (50 ng/ml) on day 3 and day 5. After incubation, cells were harvested at each time point for total RNA extraction and RT-PCR.

d) Monocyte-derived dendritic cell culture

Monocyte-derived dendritic cell differentiation: Dendritic cells were generated from monocytes purified from PBMCs from whole blood of healthy volunteers by negative selection using the EasySep® Human Monocyte Enrichment Kit and CD14+ monocyte purity was assessed by flow cytometry as previously described in macrophage cultures. Monocytes were plated into 6-well plates at 2 x 10^5 cells/ml in complete RPMI-10. Recombinant human IL-4 (500 U/ml, eBioscience) and recombinant human granulocyte-macrophage colony stimulating factor (GM-CSF; 500 U/ml, eBioscience) were added to cultures to induce monocyte differentiation into dendritic cells . Plates were incubated in 5% CO2 at 37°C for 7 days. Dendritic cell cultures were replenished with fresh medium and 500 U/ml GM-CSF and 500 U/ml IL-4 on day 3 and day 5 . $CD14^-$ $CD11c^+$ dendritic cell phenotype as confirmed by flow cytometry.

Monocyte-derived dendritic cell stimulation: Dendritic cells were stimulated with 100 ng/ml CD40L or 500 U/ml TNF for 48 hours prior to harvesting or 100 ng/ml LPS for 24 hours prior to harvesting. TNF or LPS were directly added to dendritic cell cultures, while CD40L stimulation was performed as previously described. Dendritic cell cultures in complete RPMI-10 and GM-CSF/IL-4 only were also included as unstimulated controls, and plates were incubated in 5% CO2 at 37°C. At the end of 7 days incubation, cells were harvested for TRIzol total RNA extraction and RT-PCR, and supernatants were collected for cytokine assay (Figure 2.4) (97-101).

e) Co-culture of macrophages and activated T cells

PBMCs were isolated from whole blood of healthy volunteers with Ficoll® by density gradient centrifugation. T cells were isolated by negative selection with the EasySep® Human T lymphocytes Enrichment Kit (STEMCELL Technologies, Vancouver, BC, Canada). The kit utilizes enrichment cocktail containing antibodies against cell surface antigens on undesired cell populations including: CD14, CD16, CD19, CD20, CD36, CD56, CD123, and glycophorin A. Additional two rounds of magnetic separation were performed at the end of the T cell enrichment protocol to increase the purity of isolated T

cells. CD3+ T cell purity of greater than 93% was assessed by flow cytometry. T cells (1 x 10^6 cells/ml) were stimulated by anti-CD3 (OKT3; 5 μg/ml, eBioscience) and anti-CD28 (clone CD28.2; 1 μg/ml, eBioscience) immobilized to 6 well plate. Cultures were incubated with complete RPMI-10 and recombinant human IL-2 (50 U/ml, eBioscience) in 5% CO2 at 37°C. On day 4, six - well plates were coated with anti-CD3 antibodies (OKT3; 10 μg/ml), covered plates were sealed and incubated overnight at 4 ºC. On day 5, monocyte isolation was performed for co-culture. Monocytes were purified from PBMCs isolated from whole blood of healthy volunteers with Ficoll® by density gradient centrifugation. Monocyte enrichment was performed by negative selection using the EasySep® Human Monocyte Enrichment Kit as previously described in macrophage cultures. Monocytes were resuspended in complete RPMI-10. T cells incubated for 5 days in anti CD3/anti-CD28 coated 6-well plate were collected, and were resuspended in complete RPMI-10. For co-cultures, T cells were plated into new anti-CD3 (10 μg/ml) coated 6-well plates and autologous monocytes were added in co-cultures as follows:

Transwell (no contact) co-culture: Freshly isolated monocytes were added to anti CD3-T cells (monocytes : T cells ratio = 2:1) via transwell (cell culture inserts 0.4 μm pore size) and rhIL-2 (50 U/ml) was added to cultures. Transwell culture system allows soluble factors and cytokines released to diffuse and act on cultured cells in the absence of cell-to-cell contact. Macrophages cultured alone and anti-CD3 T cultured alone were also included as controls and plates were incubated for 24 hours in 5% CO2 at 37°C (Figure 2.5).

Contact co-culture: Freshly isolated monocytes were added directly to wells in contact with anti CD3-T cells (monocytes : T cells ratio = 2:1) . Recombinant human IL-2 (50 U/ml) was added to cultures and plates were incubated in 5% CO2 at 37°C for 24 hours. Macrophages cultured alone and anti-CD3 T cultured alone were also included as controls (Figure 2.6).

After 24h incubation of co-cultures of macrophages and activated T cells (contact and no contact), cells were harvested for TRIzol total RNA extraction and RT-PCR. Supernatants were collected for cytokine assay.

2.3. FLOW CYTOMETRY

Cells were stained for flow cytometry using the following antibodies (eBioscience): APC-Cy7 labeled anti-human CD45, APC conjugated anti-human CD3, Phycoerythrin-Cy7 (PE-Cy7) anti-human CD14, PE conjugated anti-human CD19, Alexa Fluor® 488 conjugated anti-human CD56, APC conjugated anti-human CD11c . Subsequent flow cytometry data acquisition was performed on BD FACS Canto and analyzed with FCS Express software (De Novo Software, Los Angeles, CA). After gating on CD45+ viable cells, lymphocyte and myeloid cell populations were assessed as percent of CD45+ cells.

2.4. ENZYME-LINKED IMMUNOSORBENT ASSAY (ELISA)

Cytokine secretion in supernatants of cell cultures was measured by ELISA using commercially available kits for human IFNG, TNF and IL-6 (R&D Systems, Minneapolis, MN, USA) following the manufacturer's instructions. Capture antibodies were diluted in PBS at manufacturer's recommended concentrations and immobilized onto flat-bottomed 96-well plates (Dynatech Laboratories) and incubated overnight at 4ºC. Plates with immobilized antibodies were washed with wash buffer (0.5% PBS/Tween) and blocked with 200 µl assay diluent (10% FBS in PBS) and incubated at room temperature for 1-2 hours. Standards were prepared according to manufacturer's instructions, then standards and supernatant samples were added to the plate and wells were topped to reach a total volume of 100 µl per well, and plates are incubated at room temperature for 2 hours. Wells were rinsed with wash buffer three times before adding the detection antibodies to all wells containing standards or samples. After one hour, wells were rinsed three times, and avidin-HRP was added to each well at the manufacturer's recommended concentration. After incubation in the dark for 20 minutes at room temperature, wells were washed three times before adding TMB substrate (TetraMethylBenzidine, eBioscience). After sufficient color development at room temperature, 2M sulphuric acid (H_2SO_4) was added to wells to stop the reaction. Plates were read using a SPECTRAmax PLUS^{384} plate reader (Molecular Devices) and absorbance was measured at 450 nm–wavelength. For individual cytokine, concentration was calculated from the regression line for a standard curve (concentration

versus absorbance plots) generated using the corresponding highly purified recombinant cytokine at various concentrations freshly prepared with each assay.

2.5. V-PLEX CYTOKINE ASSAY

Cytokine assay in supernatants from transwell (no contact) co-cultures of macrophages and activated T cells was performed using Multiple (V-PLEX) assay kit according to the manufacturer's instructions. Briefly, multianalyte controls (provided with kit) and samples were added to wells (50 µl/well) in 96-well 10-spot MULTI SPOT® plate pre-coated with capture antibodies to different analytes. The plate was sealed with an adhesive plate seal and incubated overnight at 4ºC. The plate was washed 3 times with wash buffer (≥ 150 µl/well) and detection antibody solution (25 µl/well) was added to each well, then the plate was sealed and incubated at room temperature for 2 hours. After incubation, the plates were washed 3 times with wash buffer, and 150 µl reach buffer T was added to each well before reading the plate on the MSD instrument. Results were analyzed using the MSD DISCOVERY WORKBENCH® analysis software to determine cytokine concentrations.

2.6. RNA PREPARATION AND MICROARRAY

Samples were homogenized in Trizol reagent and total RNA was extracted and purified using the RNeasy Micro Kit (Quiagen, Ont. Canada) for kidney biopsies or Mini Kit (Quiagen, Ont. Canada) for cell cultures. RNA yield was measured by UV absorbance, and the RNA quality was assessed using the Agilent 2100 Bioanalyzer (Agilent Technologies, Palo Alto CA). Synthesis of dsDNA and cRNA was performed according to Affymetrix Technical Manual , followed by RNA labeling using GeneChip® HT One-Cycle Target Labeling and Control Kit. Labeled cRNA quality was assessed by Agilent 2100 Bioanalyzer (Agilent, Palo Alto, CA) before hybridization to human HG_U133_Plus_2.0™ GeneChip® gene expression arrays (Affymetrix, Santa Clara, CA). GeneChips were scanned using Affymetrix GeneArray Scanner and Affymetrix CEL files were generated with GeneChip® Command Console® Software Version 4.0. Microarray data were preprocessed by Robust Multichip Analysis (RMA) and gene expression data were analyzed as the raw signal values for each probe set using GeneSpring™ GX 13.0 (Agilent

Technologies, Santa Clara, CA) . RNA labeling and hybridization to HG U133 Plus 2.0 GeneChip (Affymetrix, Santa Clara, CA) was carried out by multiple technicians in the Halloran Laboratory, according to Affymetrix protocols published at www.affymetrix.com.

2.7. REAL-TIME RT-PCR

Expression of certain transcripts was confirmed by TaqMan real-time RT-PCR. Samples were homogenized in TRIzol reagent according to manufacturer's instructions. Total RNA isolation and purification was performed using the RNeasy Micro Kit (Quiagen, ON, Canada). RNA yields were measured by Nano Drop® Spectrophotometer ND-1000 (Thermo Fisher Scientific, Wilmington, DE). Subsequently, RNA was reverse transcribed using M-MLV reverse transcriptase and random primers according to manufacturer's instructions (Invitrogen Life Sciences, Carlsbad, CA) and the cDNA obtained was amplified in RT-PCR. All Primers and probes were obtained as TaqMan Gene Expression assays (PE Applied Biosystems, Foster City, CA) and all RT-PCR assays were performed in triplicates. PCR amplification conditions were 50°C for 2 min, 95°C for 10 min, followed by 40 cycles of 95°C for 15s and 65°C for 1 min. For each sample, each gene of interest and endogenous control gene were assessed in triplicate reactions. Gene expression was assessed as described by the manufacturer using the ABI PRISM 7700 Sequence Detection System (Applied Biosystems Inc. Foster City, CA). The results of RT-PCR were received as the numbers of fluorescence threshold cycles (Ct). Threshold cycle number for each gene of interest was compared with the Ct value for HPRT for the same pool. Gene expression data was expressed as relative percent of the endogenous control gene hypoxanthine phosphoribosyl transferase (HPRT) (102). The ABI gene expression IDs for the transcripts used are listed in Table 2.2.

2.8. MOUSE KIDNEY TRANSPLANTS

Mouse Strains Wild type mice: Male CBA/J (CBA; H-2k) and C57BI/6 (B6; H-2b) mice were obtained from Jackson Laboratory (Bar Harbor, ME) and were maintained in the Health Sciences Laboratory Animal Services at the University of Alberta. All maintenance and experiments conformed to approved animal care protocols. Mouse renal transplantation

was performed as a non life-supporting transplant model across full MHC and non-MHC disparities, as previously described (103;104). We used wild type CBA (H-2k) as donor and wild type CBA (H-2k) and B6 (H-2b) as recipients. Normal CBA kidneys, and CBA isografts transplanted into CBA hosts served as controls. Mice did not receive immunosuppressive therapy. Recovered mice were sacrificed and kidneys were harvested, snap frozen in liquid nitrogen and stored at -70°C. Kidneys with technical complications or infection at the time of harvesting were excluded from the study. CBA allografts transplanted into B6 hosts and CBA into CBA isografts were harvested at days 1, 2, 3, 4, 5, 7, and 21.

Mouse renal transplants were performed by Dr. Lin Fu Zhu.

RNA preparation and microarray

Samples were homogenized in TRIzol reagent according to manufacturer's instructions. Total RNA extraction and purification was performed using the RNeasy Mini Kit (Quiagen, Ont. Canada). For mouse kidneys, equal amounts of RNA from 3 mice (20-25 ug each) were pooled and purified using the RNeasy Mini Kit (Quiagen, Ont. Canada).

RNA labeling and hybridization to mouse MOE430 2.0™ GeneChip® gene expression arrays (Affymetrix, Santa Clara, CA) was performed by multiple technicians in Halloran Laboratory according to the Affymetrix published protocols (www.affymetrix.com)

2.9. STATISTICAL ANALYSES

Data analysis was performed using GraphPad Prism 5 and GeneSpring™ GX 13.0 (Agilent Technologies, Santa Clara, CA). Data were expressed as mean ± standard error (SE) unless stated otherwise. Statistical differences between different groups or conditions were analyzed by either t-test or ANOVA with Dunnett's multiple comparison test as indicated for each analysis. Class comparisons for probe set expressions between two groups was performed using moderated T test (Benjamini Hochberg). A *p* value or corrected *p* value (false discovery rate FDR) less than 0.05 was considered statistically significant.

Correlations between individual transcript expression in human allograft biopsies and macrophage transcript burden, T cell transcript burden, histologic lesion score were tested by Spearman correlation coefficient test.

2.10. TABLES

Table 2.1. Histologic diagnoses for human kidney transplant biopsies

T cell mediated rejection (TCMR)

biopsies with interstitial infiltration i ≥ 2 and tubulitis t ≥ 2

Antibody mediated rejection (ABMR)

C4d-negative

microvascular lesions of inflammation (glomerulitis [g] or peritubular capillaritis [ptc] > 0) and/or microvascular deterioration (transplant glomerulopathy [cg] > 0) with detectable donor specific antibodies (DSA) at the time of biopsy

C4d-positive

biopsies with DSA positive and C4d positive (diffuse linear C4d staining [>50% of biopsy area] was interpreted as C4d positive) and morphologic evidence of microvascular inflammation (g>0 or ptc>0) and/or and/or microvascular deterioration (cg>0)

Mixed ABMR and TCMR

biopsies that meet criteria for both ABMR and TCMR

Borderline

biopsies with foci of tubulitis (t>0) with minor interstitial infiltration (i<2) or foci of interstitial infiltration (i>1) with mild tubulitis (t1), with no arteritis (v=0)

Transplant glomerulopathy (TG)

biopsies showing double contours of glomerular basement membrane

Interstitial fibrosis and tubular atrophy (IFTA)

biopsies having a ci-score > 1 and no features of specific disease

BK polyoma virus nephropathy (BK)

biopsies showing BK nephritis (confirmed by in situ hybridization and/or electron microscopy) were designated as BK, regardless of histological signs of TCMR

No major abnormalities (NOMOA)

biopsies occurring after 42 days that also lacked histological disease features

Acute kidney injury (AKI)

biopsies for clinical indications before 42 days that lacked histological disease features

Table 2.2. RT-PCR assay on demand ID numbers (human)

TAQMAN GENE EXPRESSION ASSAYS	
Gene Symbol	ABI gene expression Assay ID
ADAMDEC1	Hs00936067_m1
CXCL13	Hs00757930_m1
CCL18	Hs00268113_m1
CCL19	Hs00171149_m1
HPRT	4326321E

2.11. FIGURES

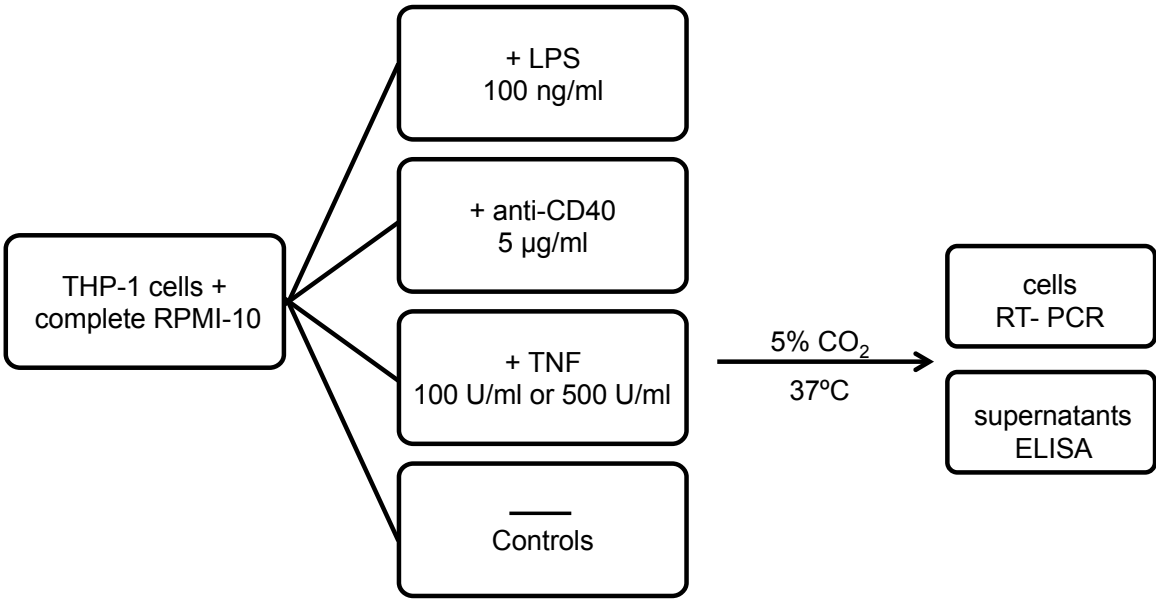

Figure 2.1. Flow chart for THP-1 cell culture and stimulation

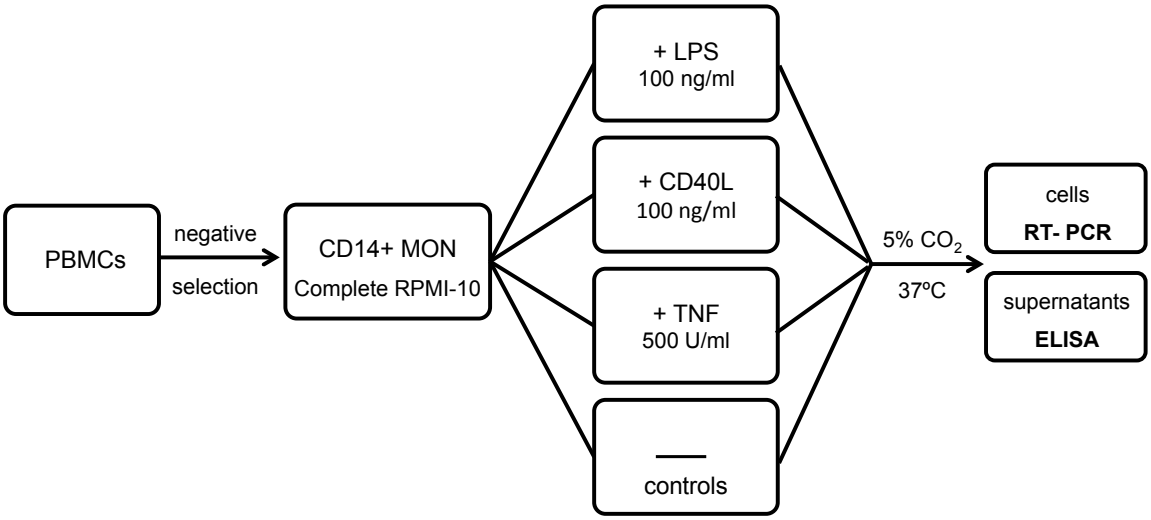

Figure 2.2. Flow chart for monocyte-derived macrophage differentiation and stimulation

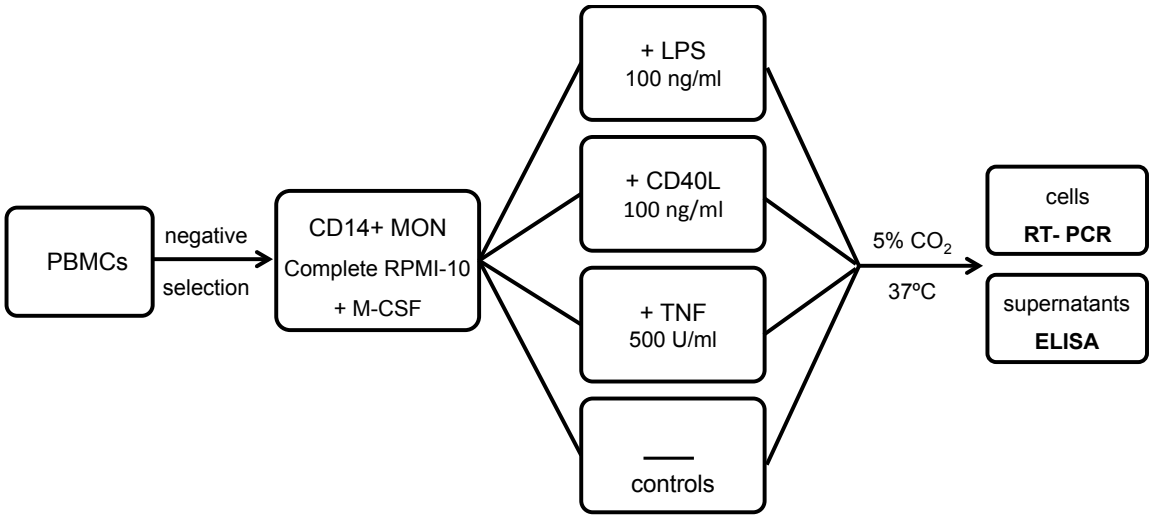

Figure 2.3. Flow chart for monocyte-derived M-CSF macrophage differentiation and stimulation

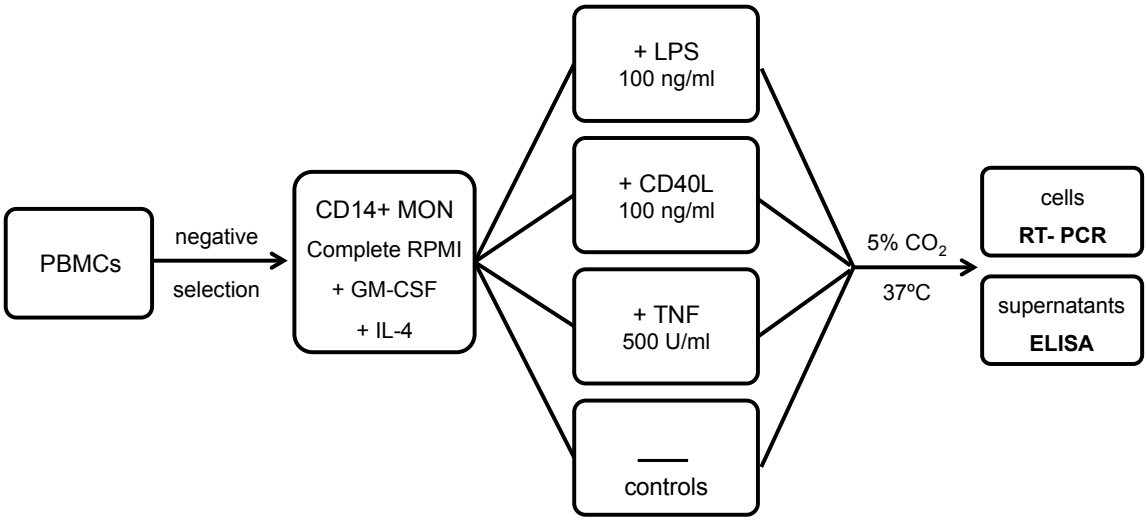

Figure 2.4. Flow chart for monocyte-derived dendritic cell differentiation and stimulation

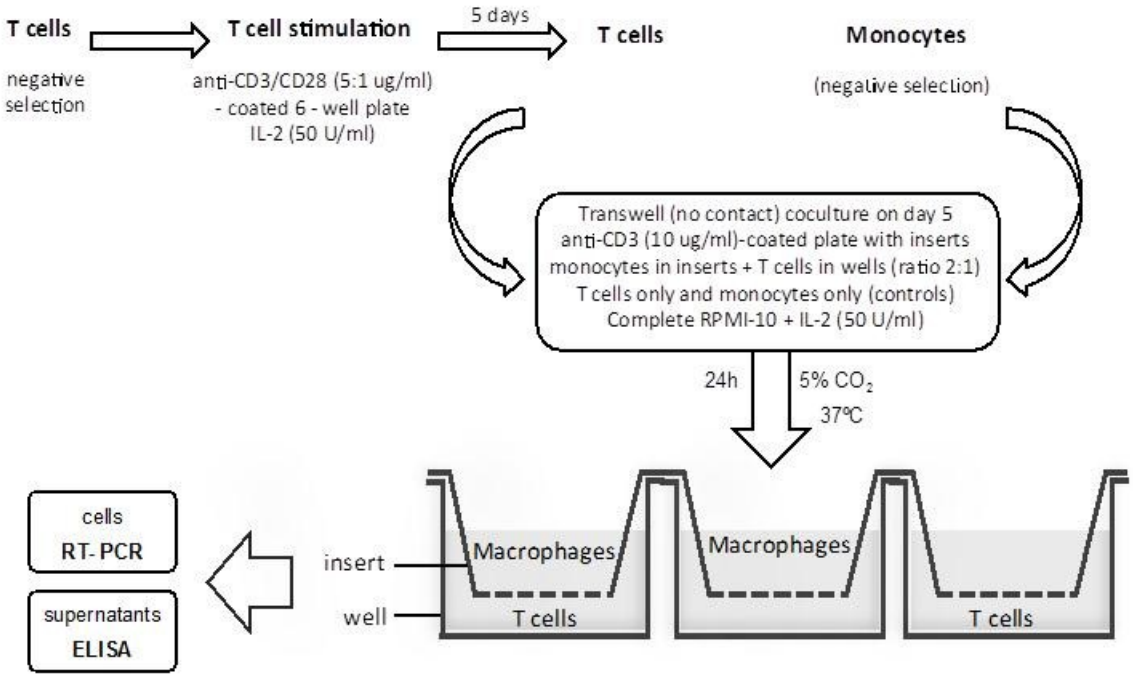

Figure 2.5. Flow chart for macrophage-activated T cell transwell (no contact) co-culture.

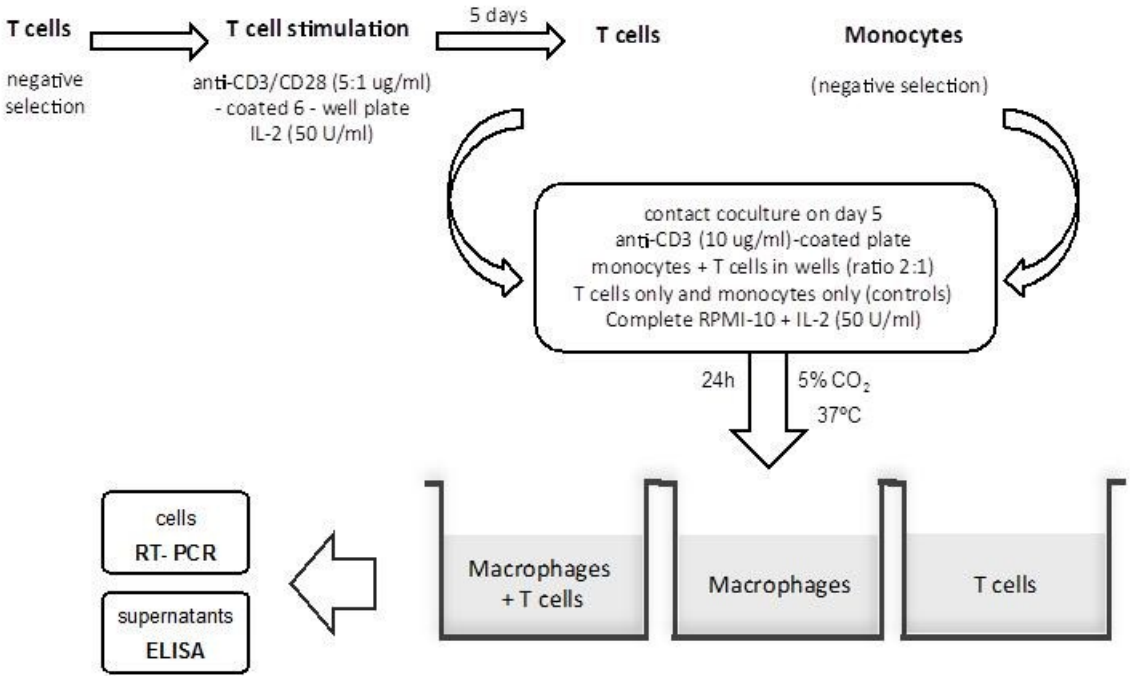

Figure 2.6. Flow chart for macrophage-activated T cell contact co culture.

CHAPTER 3

DEFINING TRANSCRIPTS PREFERENTIALLY INCREASED IN TCMR VERSUS ABMR

DEFINING TRANSCRIPTS PREFERENTIALLY INCREASED IN TCMR VERSUS ABMR

3.1. OVERVIEW

The two types of rejection recognized in Banff classification are T cell mediated rejection and antibody mediated rejection as well as the combination of both, mixed rejection. TCMR is a prototype for immune diseases mediated by cognate T cell recognition in tissues and is now recognized as the most common form of rejection in the early post-transplant period in low immunologic risk patients lacking donor specific antibodies at the time of transplant. In contrast, ABMR is a major cause for late graft loss (14-16) and requires aggressive therapeutic approaches. Thus defining the markers that distinguish between TCMR and ABMR is critical for guiding therapies, response to treatment, and graft outcome. This cannot be achieved without better understanding of the immune events and mechanisms by which the host alloimmune response mediates graft injury during rejection and their relationship to the development of the immunopathological and clinical phenotype of allograft rejection. The advances in the molecular approaches, including gene expression microarray analysis, provide valuable tools for studying the molecular phenotypes of rejection (91), identifying these mechanisms, and refining diagnosis accuracy (79-81).

In the present study, we sought to examine the molecular changes across 703 clinically indicated kidney transplant biopsies and define the transcripts that are preferentially expressed in biopsies diagnosed as TCMR. Using microarrays analyses, we initially identified transcripts with higher expression in TCMR biopsies over normal kidney control samples. The top 50 transcripts (by fold change) included many IFNG induced transcripts including the highly expressed IFNG inducible chemokines that control lymphocyte migration and recruitment to the inflamed sites, transcripts associated with tissue remodeling, and injury response related transcripts. From the transcripts showing increased

expression in TCMR compared to controls we identified the top fifty transcripts preferentially expressed in TCMR when compared to ABMR biopsies. Homeostatic chemokines and metalloprotease transcripts had the highest fold change increase of expression in differentiating TCMR over ABMR. We further assessed the significance of these transcripts in differentiating TCMR biopsies from biopsies with non specific acute kidney injury (AKI) and from non TCMR biopsies. As multiple chemokines and metalloproteases were prominent among the top transcripts preferentially increased in TCMR, we studied the molecular profile for chemokines (and chemokine receptors) and metalloproteases. In an attempt to correlate our molecular data to the alloimmune events and histopathologic lesions in biopsies, we studied the relationship between the expression of four of the top transcripts and the inflammatory burden (macrophages and T cells), histopathologic diagnoses and lesion scores in biopsies.

3.2. HUMAN POPULATION DEMOGRAPHICS AND BIOPSY DIAGNOSES

The study included 703 renal transplant indication biopsies from 579 consented patients from six kidney transplant centres, obtained between one week and 427 months post transplant. Patient demographics and clinical characteristics at time of biopsy are shown in Table 3.1.

All biopsies were assessed using the Alberta Transplant Applied Genomics Centre (ATAGC) Reference Standard (80) incorporating C4d-negative ABMR and the changes outlined in the Banff 2013 report (73). Histopathologic Banff diagnoses included T cell-mediated rejection, antibody- mediated rejection (C4d positive ABMR and C4d negative ABMR), mixed TCMR and ABMR, borderline TCMR, acute kidney injury (AKI), BK polyoma virus nephropathy (BK), transplant glomerulopathy (TG), interstitial fibrosis and tubular atrophy (IFTA), glomerulonephritis (GN), no major molecular abnormalities (NOMOA) and other. Biopsies showing BK virus by *in situ* hybridization and/or electron microscopy were designated BK polyoma virus nephropathy, regardless of whether they also had T cell-mediated rejection criteria. The histologic diagnoses for biopsies are shown in Table 3.2.

3.3. ALGORITHM FOR DEFINING TRANSCRIPTS PREFERENTIALLY INCREASED IN TCMR VERSUS ABMR

To define the transcripts that are preferentially increased in TCMR versus ABMR, we used the algorithm depicted in Figure 3.1. We wanted to exclude the transcripts that may show false increase in expression in TCMR versus ABMR due to their decrease in ABMR rather than actual increase in their expression in TCMR. This was achieved by a class comparison between TCMR and ABMR using the list of probe sets with significant higher expression in TCMR versus normal kidney control samples. This algorithm ensures that all the transcripts with significant higher expression in TCMR versus ABMR are primarily increased in TCMR versus normal kidney. As shown in Figure 3.1, the algorithm includes two main steps; 1) define a list of probe sets with significant higher expression in TCMR biopsies versus normal kidneys, then compare this list of probe sets in TCMR versus ABMR to 2) define the probe sets with significant preferential increase in TCMR versus ABMR.

3.4. DEFINING TRANSCRIPTS INCREASED IN TCMR VERSUS NORMAL KIDNEYS

We compared the expression of 54,675 non interquartile range (non-IQR) filtered probe sets on human HG_U133_Plus_2.0 GeneChips (Affymetrix) in biopsies with TCMR versus normal kidneys using moderated T test, corrected p-value (Benjamini Hochberg False Discovery Rate; FDR <0.05). We opted to avoid using IQR filter as this may eliminate transcripts with high statistical association but relatively low signal, despite the advantage of simplifying analyses.

Of the total examined 54,675 probe sets, 11,244 probe sets showed higher expression in TCMR versus control kidneys (FDR <0.05). This list of 11,244 probe sets (redundant list; a single transcript may be represented by more than one probe set) increased in TCMR versus normal kidneys (FDR <0.05) was later used in the class comparison of TCMR versus ABMR.

The top 50 transcripts with higher expression in TCMR versus normal kidneys (ordered by fold change increase of expression over normal kidneys) are listed in Table 3.3. For simplification, the table only shows a non redundant list in which each transcript is represented by only one probe set (the probe set with the higher significance/ smaller p-value). As expected, many IFNG-induced transcripts reflecting the intense IFNG response, a striking feature of T cell mediated inflammatory response including TCMR, were prominent in this list. The top transcripts with the highest increase of expression included the IFNG inducible transcripts: the chemokines CXCL9, CXCL10, and CXCL11 as well as the membrane glycoprotein FAM26F. The lymphoid chemokine CXCL13 (B cell-attracting chemokine 1; BCA-1) and the matrix metalloprotease ADAM-like decysin 1 (ADAMDEC1) were among the top highly expressed transcripts, but to a less degree than the IFNG inducible transcripts (CXCL9, CXCL10, and CXCL11 and FAM26F). Also at the top of the transcript list we found effector T cell-associated transcripts including cytotoxic molecules and membrane receptors GZMA, TRBC1, and CCR5/RANTES indicative of the vast T cell recruitment. Along with transcripts reflective of T cell recruitment, transcripts related to macrophages (TLR8, CD163, LYZ) were also identified. In addition, transcripts related to tissue injury-repair response (COL1A2, COL6A3, COL1A1, CTHRC1, CTSS, VCAN) were also prominent. This is in agreement with the expected tissue remodeling process that occurs as part of the tissue injury-repair response.

Thus the transcripts showing higher expression in TCMR versus normal kidneys reflect the intense IFNG response (IFNG inducible transcripts), the inflammatory cell recruitment and the tissue response to injury.

3.5. DEFINING TRANSCRIPTS PREFERENTIALLY INCREASED IN TCMR VERSUS ABMR

Using the algorithm described above, we identified a list of 4,449 probe sets with significant higher expression in TCMR versus ABMR. We removed redundant probe sets so that each transcript is represented by only one probe set which showed the most significant (smallest p-value/FDR) increase of expression in TCMR versus ABMR. Table 3.4 lists the top fifty transcripts preferentially increased in TCMR versus ABMR biopsies,

ordered by fold change of expression. They represented molecules related to chemotaxis and leukocyte migration (CXCL13, CCL18, CCL19 and its receptor CCR7, and SELL), matrix and tissue remodeling (ADAMDEC1, COL1A2, CTHRC1 and MMP9), effector T cells transcripts (GZMA, GZMK, CD8A, CD2, TRBC1, ITK,) and B7 family of immunoregulatory receptors (CTLA4, CD28), transcripts related to macrophage receptors (TLR8, scavenger receptor CD163), and monocyte to macrophage differentiation (APOC1). Transcripts with the highest increase (fold change) in expression in TCMR versus ABMR were CXCL13, ADAMDEC1 and CCL18 with almost 8-, 7- and 5-fold change, respectively.

3.6. THE TOP TRANSCRIPTS WITH THE HIGHEST ASSOCIATION WITH TCMR

Figure 3.2 shows the association strength (p-value) plotted on the x-axis against the fold change of expression on the y-axis. The above defined top 10 transcripts preferentially increased (fold change) in TCMR versus ABMR were CXCL13, ADAMDEC1, CCL18, PLA2G7, COL1A2, CTHRC1, MS4A1, RRM2, CD163 and APOC1. The top 10 transcripts with the highest of association (p-value) with TCMR were ADAMDEC1, CCL18, PLA2G7, CTLA4, CD84, CXCL13, SIRPG, DLGAP5, SLAMF8 and CENPF. The four transcripts ADAMDEC1, CCL18, CXCL13 and PLA2G7 had both the highest expression (fold change) in TCMR versus ABMR and highest level of association (p-value) with TCMR. This agrees with previous studies reporting many of the above transcripts such as ADAMDEC1, CXCL13, SLAMF8, SIRPG and CTLA4 among the TCMR molecular classifier transcripts (80;84). Thus ADAMDEC1, CXCL13 and CCL18 are the top transcripts most highly expressed in TCMR and with the highest association with TCMR.

3.7. THE SIGNIFICANCE OF THE TOP TRANSCRIPTS PREFERENTIALLY INCREASED IN TCMR VERSUS ABMR IN DIFFERENTIATING TCMR FROM AKI AND NON TCMR BIOPSIES

A degree of inflammation is observed with tissue injury (105) which would likely overlap with the inflammation observed in TCMR, at least to some degree. We therefore examined expression of the above defined fifty transcripts in a class comparison between biopsies with TCMR against biopsies with non specific AKI (Table 3.5). Compared to biopsies with AKI, only five transcripts of the top 50 (COL1A2, COL1A1, RRM2, MMP9 and ADAMTS2) failed to be significantly increased in TCMR versus AKI, with the top three now being CXCL13, ADAMDEC1, and CCL18 remained at the top of the list based on fold change. Thus the top transcripts preferentially increased in TCMR versus ABMR likely reflect alloimmune mechanisms characteristic for TCMR with minimal contribution from the non specific graft injury response.

Similarly, we analyzed the significance of the top 50 transcripts preferentially increased in TCMR versus ABMR in distinguishing TCMR biopsies from non TCMR biopsies. The non TCMR biopsies included all biopsy histologic diagnoses excluding TCMR, borderline, mixed TCMR and ABMR, and BK polyoma virus nephropathy i.e. we excluded biopsies with TCMR or any possible TCMR element from the non TCMR group. Biopsies with BK polyoma virus nephropathy were excluded from the non TCMR group based on recent studies showing that BK polyoma virus nephropathy is frequently associated with putative episodes of TCMR (106). In contrast to our comparison against AKI, all 50 top transcripts that were preferentially expressed in TCMR versus ABMR were also significantly increased in TCMR versus non TCMR biopsies. CXCL13 and ADAMDEC1 again remained the most highly expressed transcripts showing 10 fold change and 8 fold change increase of expression, respectively, in TCMR versus non TCMR. Other transcripts such as GBP5, CCL18 and TLR8 had higher expression in TCMR over non TCMR, but to a less degree than CXCL13 and ADAMDEC1.

Thus the top fifty transcripts preferentially increased in TCMR versus ABMR do not only differentiate TCMR from ABMR but also from all biopsies with histologic diagnoses devoid of any TCMR component. This also suggests that the top transcripts reflect mechanisms characteristic for TCMR with minimal contribution from non specific injury and all other non rejection diagnoses.

3.8. CHEMOKINES AND CHEMOKINE RECEPTORS PREFERENTIALLY INCREASED IN TCMR VERSUS ABMR

Given that chemokines and metalloproteases dominated the top transcripts most highly expressed in TCMR versus normal kidneys, we performed a comprehensive analysis of chemokines, chemokine receptors, and metalloproteases with higher expression in TCMR compared to ABMR (FDR <0.05). A better understanding of the chemokines (and chemokine receptors) and metalloproteases (and TIMP) may be critical to further understand the mechanisms of TCMR. We thought that this analysis would be pertinent to the mechanism of inflammatory cell recruitment, migration and positioning within the graft, and the extracellular matrix remodeling and tissue response to injury, all of which are observed in TCMR.

The input list was derived from our previous TCMR versus ABMR class comparison (generated by the algorithm in Figure 3.1). Of all chemokines examined, the homeostatic chemokine CXCL13 showed the highest fold change (8.1 fold) of expression in TCMR versus ABMR, followed by CCL18 (4.8 fold), and then CCL19 (Table 3.6). While CXCL13 had the highest fold change of expression, CCL18 had the strongest association with TCMR (FDR = $7x10^{-13}$) among all chemokines and chemokine receptors. The chemokine receptor CCR7 ranked third (2.4 fold change) followed by its ligand CCL19 (2.2 fold change), another important homeostatic chemokine. The higher expression of IFNG inducible chemokines (CXCL9, CXCL10, CXCL11) is part of the drastic IFNG response that is prominent in TCMR and their increased expression in rejection have been reported in many human studies (107;108). Protein levels of these chemokines are also associated with rejection; urinary CXCL9 and CXCL10 levels are elevated in patients with TCMR (109). The receptor for CXCL9, 10, and 11; CXCR3 failed to show a significant association with TCMR, likely because it is also highly expressed in NK cells found in biopsies with ABMR. The chemokine receptors (CCR5, CXCR6, CCR2 and CCR1) expressed on infiltrating T cells and macrophages, and their chemokine ligands (CCL5/RANTES, CXCL16, CCL2) these transcripts likely reflect the intense T cell and macrophage infiltration in allografts undergoing TCMR. The data emphasize a potential

role for these chemokines-chemokine receptors interaction in mediating inflammatory cell recruitment and migration within the allograft in TCMR.

3.9. METALLOPROTEASES PREFERENTIALLY INCREASED IN TCMR VERSUS ABMR

Our microarray analysis of TCMR versus ABMR biopsies yielded a list of metalloproteases that showed significant increase of expression in TCMR versus ABMR (Table 3.7). The list included matrix metalloproteases such as MMP-9, ADAMs such as ADAM12 and ADAM19, ADAMDEC1, ADAMs with thrombospondin domain such as ADAMTS2, and two tissue inhibitors of metalloproteases (TIMP1 and TIMP2) that regulate the activity of metalloproteases. The top metalloprotease showing the highest increase of expression in TCMR versus ABMR was ADAMDEC1 (7 fold change, FDR = 1.9 $x10^{-19}$). Little is known about ADAMDEC1, its exact cellular source in tissues, its substrate or its role. However, it has been linked to many human pathologies and recently was suggested as a marker in many human diseases such as neurological tumors (110) and pulmonary sarcoidosis (111). Also, ADAMDEC1 and other metalloproteases were suggested as potential markers for TCMR in renal transplant patients (112). The metalloproteases are known for their role in matrix remodeling and wound healing and a role in inflammation by their proteolytic action on chemokines that control inflammatory cell migration and recruitment. The MMP proteolytic action results in activation of certain substrate and inactivation of another one. For example, MMP-9 action on CXCL8 results in its activation while MMP-9 action on other chemokines, such as the IFNG inducible chemokines CXCL9, CXCL10 and CXCL11, results in their inactivation (68).

Thus the increased expression of these different metalloproteases (and TIMPs) in T cell-mediated rejection suggests a potential role in active control of inflammatory compartment in rejecting allograft and a role in tissue injury response and remodeling.

3.10. SELECTION OF ADAMDEC1, CXCL13, CCL18 AND CCL19 FOR FURTHER STUDY

Chemokines and their receptors are the key regulators/main orchestrator of leukocyte trafficking. The expression of many chemokines is induced in cells and tissues during immune responses to regulate leukocyte migration to inflamed tissue. However, some chemokines are constitutively expressed in secondary lymphoid organs and regulate leukocyte homing and movement during homeostasis, thus known as homeostatic chemokines. Interestingly, three lymphoid chemokines, CXCL13, CCL18 and CCL19 (in addition to the metalloprotease ADAMDEC1) had the highest expression in TCMR over ABMR. Although homeostatic chemokines are well characterized in secondary lymphoid organs (64), little is known about their role in peripheral tissues. Thus we proceed with detailed in vitro studies focusing on these four top highly expressed transcripts.

3.11. EXPRESSION OF ADAMDEC1, CXCL13, CCL18 AND CCL19 IN DIFFERENT HISTOLOGIC DIAGNOSES

Expression of ADAMDEC1, CXCL13, CCL18 and CCL19 was assessed by microarrays in different histologic diagnoses across 703 kidney transplant biopsies. We compared the expression of individual transcripts in each diagnostic category to normal kidney control samples (nephrectomies) using one-way ANOVA with Dunnett's multiple comparison test (Figure 3.3). Among all histologic diagnoses, biopsies with TCMR showed the highest expression ($p < 0.01$) of ADAMDEC1, CXCL13, CCL18 and CCL19 compared to controls. The expression of ADAMDEC1 and CXCL13, although not significant ($p<0.05$), in biopsy with BK polyoma virus nephropathy can be explained by the recent reports showing putative TCMR episodes in biopsies diagnosed as BK polyoma virus nephropathy (106). Similarly, biopsies with mixed TCMR and ABMR expressed considerable levels of ADAMDEC1, but this was not significant, and that can be attributed to the presence of TCMR element in these biopsies. Although no other diagnostic category besides TCMR showed higher expression than controls, CCL19 showed high average expression in many diagnoses. None of the four transcripts showed higher expression in either ABMR or AKI compared to controls. This is of particular interest because it differentiates biopsies with

TCMR from the other type of rejection (ABMR) and from the non specific AKI response that is part of the tissue response to injury but not an alloimmune injury. Thus high expression of ADAMDEC1, CXCL13, CCL18 and CCL19 over normal kidneys is a characteristic molecular feature for TCMR that distinguish it from all other histologic diagnoses, including biopsies with ABMR and biopsies with AKI.

3.12. THE RELATIONSHIP BETWEEN ADAMDEC1, CXCL13, CCL18 AND CCL19 EXPRESSION AND HISTOLOGIC LESIONS

Although the four transcripts of interest showed associations with the histologic diagnosis of TCMR, we sought to examine associations with the individual histologic lesions used for the TCMR diagnosis, which are also more granular. The relationship between expression of ADAMDEC1, CXCL13, CCL18 and CCL19 and the histologic lesions in biopsies was examined using Spearman correlations (Table 3.8). Across 703 biopsies, the strongest, and most consistent, correlations between the expression of ADAMDEC1, CXCL13, CCL18 and CCL19 ($p < 0.0001$) were observed with the lesions of interstitial inflammation (i-score; $r = 0.45$, $r = 0.40$, $r = 0.33$ and $r = 0.31$, respectively) and tubulitis (t-score; $r = 0.43$, $r = 0.40$, $r = 0.31$ and $r = 0.28$, respectively). This corroborates the associations observed with TCMR as interstitial inflammation and tubulitis are the lesions most characteristic for TCMR. The correlation of the expression of the four transcripts with intimal arteritis (v-score) was weaker than those observed with i- and t- scores (ADAMDEC1; $r = 0.25$, CXCL13; $r = 0.20$, CCL18; $r = 0.21$, and CCL19; $r = 0.19$, $p < 0.0001$) likely due to its more recently found association with ABMR (113).

The associations with the lesions above are expected, but for the four selected transcripts to be truly associated with TCMR and not ABMR we should also observed a lack of or weaker correlation with lesions that depict ABMR. We examined the correlation between transcript expression and the histologic lesions for ABMR i.e. glomerulitis (g-score), peritubular capillaritis (ptc-score), and glomerular double contours (cg-score). The expression of ADAMDEC1, CXCL13, CCL18 and CCL19 showed no correlation in relation to g-score, weak correlation (all transcripts except CCL18) in relation to ptc-score

and with cg-score (all transcripts except CCL19). The weak positive correlations observed with ptc-scores are likely due to the presence of this lesion in TCMR (114).

The remaining Banff lesion scores were also examined. We studied the correlations between transcript expression and histologic lesions related to atrophy and scarring i.e. interstitial fibrosis (ci-score), tubular atrophy (ct-score), arterial fibrous intimal thickening (cv-score) and arteriolar hyalinosis (ah-score). We found either no correlation (all four transcripts with cv-score), weak correlation (ADAMDEC1 and CXCL13 in relation to ci- and ct-score) or negative correlations (all transcripts except CCL19 in relation to ah-score). Interestingly, CCL19 expression had a relatively stronger correlation, compared to the other three transcripts, with interstitial fibrosis (ci-score) and tubular atrophy (ct-score). Interstitial fibrosis and tubular atrophy generally occur late and may contain lymphoid aggregates in which CCL19 (115), a lymphoid homing chemokine, may be secreted, which may justify the correlation between this lesion and CCL19.

Thus the expression of ADAMDEC1, CXCL13, CCL18, and CCL19 had the strongest correlations with histologic lesions diagnostic for TCMR and weak or negative correlations with lesions diagnostic for ABMR.

3.13. PATHOGENESIS BASED TRANSCRIPT SETS

For assessment of the transcriptome disturbances during rejection, we have coined the term pathogenesis based transcript sets (PBTs) (82) to define a number of transcript sets that measure characteristic transcriptional changes associated with the inflammatory burden in kidney transplant biopsies. These PBTs reflect the major biologic events during the rejection process, such as IFNG effects (116), T cell infiltration and macrophage infiltration (80;117;118). PBTs were derived from mouse kidney transplant models and *in vitro* human cell lines. Each PBTs (e.g. macrophage-associated transcript set) is represented by a number of probesets and is expressed as a score, PBTs score. For each biopsy, this score is calculated using the probesets included in each PBTs as follows: the fold change of each probe set in the PBTs versus the mean value of that probe set in controls (normal kidney samples from nephrectomy). The mean of these fold changes

across all probesets in the PBTs was then used as that biopsy's PBTs score. Calculation of the different PBTs scores is a useful quantitative tool for assessment of the biological events in rejecting biopsies. In our study, the inflammatory burden (T cells and macrophages) was assessed by the T cell transcript burden score and macrophage transcript burden score.

3.14. THE RELATIONSHIP BETWEEN ADAMDEC1, CXCL13, CCL18 AND CCL19 EXPRESSION AND INFLAMMATORY CELL BURDEN

Our laboratory previously identified five relatively specific effector T cell transcripts that are capable of quantifying the T cell transcript burden (TCtb) with minimal concerns about overlap with NK cells (80). Similarly, a set of classical macrophage transcripts and a second set of alternative macrophage transcripts have been described (118) and are capable of quantifying macrophage (classical and alternative macrophages, respectively) transcript burden in renal transplant biopsies. We assessed the relationship between expression of ADAMDEC1, CXCL13, CCL18 and CCL19 and inflammatory cell burden (T cells and macrophages) across all 703 biopsies and across TCMR biopsies (n=67). T cell burden was represented by the T cell transcript burden (TCtb) score, while macrophage burden was represented by both classical macrophages transcript burden (CMACtb) score and alternative macrophage transcript burden (AMACtb) score. Each of the three scores was calculated for each biopsy and its relationship and Spearman correlations to expression of individual transcript were calculated.

Table 3.9 shows the relationship between expression of individual transcripts and T cell (TCtb) and macrophage (CMACtb and AMACtb) burden. Strong associations were observed between TCtb and all four transcripts ($p < 0.0001$). The strongest correlation with TCtb was in relation to expression of ADAMDEC1 ($r = 0.75$), CCL19 ($r = 0.74$) and CXCL13 ($r = 0.73$). However, TCtb correlation with CCL18 expression was moderate ($r = 0.49$) and considerably weaker than the other three transcripts. There was an association between both CMACtb and AMACtb and expression of all four transcripts across all 703 biopsies (Table 3.9). ADAMDEC1 expression was equally correlated to CMACtb and AMACtb ($r = 0.78$, $p < 0.0001$), and these correlations were the strongest among all four

transcripts in relation to CMACtb and AMACtb . Also, the expression of CCL18 , CCL19 and CXL13 correlated with CMACtb (r = 0.62, r=0.60 and r = 0.57, respectively) and to a comparable degree with AMACtb (r = 0.64, r=0.53 and r = 0.56, respectively). Thus there is an association between the expression of ADAMDEC1, CXCL13, CCL18 and CCL19 and the macrophage burden in biopsies with no apparent preference to a particular macrophage activation phenotype (classical and alternative). It is noteworthy that while CXCL13 and CCL19 expression had stronger correlations with TCtb than macrophage burden (both CMACtb and AMACtb), CCL18 showed stronger correlations with macrophage burden (both CMACtb and AMACtb). This is important to be considered while studying the biology and mechanisms of rejection, particularly the events related to migration of inflammatory cells within the inflamed tissue, their positioning during interaction, and the process of matrix remodeling and tissue response to injury. The chemokines CXCL13, CCL18, and CCL19 and the matrix metalloprotease ADAMDEC1 could be potential candidates, particularly that little is known about these molecules and their role in peripheral tissues.

The same analysis was repeated but limited to within TCMR biopsies only (Table 3.10). T cell transcript burden (TCtb) correlated strongly ($p<0.0001$) with the expression of CXCL13 (r = 0.78), and less strongly with ADAMDEC1 (r = 0.60), CCL19 (r = 0.55) and CCL18 (r = 0.50). Both macrophage transcript burden scores strongly correlated with ADAMDEC1 (r = 0.79 and r= 0.74, respectively), and less strongly with CCL18 (r = 0.66 and r = 0.67) and CXCL13 (r = 0.45 and r = 0.36) and CCL19 (r = 0.34, p = 0.0048 and r = 0.32, $p <0.0001$). The correlations between expression of individual transcripts and macrophage transcript burden did not show major variation between the two macrophage phenotypes; classical (CMACtb) and alternative (AMACtb). While CXCL13 and CCL19 correlations were stronger with TCtb than CMACtb or AMACtb, ADAMDEC1 and CCL18 correlations were stronger with macrophage burden (CMACtb and AMACtb) than T cell burden (TCtb). This is similar to the pattern we had across the aforementioned correlations across all 703 biopsies, except that ADAMDEC1 correlations with T cell burden and macrophage burden were comparable across all 703 biopsies, while across

TCMR biopsies the correlation was stronger with macrophage burden than with T cell burden.

3.15. SELECTIVITY OF ADAMDEC1, CXCL13, CCL18 AND CCL19 EXPRESSION FOR TCMR

One final way to demonstrate the associations with TCMR was the calculation of area under the curve (AUC) for selecting TCMR from selected sets of biopsies. AUCs for ADAMDEC1, CXCL13, CCL18 and CCL19 transcripts in discriminating TCMR biopsies from ABMR (Figure 3.4), AKI (Figure 3.5) and non-TCMR biopsies (Figure 3.6) were examined. CCL19 expression showed the smallest AUC (0.73), while CXCL13, ADAMDEC1 and CCL18 all showed higher AUCs; 0.81, 0.87 and 0.88, respectively. AUC's were also calculated for differentiating TCMR from AKI biopsies (Figure 3.4). Among all four transcripts, CXCL13 expression had the best AUC value (0.91), followed by ADAMDEC1 expression with an AUC of 0.88. Using the expression of the other 2 transcripts markedly lowered the AUCs values to 0.79 for CCL19 and 0.78 for CCL18. Similarly, we assessed the AUCs when selecting TCMR from non-TCMR biopsies using the expression of individual transcript (Figure 3.6). The non-TCMR biopsies included all biopsies except biopsies with TCMR, borderline TCMR, mixed TCMR and ABMR, and BK polyoma virus nephropathy. ADAMDEC1 expression had the best AUC value reaching 0.89 for selecting TCMR from non TCMR biopsies, followed by CCL18 (AUC = 0.86) and CXCL13 (AUC = 0.84). However, using CCL19 expression led to an AUC of 0.76, the lowest AUC among all four transcripts.

Thus the best transcripts for selecting TCMR biopsies from ABMR, AKI and non TCMR biopsies were ADAMDEC1 and CXCL13, then CCL18, while CCL19 had the least selectivity for TCMR (compared to the other three transcripts).

3.16. ESTABLISHING REAL-TIME RT-PCR METHOD FOR ASSESSMENT OF ADAMDEC1, CXCL13, CCL18, AND CCL19 EXPRESSION

All of the associations between expression of the four transcripts of interest and parameters related to diagnosis and biopsy findings have thus far been based on gene expression microarray data. However, the subsequent *in vitro* studies would require a less expensive method to assess gene expression. We opted to use TaqMan real-time RT-PCR as this is a method with which our laboratory has extensive experience (96). The primers and probes used were all commercially sourced and their performance thus validated by the vendor. Nonetheless we validated their use before proceeding on to assessing expression in the *in vitro* experiments.

The validation was limited to CXCL13 and ADAMDEC1 as these were the top transcripts associated with TCMR. Due to the limited amount of mRNA available from kidney transplant biopsies, we validated CXCL13 and ADAMDEC1 expression across 78 biopsies that included 11 and 12 biopsies with the diagnosis of TCMR and ABMR, respectively. In agreement with our microarray data, RT-PCR showed equal trends for each transcript showing stronger expression of CXCL13 mRNA ($p = 0.0073$) and ADAMDEC1 mRNA ($p = 0.0006$) in TCMR compared to ABMR biopsies (Figure 3.7).

3.17. TABLES

Table 3.1. Patient demographics and clinical characteristics at time of biopsy

Patient characteristics	**Patients (n = 579)**
Mean recipient age (years)	48 (10 - 86)
Recipient Gender (% male) [n = 579]	375 (65%)
Race [n = 579]	
Caucasian	431 (74%)
Black	45 (8%)
Other	75 (13%)
NA	28 (5%)
Primary disease [n = 579]	
Diabetic nephropathy	95 (16%)
Hypertension / large vessel disease	38 (7%)
Glomerulonephritis / vasculitis	154 (27%)
Interstitial nephritis / pyelonephritis	27 (5%)
Polycystic kidney disease	64 (11%)
Others	40 (7%)
Unknown etiology	161 (28%)
Mean donor age (years)	41 (1 - 75)
Donor gender (% male)	223 (39%)
Donor type (% deceased donor transplants)	314 (54%)
Clinical characteristics at time of biopsy	**Biopsies (n = 703)**
Median and range time from transplant to biopsy (months)	19 (0.25 - 427)
Indication for biopsy	
Primary non-function	11 (2%)
Rapid deterioration of graft function	161 (23%)
Slow deterioration of graft function	216 (31%)
Stable impaired graft function	88 (13%)
Investigate proteinuria	103 (15%)
Follow-up from previous biopsy	20 (3%)
Others	76 (11%)
Indication unknown	28 (4%)
Maintenance immunosuppressive regimens at biopsy	
MMF, tacrolimus, steroid	284 (40%)
MMF, cyclosporine, steroid	126 (18%)
Others	293 (42%)

Table 3.2. Histologic diagnoses for biopsies

Histologic Biopsy Diagnosis	Biopsies (n = 703)
Rejection	
TCMR	67 (10%)
C4d-negative ABMR	80 (11%)
C4d-positive ABMR	30 (4%)
Mixed rejection	28 (4%)
Abnormal	
Transplant glomerulopathy (TG)	27 (4%)
Borderline	89 (13%)
BK polyoma virus nephropathy (BK)	25 (4%)
Glomerulonephritis (GN)	81 (12%)
Interstitial fibrosis and tubular atrophy (IFTA)	72 (10%)
Other	24 (3%)
Relatively normal	
Acute kidney injury (AKI)	64 (9%)
No major abnormalities (NOMOA)	116 (17%)

Table 3.3. The top 50 transcripts in TCMR versus normal kidney control biopsies

Probe Set ID	Gene Symbol	Gene Title	TCMR vs Normal kidney		
			Fold Change	p- value	FDR
211122_s_at	CXCL11	chemokine (C-X-C motif) ligand 11	49.36	9.02E-12	4.42E-09
229390_at	FAM26F	family with sequence similarity 26, member F	31.53	3.36E-14	7.65E-11
203915_at	CXCL9	chemokine (C-X-C motif) ligand 9	28.73	5.97E-15	2.17E-11
204533_at	CXCL10	chemokine (C-X-C motif) ligand 10	23.18	9.41E-14	1.60E-10
205242_at	CXCL13	chemokine (C-X-C motif) ligand 13	22.61	5.92E-06	8.69E-05
206134_at	ADAMDEC1	ADAM-like, decysin 1	18.73	1.34E-09	1.57E-07
202404_s_at	COL1A2	collagen, type I, alpha 2	16.06	1.01E-11	4.66E-09
225681_at	CTHRC1	collagen triple helix repeat containing 1	16.00	3.54E-10	5.69E-08
34210_at	CD52	CD52 molecule	14.77	1.16E-15	5.22E-12
206584_at	LY96	lymphocyte antigen 96	13.51	2.77E-15	1.08E-11
234987_at	SAMHD1	SAM domain and HD domain 1	11.49	6.67E-14	1.35E-10
220330_s_at	SAMSN1	SH3 domain and nuclear localization signals 1	11.48	9.95E-11	2.22E-08
212588_at	PTPRC	protein tyrosine phosphatase, receptor type, C	10.96	1.24E-13	1.83E-10
219014_at	PLAC8	placenta-specific 8	10.55	9.36E-10	1.20E-07
205269_at	LCP2	lymphocyte cytosolic protein 2	10.53	3.95E-13	4.24E-10
1554899_s_at	FCER1G	Fc fragment of IgE, high affinity I, receptor for gamma polypeptide	10.40	4.26E-11	1.23E-08
205488_at	GZMA	granzyme A	10.25	2.66E-12	1.84E-09
204655_at	CCL5	chemokine (C-C motif) ligand 5	10.02	3.18E-12	2.10E-09
202902_s_at	CTSS	cathepsin S	9.91	6.24E-13	5.79E-10
223501_at	TNFSF13B	tumor necrosis factor (ligand) superfamily, member 13b	9.83	5.13E-12	2.95E-09
202953_at	C1QB	complement component 1, q subcomponent, B chain	9.71	2.16E-10	3.98E-08
203741_s_at	ADCY7	adenylate cyclase 7	9.50	6.90E-14	1.35E-10
222838_at	SLAMF7	SLAM family member 7	9.43	1.01E-08	7.18E-07
219607_s_at	MS4A4A	membrane-spanning 4-domains, subfamily A, member 4A	9.43	5.76E-12	3.23E-09
230550_at	MS4A6A	membrane-spanning 4-domains, subfamily A, member 6A	9.38	4.90E-12	2.89E-09
205890_s_at	UBD	ubiquitin D	9.36	4.19E-10	6.51E-08
229560_at	TLR8	toll-like receptor 8	9.18	5.89E-09	4.78E-07
207957_s_at	PRKCB	protein kinase C, beta	9.17	9.44E-11	2.13E-08
223122_s_at	SFRP2	secreted frizzled-related protein 2	9.14	1.53E-04	9.72E-04
201438_at	COL6A3	collagen, type VI, alpha 3	8.96	6.17E-13	5.79E-10
205159_at	CSF2RB	colony stimulating factor 2 receptor, beta, low-affinity	8.91	6.36E-10	8.89E-08
215049_x_at	CD163	CD163 molecule	8.88	3.87E-11	1.14E-08
227346_at	IKZF1	IKAROS family zinc finger 1 (Ikaros)	8.85	2.08E-11	7.63E-09
1559584_a_at	C16orf54	chromosome 16 open reading frame 54	8.85	1.05E-10	2.31E-08
211796_s_at	TRBC1	T cell receptor beta constant 1	8.59	1.72E-09	1.88E-07
203923_s_at	CYBB	cytochrome b-245, beta polypeptide	8.56	5.49E-08	2.61E-06
238581_at	GBP5	guanylate binding protein 5	8.54	7.18E-07	1.81E-05
231577_s_at	GBP1	guanylate binding protein 1, interferon-inducible	8.38	9.19E-11	2.12E-08
201645_at	TNC	tenascin C	8.38	1.14E-13	1.78E-10
202345_s_at	FABP5	fatty acid binding protein 5 (psoriasis-associated)	8.33	3.37E-11	1.04E-08
221872_at	RARRES1	retinoic acid receptor responder 1	8.31	1.75E-11	6.88E-09
210029_at	IDO1	indoleamine 2,3-dioxygenase 1	8.18	3.85E-08	1.97E-06
205681_at	BCL2A1	BCL2-related protein A1	8.08	6.88E-10	9.33E-08
213975_s_at	LYZ	lysozyme	8.00	2.44E-13	3.13E-10
230741_at	unannotated	unannotated	7.96	2.53E-11	8.75E-09
221731_x_at	VCAN	versican	7.72	5.03E-11	1.40E-08
215076_s_at	COL3A1	collagen, type III, alpha 1	7.65	5.68E-12	3.23E-09
204971_at	CSTA	cystatin A (stefin A)	7.65	2.60E-09	2.58E-07
214511_x_at	FCGR1B	Fc fragment of IgG, high affinity Ib, receptor (CD64)	7.62	3.04E-08	1.65E-06
206420_at	IGSF6	immunoglobulin superfamily, member 6	7.53	4.63E-06	7.28E-05

Table 3.4. The top 50 transcripts in TCMR versus ABMR biopsies

Probe Set ID	Gene Symbol	Gene Title	TCMR vs ABMR		
			Fold change	*p*-Value	FDR
205242_at	CXCL13	chemokine (C-X-C motif) ligand 13	8.12	4.52E-16	7.26E-13
206134_at	ADAMDEC1	ADAM-like, decysin 1	7.11	1.72E-23	1.94E-19
32128_at	CCL18	chemokine (C-C motif) ligand 18	4.83	1.04E-20	5.85E-17
206214_at	PLA2G7	phospholipase A2, group VII	2.78	8.72E-20	3.27E-16
202404_s_at	COL1A2	collagen, type I, alpha 2	2.72	6.38E-12	4.95E-10
225681_at	CTHRC1	collagen triple helix repeat containing 1	2.66	1.01E-09	2.81E-08
228592_at	MS4A1	membrane-spanning 4-domains, subfamily A, member 1	2.65	1.16E-07	1.47E-06
209773_s_at	RRM2	ribonucleotide reductase M2	2.65	2.87E-15	1.79E-12
203645_s_at	CD163	CD163 molecule	2.56	1.24E-13	3.41E-11
204416_x_at	APOC1	apolipoprotein C-I	2.56	5.31E-15	2.71E-12
201292_at	TOP2A	topoisomerase (DNA) II alpha 170kDa	2.52	2.50E-15	1.76E-12
229560_at	TLR8	toll-like receptor 8	2.50	2.07E-11	1.21E-09
212827_at	IGHM	immunoglobulin heavy constant mu	2.49	3.14E-10	1.08E-08
206420_at	IGSF6	immunoglobulin superfamily, member 6	2.44	1.80E-07	2.16E-06
205569_at	LAMP3	lysosomal-associated membrane protein 3	2.43	5.60E-14	1.97E-11
205758_at	CD8A	CD8a molecule	2.41	3.10E-12	3.06E-10
236341_at	CTLA4	cytotoxic T-lymphocyte-associated protein 4	2.41	2.18E-16	4.89E-13
206337_at	CCR7	chemokine (C-C motif) receptor 7	2.40	1.56E-13	3.89E-11
211796_s_at	TRBC1	T cell receptor beta constant 1	2.40	1.19E-10	4.66E-09
214511_x_at	FCGR1B	Fc fragment of IgG, high affinity Ib, receptor (CD64)	2.37	2.07E-11	1.21E-09
229390_at	FAM26F	family with sequence similarity 26, member F	2.37	9.47E-09	1.75E-07
204563_at	SELL	selectin L	2.36	9.71E-13	1.40E-10
34210_at	CD52	CD52 molecule	2.36	2.42E-12	2.52E-10
211339_s_at	ITK	IL2-inducible T-cell kinase	2.36	4.27E-11	2.17E-09
229437_at	MIR155/MIR155HG	microRNA 155/MIR155 host gene	2.35	3.22E-12	3.13E-10
202953_at	C1QB	complement component 1, q subcomponent, B chain	2.35	1.58E-11	1.00E-09
238581_at	GBP5	guanylate binding protein 5	2.33	3.72E-08	5.61E-07
202503_s_at	KIAA0101/ PCLAF	KIAA0101/ PCNA clamp associated factor	2.33	7.09E-13	1.12E-10
216950_s_at	FCGR1A/1B/1C	Fc fragment of IgG, high affinity Ia/ Ib/Ic, receptor (CD64)	2.31	3.34E-12	3.18E-10
220485_s_at	SIRPG	signal-regulatory protein gamma	2.30	5.32E-16	7.48E-13
203936_s_at	MMP9	matrix metallopeptidase 9	2.29	2.11E-12	2.27E-10
206545_at	CD28	CD28 molecule	2.29	1.07E-13	3.17E-11
205831_at	CD2	CD2 molecule	2.27	2.96E-12	2.98E-10
242943_at	ST8SIA4	ST8 alpha-N-acetyl-neuraminide alpha-2,8-sialyltransferase 4	2.27	6.67E-13	1.07E-10
202917_s_at	S100A8	S100 calcium binding protein A8	2.25	1.11E-08	2.00E-07
223502_s_at	TNFSF13B	tumor necrosis factor (ligand) superfamily, member 13b	2.24	5.08E-13	9.19E-11
1556499_s_at	COL1A1	collagen, type I, alpha 1	2.21	3.18E-12	3.11E-10
206666_at	GZMK	granzyme K (granzyme 3; tryptase II)	2.21	9.24E-11	3.86E-09
219607_s_at	MS4A4A	membrane-spanning 4-domains, subfamily A, member 4A	2.21	2.76E-10	9.64E-09
209795_at	CD69	CD69 molecule	2.19	3.76E-10	1.26E-08
236226_at	BTLA	B and T lymphocyte associated	2.18	2.29E-14	9.54E-12
206632_s_at	APOBEC3B	apolipoprotein B mRNA editing enzyme, catalytic polypeptide-like 3B	2.18	1.48E-11	9.52E-10
226311_at	ADAMTS2	ADAM metallopeptidase with thrombospondin type 1 motif, 2	2.18	5.27E-15	2.71E-12
210072_at	CCL19	chemokine (C-C motif) ligand 19	2.18	4.72E-07	5.01E-06
209969_s_at	STAT1	signal transducer and activator of transcription 1	2.18	2.19E-11	1.27E-09
225353_s_at	C1QC	complement component 1, q subcomponent, C chain	2.17	1.02E-10	4.12E-09
201438_at	COL6A3	collagen, type VI, alpha 3	2.17	1.20E-12	1.63E-10
229543_at	unannotated	unannotated	2.17	3.08E-07	3.44E-06
219918_s_at	ASPM	asp (abnormal spindle) homolog, microcephaly associated	2.16	1.61E-12	1.93E-10
230391_at	CD84	CD84 molecule	2.16	2.83E-16	5.30E-13

Table 3.5. The top 50 transcripts preferentially increased in TCMR versus ABMR compared in TCMR versus AKI and non TCMR biopsies

Probe Set ID	Gene Symbol	TCMR vs AKI			TCMR vs non TCMR		
		Fold Change	p-value	FDR	Fold Change	p-value	FDR
205242_at	CXCL13	16.80	9.44E-22	5.44E-20	10.02	3.72E-36	2.99E-34
206134_at	ADAMDEC1	7.74	1.87E-20	6.36E-19	8.02	0.00E+00	0.00E+00
32128_at	CCL18	3.40	1.79E-09	6.28E-09	4.32	1.34E-31	3.64E-30
206214_at	PLA2G7	2.05	1.45E-06	3.28E-06	2.88	2.53E-31	6.37E-30
202404_s_at	COL1A2	1.11	5.48E-01	5.69E-01	2.25	1.76E-08	3.32E-08
225681_at	CTHRC1	2.07	6.85E-04	1.03E-03	2.72	1.06E-10	2.52E-10
228592_at	MS4A1	6.50	8.88E-17	1.05E-15	3.66	2.46E-15	8.69E-15
209773_s_at	RRM2	1.31	6.05E-02	6.99E-02	2.84	1.47E-30	3.33E-29
203645_s_at	CD163	2.67	1.70E-10	7.09E-10	3.27	4.32E-29	7.65E-28
204416_x_at	APOC1	2.48	2.97E-10	1.19E-09	2.94	1.99E-29	3.72E-28
201292_at	TOP2A	1.48	9.25E-03	1.19E-02	2.74	1.08E-31	3.03E-30
229560_at	TLR8	4.54	8.77E-17	1.04E-15	3.99	1.01E-32	3.56E-31
212827_at	IGHM	3.76	1.83E-14	1.40E-13	2.88	3.38E-21	1.93E-20
206420_at	IGSF6	3.40	1.62E-09	5.71E-09	3.11	6.53E-18	2.86E-17
205569_at	LAMP3	3.51	5.05E-17	6.44E-16	2.98	3.63E-30	7.82E-29
205758_at	CD8A	4.78	8.04E-24	1.39E-21	3.66	5.66E-37	6.02E-35
236341_at	CTLA4	3.08	3.69E-19	8.21E-18	2.77	0.00E+00	0.00E+00
206337_at	CCR7	3.12	8.24E-15	6.69E-14	2.79	2.42E-28	3.43E-27
211796_s_at	TRBC1	6.96	2.87E-24	8.60E-22	3.97	3.79E-27	4.37E-26
214511_x_at	FCGR1B	3.60	3.99E-16	4.16E-15	3.62	1.31E-37	1.55E-35
229390_at	FAM26F	7.50	1.28E-20	4.58E-19	5.17	4.21E-30	9.52E-29
204563_at	SELL	4.14	1.49E-17	2.25E-16	3.08	1.17E-27	1.51E-26
34210_at	CD52	5.15	1.71E-17	2.51E-16	3.87	2.42E-25	2.21E-24
211339_s_at	ITK	5.51	7.55E-24	1.38E-21	3.62	1.38E-31	3.73E-30
229437_at	MIR155/MIR155HG	4.06	1.20E-22	1.04E-20	3.45	8.79E-37	9.06E-35
202953_at	C1QB	3.53	2.96E-15	2.60E-14	3.74	1.70E-33	7.38E-32
238581_at	GBP5	6.56	2.64E-22	1.85E-20	4.54	2.97E-36	2.64E-34
202503_s_at	KIAA0101/ PCLAF	1.34	3.07E-02	3.70E-02	2.60	3.64E-25	3.21E-24
216950_s_at	FCGR1A/FCGR1B/FCGR1C	3.10	1.65E-15	1.53E-14	3.25	1.18E-39	2.43E-37
220485_s_at	SIRPG	2.77	2.25E-16	2.46E-15	2.71	2.80E-45	1.32E-42
203936_s_at	MMP9	1.39	5.52E-02	6.43E-02	2.11	2.33E-13	6.95E-13
206545_at	CD28	2.68	6.03E-14	4.24E-13	2.45	1.19E-35	8.70E-34
205831_at	CD2	4.79	2.34E-22	1.67E-20	3.38	1.47E-31	3.93E-30
242943_at	ST8SIA4	3.31	5.90E-18	9.97E-17	2.93	7.61E-35	4.92E-33
202917_s_at	S100A8	1.64	3.16E-03	4.34E-03	2.53	3.68E-15	1.28E-14
223502_s_at	TNFSF13B	3.99	2.65E-20	8.62E-19	3.38	4.09E-34	2.17E-32
1556499_s_at	COL1A1	1.05	7.27E-01	7.42E-01	1.97	4.01E-09	8.16E-09
206666_at	GZMK	4.72	7.72E-22	4.62E-20	3.36	1.24E-28	1.93E-27
219607_s_at	MS4A4A	2.88	3.30E-11	1.54E-10	2.88	9.26E-22	5.57E-21
209795_at	CD69	5.48	4.67E-24	1.07E-21	3.53	1.91E-28	2.82E-27
236226_at	BTLA	2.64	9.38E-15	7.55E-14	2.46	2.56E-43	8.45E-41
206632_s_at	APOBEC3B	1.47	3.85E-03	5.23E-03	2.41	9.25E-24	6.93E-23
226311_at	ADAMTS2	1.26	5.25E-02	6.14E-02	2.03	4.80E-15	1.65E-14
210072_at	CCL19	3.74	5.80E-11	2.59E-10	2.82	9.67E-14	3.00E-13
209969_s_at	STAT1	3.63	1.51E-17	2.27E-16	3.22	3.03E-32	9.24E-31
225353_s_at	C1QC	3.06	1.21E-13	8.14E-13	3.14	5.56E-29	9.50E-28
201438_at	COL6A3	1.39	1.02E-02	1.30E-02	2.04	3.53E-11	8.76E-11
229543_at	unannotated	4.47	1.23E-16	1.42E-15	3.51	1.01E-31	2.84E-30
219918_s_at	ASPM	1.51	5.50E-03	7.31E-03	2.34	3.61E-27	4.20E-26
230391_at	CD84	2.96	2.78E-17	3.74E-16	2.75	3.40E-34	1.84E-32

Table 3.6. Chemokines and chemokine receptors increased in TCMR versus ABMR biopsies

Chemokines					
Probe Set ID	**Symbol**	**Gene Title**	**Fold change**	***p*-Value**	**FDR**
205242_at	CXCL13	chemokine (C-X-C motif) ligand 13	8.12	4.52E-16	7.26E-13
32128_at	CCL18	chemokine (C-C motif) ligand 18	4.83	1.04E-20	5.85E-17
210072_at	CCL19	chemokine (C-C motif) ligand 19	2.18	4.72E-07	5.01E-06
204655_at	CCL5	chemokine (C-C motif) ligand 5	2.16	7.88E-10	2.27E-08
203915_at	CXCL9	chemokine (C-X-C motif) ligand 9	2.11	1.29E-07	1.63E-06
211122_s_at	CXCL11	chemokine (C-X-C motif) ligand 11	1.85	1.45E-03	5.52E-03
204533_at	CXCL10	chemokine (C-X-C motif) ligand 10	1.78	2.89E-05	1.87E-04
214567_s_at	XCL1/XCL2	chemokine (C motif) ligand 1/ chemokine (C motif) ligand 2	1.59	1.45E-05	1.02E-04
206407_s_at	CCL13	chemokine (C-C motif) ligand 13	1.36	5.71E-06	4.47E-05
204103_at	CCL4	chemokine (C-C motif) ligand 4	1.34	1.15E-02	3.14E-02
210133_at	CCL11	chemokine (C-C motif) ligand 11	1.31	1.42E-03	5.44E-03
223454_at	CXCL16	chemokine (C-X-C motif) ligand 16	1.26	1.26E-04	6.67E-04
Chemokine receptors					
Probe Set ID	**Symbol**	**Gene Title**	**Fold change**	***p*-Value**	**FDR**
206337_at	CCR7	chemokine (C-C motif) receptor 7	2.40	1.56E-13	3.89E-11
217028_at	CXCR4	chemokine (C-X-C motif) receptor 4	2.10	5.75E-09	1.14E-07
206991_s_at	CCR5	chemokine (C-C motif) receptor 5	1.94	1.06E-11	7.15E-10
206978_at	CCR2	chemokine (C-C motif) receptor 2	1.70	5.36E-06	4.26E-05
206974_at	CXCR6	chemokine (C-X-C motif) receptor 6	1.70	5.55E-11	2.60E-09
205098_at	CCR1	chemokine (C-C motif) receptor 1	1.63	2.07E-08	3.37E-07
220351_at	CCRL1	chemokine (C-C motif) receptor-like 1	1.46	5.00E-06	3.99E-05
206983_at	CCR6	chemokine (C-C motif) receptor 6	1.40	1.54E-05	1.08E-04

Table 3.7. Metalloproteases increased in TCMR versus ABMR biopsies

Probe Set ID	Symbol	Gene Title	TCMR vs ABMR		
			Fold change	*p*-Value	FDR
206134_at	ADAMDEC1	ADAM-like, decysin 1	7.11	1.72E-23	1.94E-19
203936_s_at	MMP9	matrix metallopeptidase 9	2.29	2.11E-12	2.27E-10
226311_at	ADAMTS2	ADAM metallopeptidase with thrombospondin type 1 motif, 2	2.18	5.27E-15	2.71E-12
226777_at	ADAM12/ ADAM12-OT1	ADAM metallopeptidase domain 12/ ADAM12 overlapping transcript 1	2.02	2.98E-08	4.65E-07
202952_s_at	ADAM12	ADAM metallopeptidase domain 12	1.57	1.20E-07	1.52E-06
201666_at	TIMP1	TIMP metallopeptidase inhibitor 1	1.47	4.81E-06	3.85E-05
209765_at	ADAM19	ADAM metallopeptidase domain 19	1.40	1.11E-09	3.02E-08
203167_at	TIMP2	TIMP metallopeptidase inhibitor 2	1.31	1.09E-06	1.06E-05
205180_s_at	ADAM8	ADAM metallopeptidase domain 8	1.28	3.34E-08	5.13E-07
214913_at	ADAMTS3	ADAM metallopeptidase with thrombospondin type 1 motif, 3	1.26	4.96E-03	1.56E-02
226997_at	ADAMTS12	ADAM metallopeptidase with thrombospondin type 1 motif, 12	1.22	1.04E-04	5.68E-04
205997_at	ADAM28	ADAM metallopeptidase domain 28	1.20	6.90E-03	2.05E-02
213532_at	ADAM17	ADAM metallopeptidase domain 17	1.16	1.11E-03	4.38E-03

Table 3.8. Relationship between ADAMDEC1, CXCL13, CCL18 and CCL19 expression and histologic lesions across all 703 biopsies

Histologic lesions		ADAMDEC1		CXCL13		CCL18		CCL19	
		Spearman r	p value	Spearman r	p value	Spearman r	p value	Spearman r	p value
TCMR lesions	Interstitial inflammation (i)	**0.45**	< 0.0001	**0.40**	< 0.0001	**0.33**	< 0.0001	**0.31**	< 0.0001
	Tubulitis (t)	**0.43**	< 0.0001	**0.40**	< 0.0001	**0.31**	< 0.0001	**0.28**	< 0.0001
TCMR and ABMR lesions	Intimal arteritis (v)	**0.25**	< 0.0001	**0.20**	< 0.0001	**0.21**	< 0.0001	**0.19**	< 0.0001
ABMR lesions	Peritubular capillaritis (ptc)	**0.16**	< 0.0001	**0.15**	0.0001	0.04	0.3227	**0.11**	0.0038
	Glomerulitis (g)	0.03	0.4238	0.02	0.5486	-0.07	0.0504	0.07	0.0602
	Glomerular double contours (cg)	**-0.10**	0.008	**-0.09**	0.0169	**-0.17**	< 0.0001	0.05	0.2111
Atrophy-scarring lesions	Interstitial fibrosis (ci)	**0.12**	0.002	**0.16**	< 0.0001	-0.01	0.7275	**0.22**	< 0.0001
	Tubular atrophy (ct)	**0.13**	0.0005	**0.17**	< 0.0001	0.01	0.8382	**0.23**	< 0.0001
	Arterial fibrous intimal thickening (cv)	-0.07	0.0741	-0.02	0.6496	-0.03	0.4860	0.07	0.0643
	Arteriolar hyalinosis (ah)	**-0.17**	< 0.0001	**-0.15**	0.0001	**-0.17**	< 0.0001	0.01	0.7833

The relationship between individual transcript expression (microarrays) and histologic lesions was assessed across all 703 biopsies by Spearman r correlation coefficient. Significant $p < 0.05$ are bolded.

Table 3.9. Relationship between ADAMDEC1, CXCL13, CCL18 and CCL19 expression and T cell transcript burden and macrophage transcript burden across all 703 biopsies

Kidney transplant biopsies (n=703)						
GENE SYMBOL	**TCtb***		**CMACtb***		**AMACtb***	
	Spearman r	p value	Spearman r	p value	Spearman r	p value
ADAMDEC1	**0.75**	< 0.0001	**0.78**	< 0.0001	**0.78**	< 0.0001
CXCL13	**0.73**	< 0.0001	**0.57**	< 0.0001	**0.56**	< 0.0001
CCL18	**0.49**	< 0.0001	**0.62**	< 0.0001	**0.64**	< 0.0001
CCL19	**0.74**	< 0.0001	**0.60**	< 0.0001	**0.53**	< 0.0001

The relationship between individual transcript expression and inflammatory burden (TCtb, CMACtb and AMACtb) was assessed across all 703 biopsies by Spearman r correlation coefficient. Significant $p < 0.05$ are bolded. TCtb; T cell transcript burden, CMACtb; classical macrophage transcript burden, AMACtb; alternative macrophage transcript burden.* ADAMDEC1, CXCL13, CCL18 and CCL19 transcripts are not included in TCtb, CMACtb and AMACtb scores

Table 3.10. Relationship between ADAMDEC1, CXCL13, CCL18 and CCL19 expression and T cell transcript burden and macrophage transcript burden in TCMR biopsies

T cell mediated rejection biopsies (n=67)						
GENE SYMBOL	**TCtb***		**CMACtb***		**AMACtb***	
	Spearman r	*p* value	Spearman r	*p* value	Spearman r	*p* value
ADAMDEC1	**0.60**	< 0.0001	**0.79**	< 0.0001	**0.74**	< 0.0001
CXCL13	**0.78**	< 0.0001	**0.45**	< 0.0001	**0.36**	< 0.0001
CCL18	**0.50**	< 0.0001	**0.66**	< 0.0001	**0.67**	< 0.0001
CCL19	**0.55**	< 0.0001	**0.34**	0.0048	**0.31**	< 0.0001

The relationship between individual transcript expression and inflammatory burden (TCtb, CMACtb and AMACtb) was assessed across TCMR biopsies (n=67) by Spearman correlation coefficient. Significant $p < 0.05$ are bolded. TCtb; T cell transcript burden, CMACtb; classical macrophage transcript burden, , AMACtb; alternative macrophage transcript burden.

3.18. FIGURES

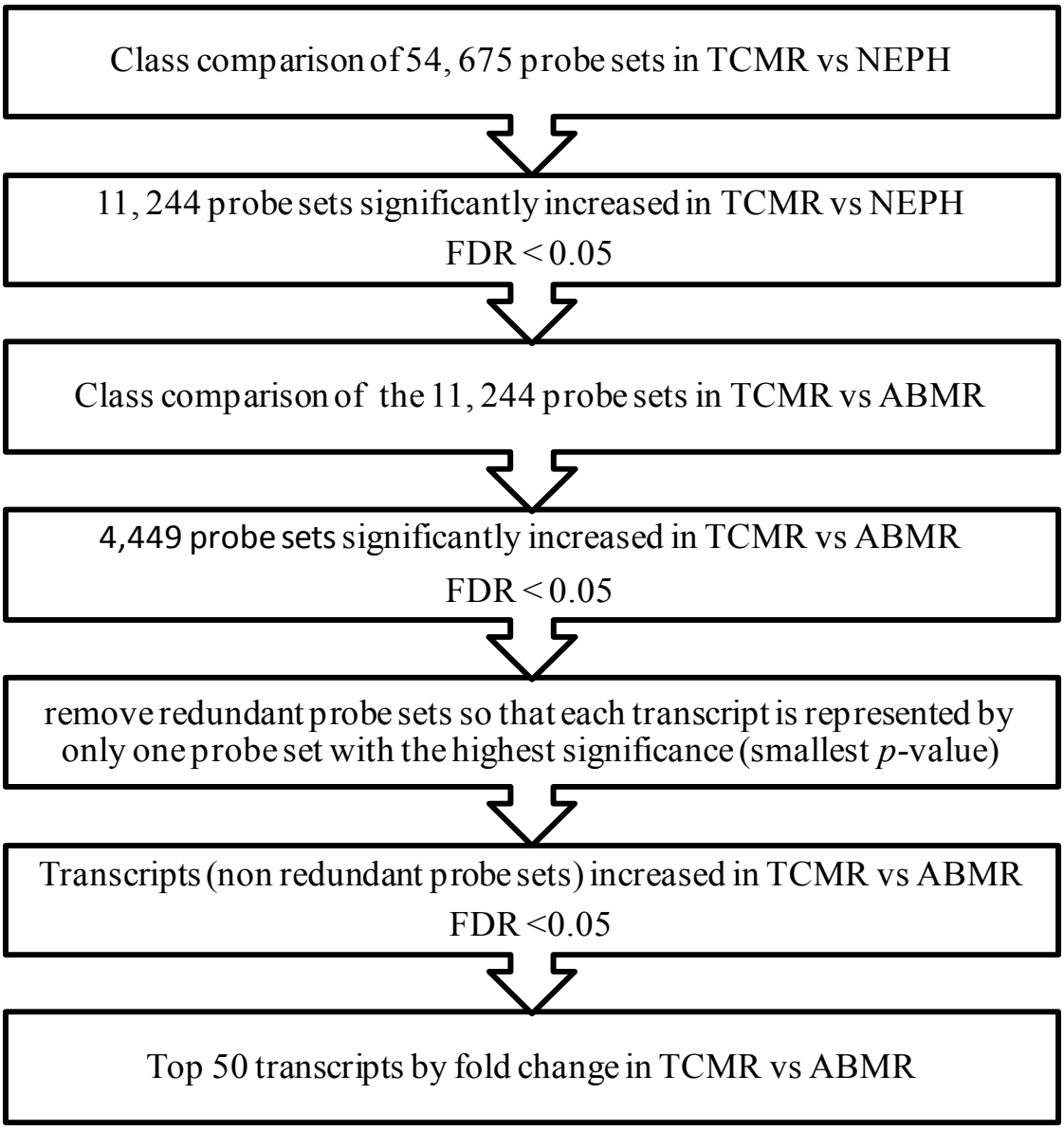

Figure 3.1. Algorithm for defining the top transcripts preferentially increased in TCMR versus ABMR biopsies

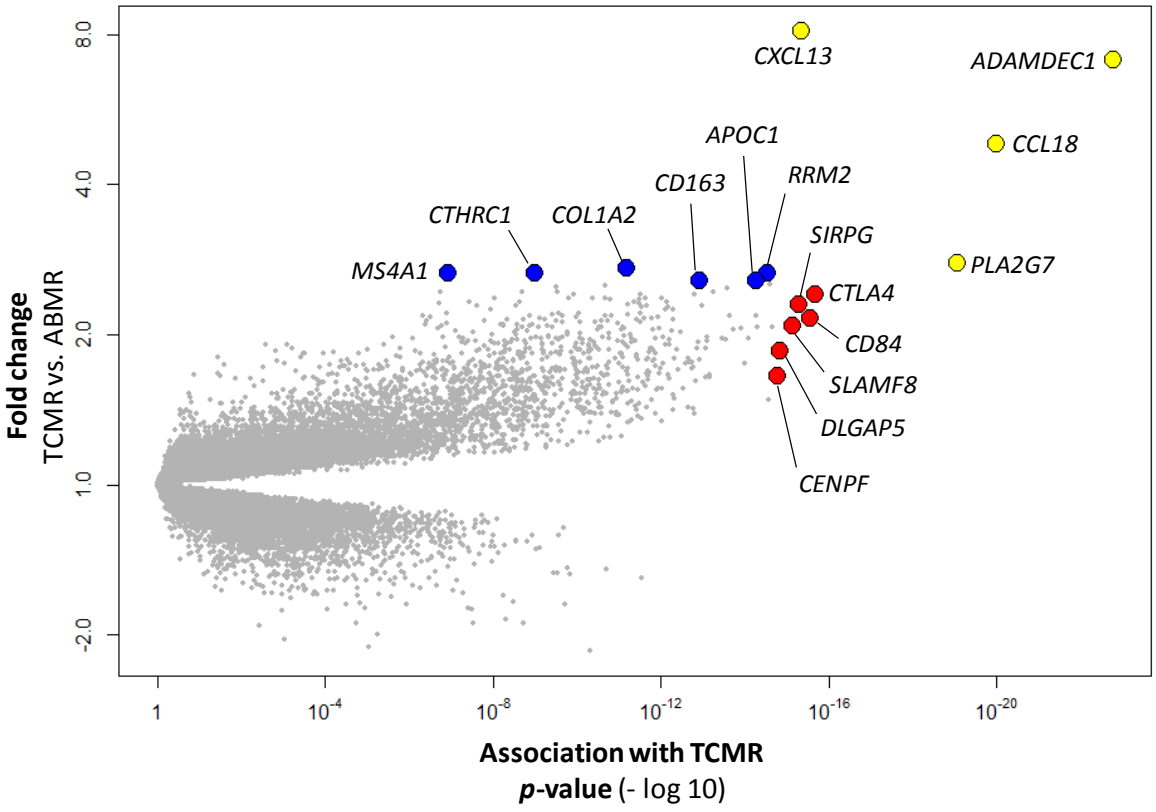

Figure 3.2. TCMR association with the top transcripts preferentially increased in TCMR versus ABMR biopsies. Dots represent individual probe sets. The x-axis represents p-value (-log 10) for the association of individual transcript with TCMR, with fold change on the y-axis for TCMR versus ABMR across 703 kidney transplant biopsies. The top 10 probe sets with the highest association with TCMR (p-value), are represented by red dots, the top 10 probe sets with the highest fold change increase in TCMR versus ABMR are represented by blue dots, and the overlapping probe sets with both the highest association and highest fold change in TCMR versus ABMR are represented by yellow dots.

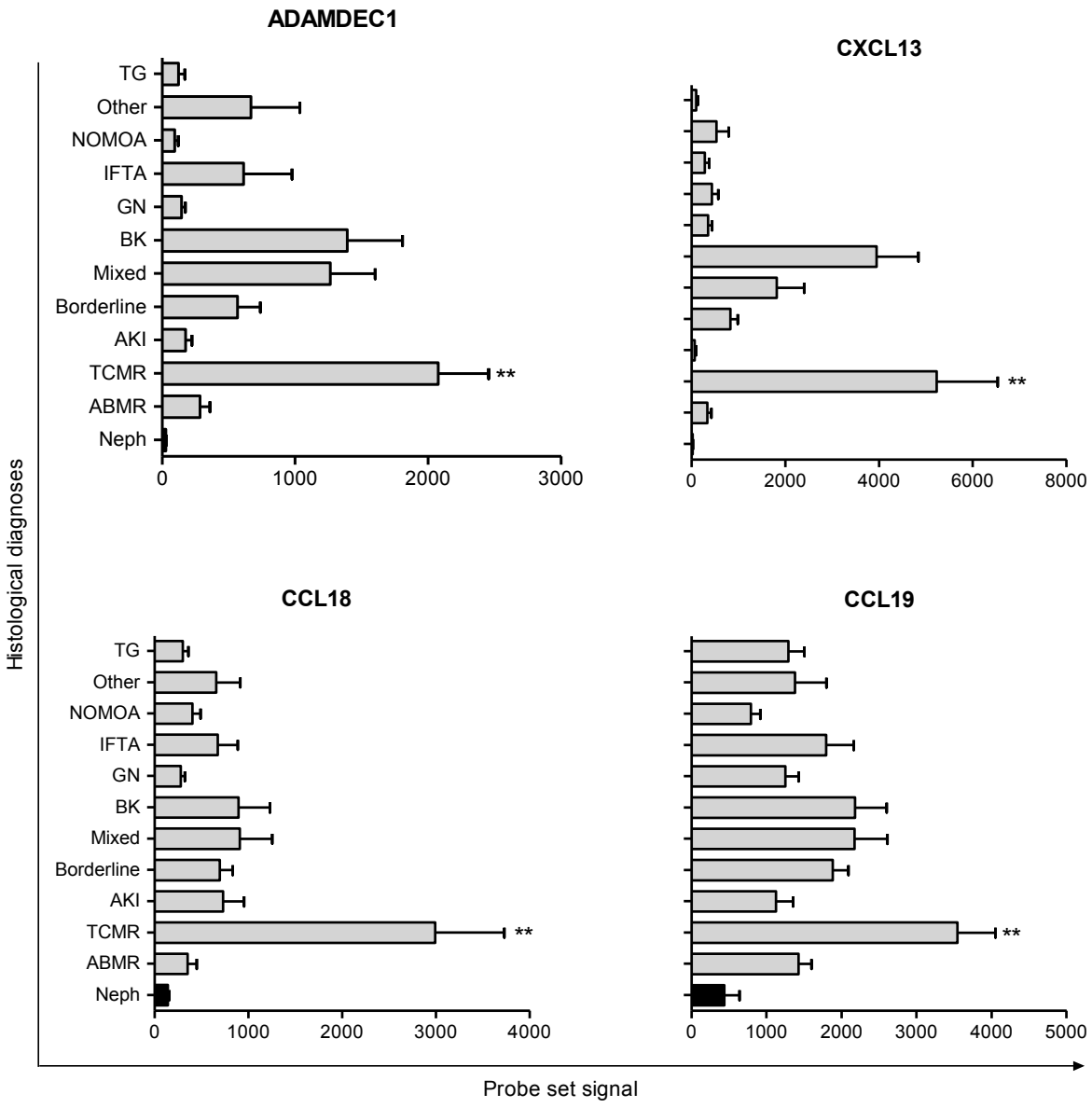

Figure 3.3. ADAMDEC1, CXCL13, CCL18 and CCL19 expression across 703 kidney transplant biopsies (microarrays). Neph; nephrectomies (n=8), ABMR; antibody-mediated rejection (n=110), TCMR; T cell-mediated rejection (n=67), AKI; acute kidney injury (n=64), Borderline (n=89), Mixed; mixed TCMR and ABMR (n=28), BK; polyoma virus nephropathy (n=25), GN; glomerulonephritis (n=81), IFTA; interstitial fibrosis and tubular atrophy (n=72), NOMOA; no major molecular abnormalities (n=116), Other (n=24), TG; transplant glomerulopathy (n=27). Probe set signals (mean ± SE) in each histological diagnosis were compared to normal kidney control samples (nephrectomies) using One-way ANOVA with Dunnett's Multiple Comparison Test. **$p<0.01$.

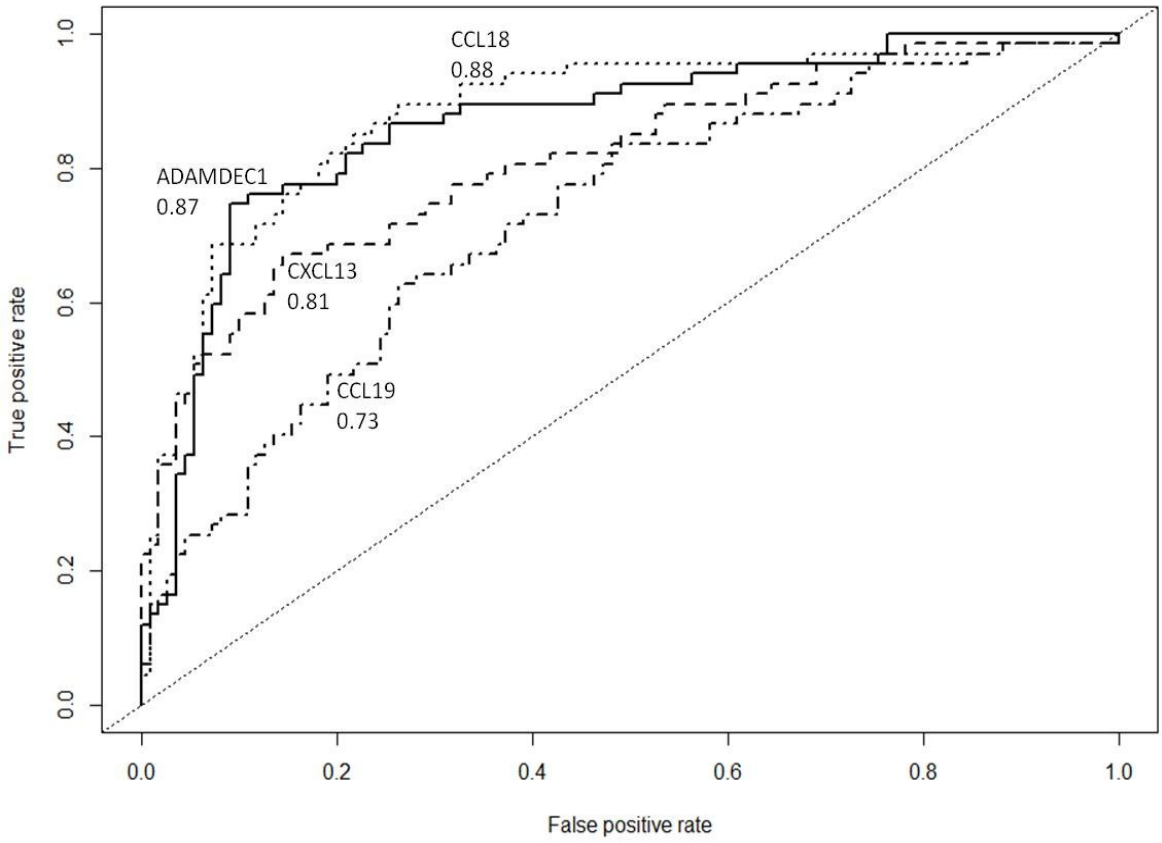

Figure 3.4. ROC curves of ADAMDEC1, CXCL13, CCL18 and CCL19 in TCMR versus ABMR biopsies. Area under the curve (AUC) is indicated for each transcript.

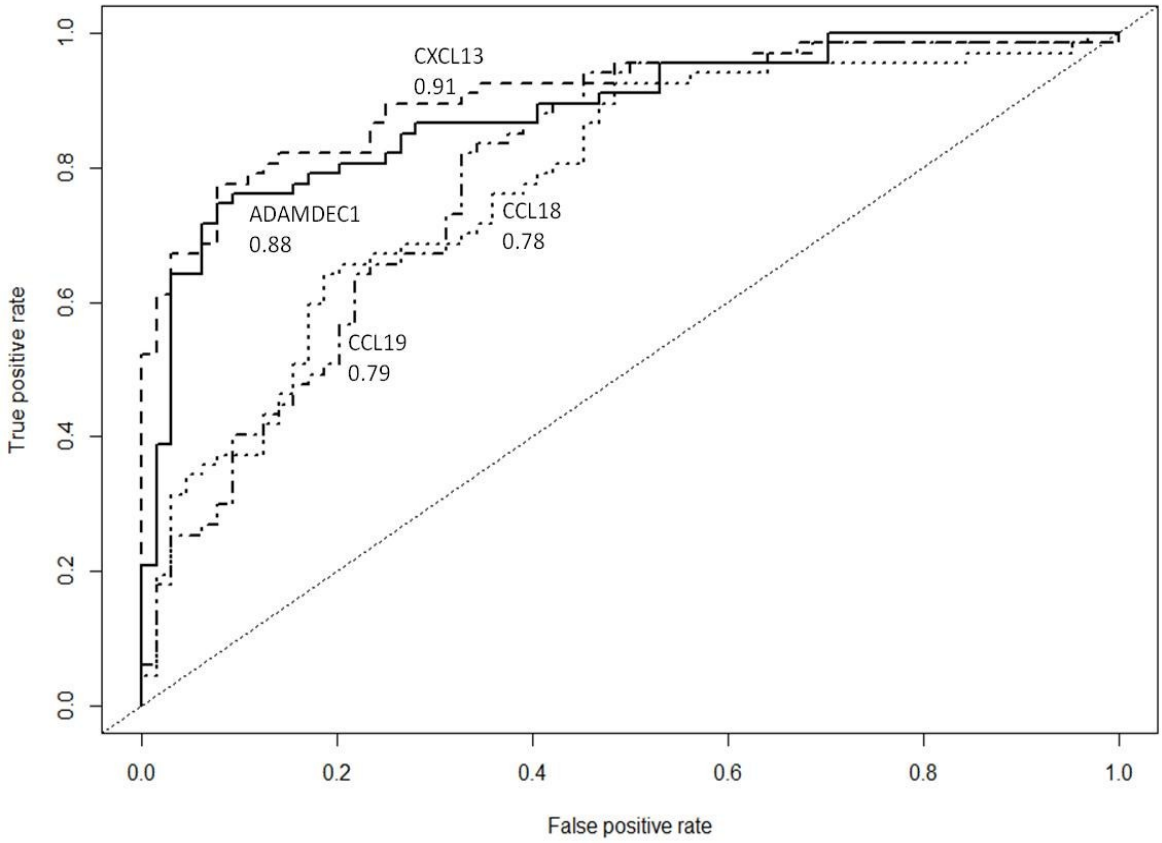

Figure 3.5. ROC curves of ADAMDEC1, CXCL13, CCL18 and CCL19 in TCMR versus AKI biopsies. Area under the curve (AUC) is indicated for each transcript.

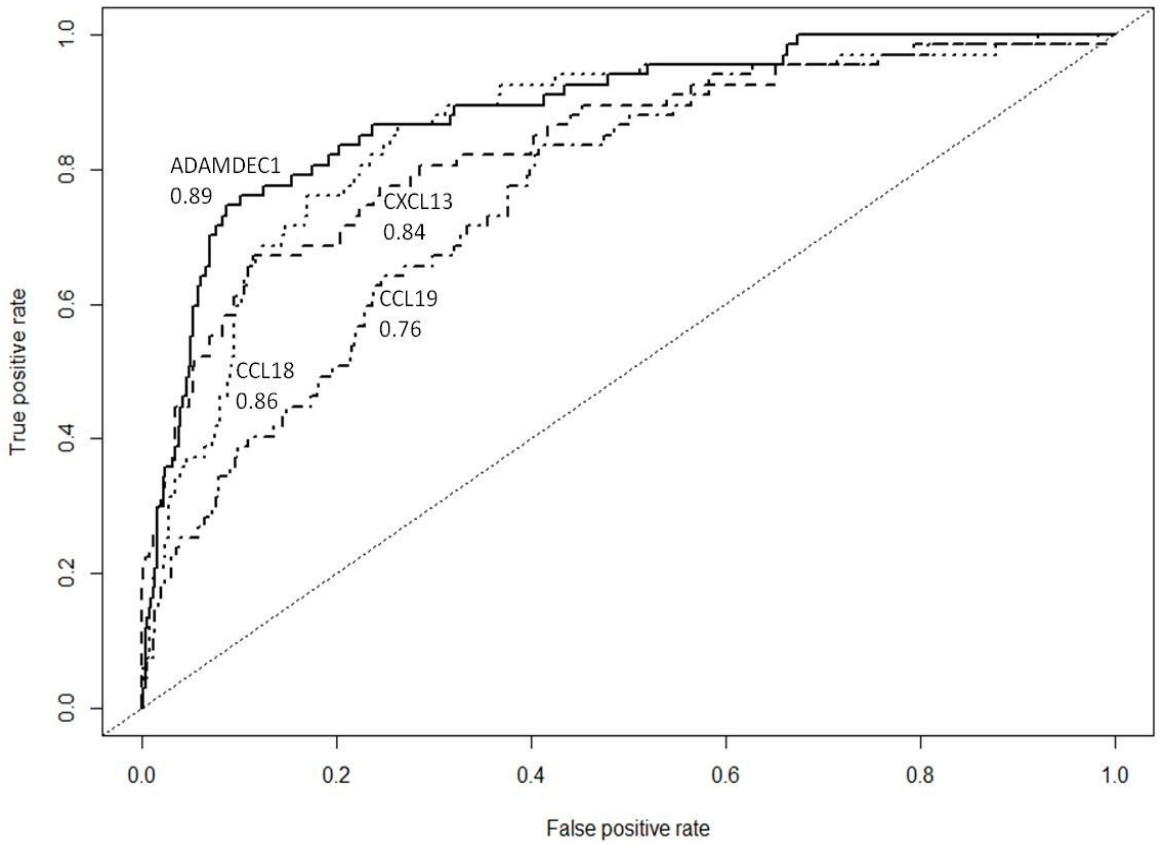

Figure 3.6. ROC curves of ADAMDEC1, CXCL13, CCL18 and CCL19 in TCMR versus non TCMR biopsies. Area under the curve (AUC) is indicated for each transcript.

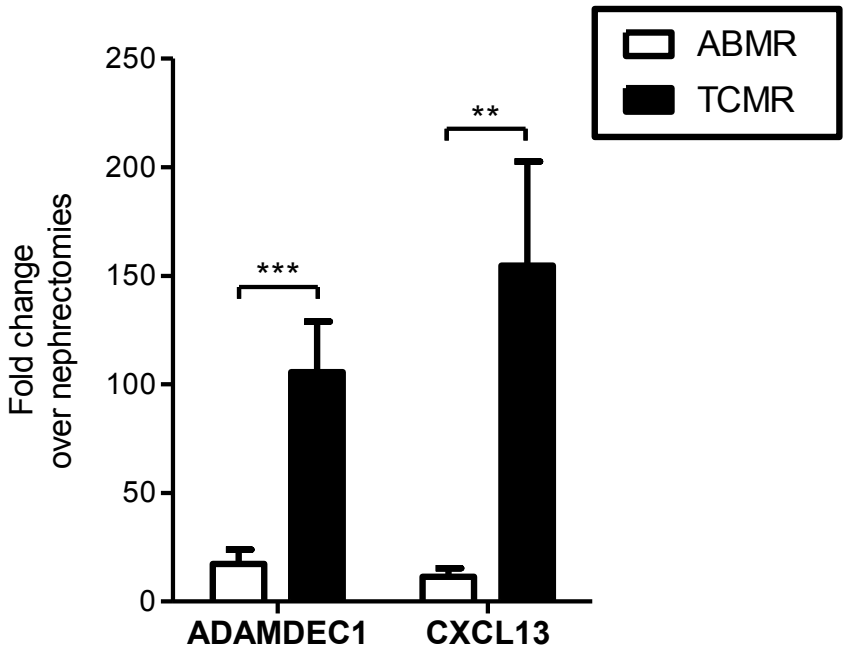

Figure 3.7. ADAMDEC1 and CXCL13 expression in TCMR versus ABMR biopsies (RT-PCR). ADAMDEC1 and CXCL13 mRNA levels were expressed as fold change (mean ± SE) over normal kidney control samples (nephrectomies), and were compared in TCMR (n=11) versus ABMR (n=12) using unpaired t test , ** p = 0.0073, *** p = 0.0006

CHAPTER 4

CHARACTERIZATION OF ADAMDEC1, CXCL13, CCL18 AND CCL19 EXPRESSION IN HUMAN MMDC

CHARACTERIZATION OF ADAMDEC1, CXCL13, CCL18 AND CCL19 EXPRESSION IN HUMAN MMDC

4.1. OVERVIEW

During rejection, cognate interactions between the infiltrating effector T cells and antigen presenting cells within the graft may trigger the release of soluble factors (such as cytokines, enzymes, and reactive oxygen and nitrogen oxide species). The reaction between effector T cells and APC is bidirectional, therefore both types of cells may contribute to the production of these mediators and their release into the inflamed graft (36;37). Meanwhile, either cell population (effector T cells or APCs) could also be a target population responding to the action of soluble factors produced by the other interacting cell population. These interactions between effector T cells and APCs in inflamed grafts could be indirect (contact-independent) interactions or direct (contact-dependent) interactions. The contact-independent interactions do not require direct cell-cell contact but are mediated indirectly through the release of soluble mediators that exert their actions on all reactive cells in the vicinity. In contrast, the contact dependent interactions require direct cell-cell contact between effector T cells and APCs, and are mediated through wide range of receptor/ligand interactions expressed on the surface of interacting cells.

We hypothesized that the expression of ADAMDEC1, CXCL13, CCL18 and CCL19 (the transcripts preferentially increased in TCMR versus ABMR) is regulated during the cognate effector T cell: macrophage interaction including both contact-independent and/or contact dependent interactions. We tested our hypothesis using in vitro experiments that first examined human monocytic cell lines, then primary macrophages and T cells isolated from whole blood of healthy volunteers.

4.2. THP-1 MONOCYTIC CELL LINE AS IN VITRO MODEL TO STUDY ADAMDEC1 AND CXCL13

THP-1 cells (myeloid cell line) (119) are one of the most commonly used cell lines to study human monocytes and macrophages. We examined THP-1 as a suitable primary monocyte substitute because of the difficulty involved with primary monocytes from healthy volunteers based on previous experience in our laboratory. However, the degree to which THP-1 cells mimic monocytes and macrophages is unclear, particularly that this cell line (THP-1) is derived from the blood of acute monocytic leukemia patient. Previous studies reported that macrophage characteristics vary with different protocols used to induce macrophage differentiation in THP-1 cells (120;121). Also the transcripts that we focus on in our study may be affected by treatment used to induce THP-1 differentiation into macrophages. Indeed, Vitamin D3, used in induction of macrophage differentiation in monocytic cell lines, stimulates expression of ADAMDEC1 (122). Therefore we examined the possibility of using THP-1 cells as surrogates for primary monocytes/macrophages without treatments, such as 1, 25-dihydroxyvitamin D3 and Phorbol-12-myristate-13-acetate (PMA), that would likely alter transcript expression and thus affect interpretation of our *in vitro* data.

Our approach was justified by a previous study by others in our laboratory in which THP-1 cells without PMA treatment were used to mimic primary macrophages in cell culture experiments. In a pilot experiment, both THP-1 cells (without PMA) and monocyte derived macrophages were examined for their ability to induce T cell activation. Both primary macrophages and THP-1 cells induced comparable T cell proliferation and cytokine secretion. Therefore we explored the possibility of using THP-1 cells (without PMA) as an alternative/surrogate to monocyte-derived macrophages in our *in vitro* culture model. For that purpose, THP-1 cells were maintained in polystyrene tissue culture flasks in complete RPMI-10 medium where they remain as a suspension cell. Cells were harvested by centrifugation and were resuspended in fresh medium. Then the cells were used for the following experiments to examine expression of ADAMDEC1 and CXCL13 in THP-1 cell line compared to primary macrophages. We also examined the effect of different stimuli on

expression of ADAMDEC1 and CXCL13 in THP-1 cells. Since this was only an exploratory set of experiments, the analyses were limited to ADAMDEC1 and CXCL13.

a) ADAMDEC1 and CXCL13 expression in THP-1 cells versus primary monocytes

$CD14^+$ primary human monocytes were purified from PBMCs of healthy donors using Ficoll centrifugation followed by positive selection using immunomagnetic beads. Freshly isolated monocytes and THP-1 cells were separately suspended in complete RPMI-10 medium and cultured in six-well plate. After 24 hours incubation, macrophages (24h incubated monocytes) and THP-1 cells were harvested for total RNA extraction and RT-PCR. ADAMDEC1 and CXCL13 mRNA levels in 24 hours incubated THP-1 cells and primary macrophages are shown in Figure 4.1. By RT-PCR, 24 hours incubated THP-1 cells expressed markedly low levels of ADAMDEC1 ($p < 0.0001$) and CXCL13 ($p < 0.01$) compared to the noticeably higher levels of expression in primary macrophages (24h incubated monocytes). Thus there is marked difference in expression of ADAMDEC1 and CXCL13 between THP-1 cell line and primary monocytes/macrophages.

b) Effect of THP-1 stimulation on expression of ADAMDEC1 and CXCL13

Different inflammatory mediators can activate cells of the monocyte-macrophage-dendritic cell series infiltrating kidney allografts during TCMR and induce expression of effector molecules. Thus we examined the effect of different activation stimuli on expression of ADAMDEC1 and CXCL13 in THP-1 monocytic cell line. THP-1 cells suspended in complete RPMI-10 medium were cultured in six well plates. Cells were either incubated in medium only (unstimulated controls) or with LPS, TNF (100 U/ml and 500 U/ml) or anti-CD40 (immobilized to six well plate). After incubation, cells were harvested for total RNA extraction and ADAMDEC1 and CXCL13 expression was assessed by RT-PCR. Compared to unstimulated THP-1 controls, the expression of ADAMDEC1 and CXCL13 did not increase ($p > 0.05$) in response to stimulation of THP-1 cells with either anti-CD40 or LPS (Figure 4.2). However, both ADAMDEC1 and CXCL13 showed significant increase in expression levels in THP-1 cells stimulated with TNF compared to unstimulated controls. Stimulation of THP-1 cells with 100 U/ml TNF and 500 U/ml TNF increased

ADAMDEC1 expression by 3.6 fold ($p < 0.001$) and 7.6 fold ($p < 0.001$), respectively, compared to unstimulated controls. Similarly stimulation with 100 U/ml TNF and 500 U/ml TNF increased CXCL13 expression by 10.4 fold ($p < 0.001$) and 15.6 fold ($p < 0.001$) compared to controls. Although TNF stimulated expression of ADAMDEC1 and CXCL13 in THP-1 cells, the levels were a lot less than the increase in primary monocytes.

Thus there is differential regulation of expression of ADAMDEC1 and CXCL13 in the monocytic THP-1 cell line in response to stimulation with TNF, leading to marked increase in expression, but not anti-CD40 or LPS. However, ADAMDEC1 and CXCL13 expression varied markedly between the monocytic THP-1 cells and primary monocytes/macrophages cultures, and expression was much weaker in cell line than primary cells.

4.3. ADAMDEC1, CXCL13, CCL18 AND CCL19 EXPRESSION IN HUMAN CELLS

We sought to identify which cell types express ADAMDEC1, CXCL13, CCL18, and CCL19. We used global gene expression microarrays to examine a primary human cell panel representing cell types commonly found in rejecting human kidney transplants using normal kidney as a control (Figure 4.3). The human cell culture panel included: renal proximal tubular epithelial cells (RPTEC), human umbilical vein endothelial cells (HUVEC), $CD4^+$ and $CD8^+$ allo-stimulated effector T cells, B cells, NK cells, monocytes and macrophages (24 hours incubated monocytes).

By gene expression microarrays, we compared the expression (probe set signal) for ADAMDEC1, CXCL13, CCL18 and CCL19 transcripts in individual cell types represented in the panel to their expression in normal control kidneys. There was no significant difference in expression of ADAMDEC1, CXCL13 and CCL18 between control kidneys and monocytes, NK cells, effector $CD4^+$ and $CD8^+$ T cells, B cells, RPTEC and HUVEC. Of all cells on the panel, only macrophages expressed significantly high levels of ADAMDEC1 ($p < 0.001$), CXCL13 ($p < 0.01$) and CCL18 ($p < 0.05$) compared to control kidneys. Although CCL19 probe set signal was higher in normal kidney controls compared to all other cell types in the cell panel, macrophages and monocytes had a

relatively higher, although not significant, probe set signal among all other examined human cell types. Thus ADAMDEC1, CXCL13, CCL18 and CCL19 are most highly expressed in MMDC.

4.4. EFFECT OF IFNG ON ADAMDEC1, CXCL13, CCL18 AND CCL19 EXPRESSION

IFNG is a major proinflammatory cytokine that plays important role in the immune response through its actions on many immune cells including all cells of myeloid origin as well as non-marrow derived cells such as epithelial and endothelial cells (123). An increase in IFNG and IFNG-inducible transcripts is a striking feature of T cell mediated inflammatory responses such as TCMR (82;84;91). IFNG is also the principle inducer of classical macrophage activation, and many transcripts are induced in infiltrating host macrophages in response to IFNG (116). Therefore we sought to examine the effect of IFNG treatment of macrophages, epithelial cells, and endothelial cells on ADAMDEC1, CXCL13, CCL18 and CCL19 expression *in vitro*.

By microarray analysis, we examined the expression of ADAMDEC1, CXCL13, CCL18 and CCL19 in epithelial cells (RPTEC), endothelial cells (HUVEC) and macrophages (24h incubated monocytes) incubated in culture medium alone or with IFNG (Figure 4.4). Compared to their unstimulated controls, the expression of ADAMDEC1 and CXCL13 did not show any significant change ($p > 0.05$) in response to IFNG treatment of macrophages, endothelial cells and epithelial cells. Similar results were obtained for CCL18 with no significant changes ($p > 0.05$) in expression were detected in response to IFNG treatment. CCL19 was the only transcript that appeared to be IFNG responsive, but the increase was not significant. Interestingly, CCL18 is known as an alternative macrophage activation marker but not IFNG -induced classical macrophage activation (47). So, one would expect to see a decrease of CCL18 expression in macrophages treated with IFNG. However, our data failed to show any significant change in response to IFNG compared to non-IFNG treated controls.

Thus ADAMDEC1, CXCL13, and CCL18 transcripts are most highly expressed in macrophages and their expression is IFNG-independent i.e. they are not IFNG-inducible transcripts. In contrast, CCL19 showed little increase in response to IFNG, but its expression remained limited to IFNG-treated macrophages and not other IFNG-treated cells in our panel.

HETEROGENEITY OF EXPRESSION OF ADAMDEC1, CXCL13, CCL18 AND CCL19 IN MMDC

Primary monocytes are the circulating precursors for macrophages and myeloid dendritic cells. During an immune response, they are continuously recruited from blood into inflamed tissues. While *in vitro*, monocytes can be differentiated into macrophages or dendritic cells using distinct culture conditions, the *in vivo* factors that trigger the differentiation of monocytes to macrophages or dendritic cells remain incompletely understood. Heterogeneity in expression of various transcripts have been reported among different types of monocyte, macrophage, dendritic cell lineage in human and animal models. Using RT-PCR we examined gene expression of ADAMDEC1, CXCL13, CCL18 and CCL19 in freshly isolated human monocytes and after their *in vitro* differentiation to macrophages and to dendritic cells.

4.5. ADAMDEC1, CXCL13, CCL18 AND CCL19 EXPRESSION DURING DIFFERENTIATION OF MONOCYTE-DERIVED MACROPHAGES AND DENDRITIC CELLS

Following isolation of PBMCs from whole blood of healthy volunteers, monocytes were enriched by negative selection using immunomagnetic beads. Monocytes were resuspended in complete RPMI-10 medium and were differentiated into macrophages or dendritic cells. Macrophages were generated by 24 hours incubation of monocytes in six-well plate in complete RPMI-10 medium. Dendritic cells were differentiated by incubating monocytes in six-well plate in complete RPMI-10 medium in the presence of GM-CSF and IL-4 for 7 days. Dendritic cell cultures were replenished at day 3 and day 5 with fresh culture medium

containing GM-CSF and IL-4**.** Freshly isolated monocytes expressed low levels of ADAMDEC1 and only detectable levels of CCL19, but did not express CXCL13 and CCL18 (Figure 4.5). Monocyte differentiation to macrophages (through adherence to tissue-culture treated polystyrene plates) markedly increased ADAMDEC1 expression (1000 fold, $p < 0.0001$) compared their freshly isolated monocyte precursors. Also, macrophage differentiation induced the expression of CXCL13 ($p < 0.0001$) and CCL18 ($p < 0.0001$), both being not detectable in freshly isolated monocytes. The increase in expression levels was similar between CXCL13 and CCL18. Dendritic cells seem to regulate expression of these transcripts differently than macrophages. In contrast to macrophages, monocyte differentiation to dendritic cells (Figure 4.6) decreased expression of ADAMDEC1 ($p < 0.01$) yet induced expression of CXCL13 ($p < 0.0001$) and CCL18 ($p < 0.0001$). The expression levels were highest with CCL18 and at lower levels with CXCL13. However, CCL19 expression did not significantly change when monocytes were differentiated to dendritic cells.

Thus these data show differential regulation of ADAMDEC1, CXCL13, CCL18 and CCL19 upon MMDC differentiation with marked heterogeneity in the expression pattern across MMDC. Increased ADAMDEC1 expression was a characteristic feature for macrophage differentiation, but not dendritic cell differentiation, while CXCL13 and CCL18 were induced by macrophage as well as dendritic cell differentiation.

4.6. ADAMDEC1, CXCL13, CCL18 AND CCL19 EXPRESSION DURING MACROPHAGE STIMULATION

The costimulatory CD40/CD40L pathway, TLR agonists (e.g. LPS) and inflammatory cytokines (e.g. TNF) play an important role in activation of macrophages and dendritic cells and induction of various effector molecules in inflamed tissues such as rejecting allografts (48;124-126). We sought to study the effect of these different stimuli on expression of ADAMDEC1, CXCL13, CCL18, and CCL19 in *in vitro* cultured monocyte-derived macrophages. Understanding the effect of these stimuli on transcript expression may shed some light on their potential contribution to regulation of expression of these transcripts *in vivo* in inflamed sites such as rejecting allograft. Macrophages were

generated from monocytes incubated either in complete RPMI-10 medium only (unstimulated controls) or were stimulated by CD40L or TNF or LPS added to the cultures as described in materials and methods. After 24 hours incubation, cells were harvested for total RNA extraction and RT-PCR, and supernatant was collected for cytokine assays.

Different patterns of gene expression were observed for ADAMDEC1, CXCL13, CCL18 and CCL19 in response to the stimuli tested. Macrophage stimulation with TNF or LPS significantly increased expression of ADAMDEC1, CXCL13, CCL18 and CCL19 compared to unstimulated controls (Figure 4.7). In macrophages, ADAMDEC1 expression was only increased ($p < 0.01$) in response to TNF stimulation, but not CD40L or LPS. However, expression of CXCL13, CCL18 and CCL19 increased to a variable degree in response to both TNF and LPS stimulation. While the increase in CXCL13 expression was stronger in response to TNF stimulation ($p < 0.001$) than LPS stimulation ($p < 0.05$), the increase in CCL19 expression was stronger with LPS ($p < 0.001$) than TNF ($p < 0.05$). The increase in expression of CCL18 was comparable for both TNF and LPS, and both stimuli resulted in marked increase ($p < 0.001$) in expression. Overall, CD40L was the weakest stimulant showing only trends towards increased expression of all four transcripts but none statistically significant.

To confirm cell culture activation in response to different stimuli, we analyzed IL-6 concentration in the supernatant of these cultures by ELISA (Figure 4.8). IL-6 levels increased ($p < 0.001$) after macrophage stimulation with all three stimuli, including CD40L, compared to their unstimulated controls.

Thus TNF was the only stimulus, among all three tested stimuli, capable of increasing expression of all four transcripts, particularly ADAMDEC1, CXCL13 and CCL18, and to less degree CCL19. There was a distinct pattern of regulation of expression for each transcript, and that pattern varied with different stimuli.

4.7. ADAMDEC1, CXCL13, CCL18 AND CCL19 EXPRESSION DURING DENDRITIC CELL STIMULATION

Similar to macrophage stimulation, we also examined the effect of CD40/CD40L costimulation, LPS and TNF stimulation on expression of ADAMDEC1, CXCL13, CCL18 and CCL19 in *in vitro* cultured monocyte-derived dendritic cells. Dendritic cell cultures were differentiated from freshly isolated monocytes in presence of GM-CSF and IL-4 in complete RPMI-10. Cultures were replenished with fresh medium, GM-CSF and IL-4 on day 3 and day 5 as previously described. Dendritic cells were stimulated by adding CD40L, TNF, or LPS to cultures on day six of culture. After incubation, cells were harvested for RNA extraction and RT-PCR, and supernatant was collected for cytokine assay.

In contrast to macrophage stimulation, dendritic cell stimulation with CD40L, TNF or LPS did not increase the expression of ADAMDEC1, CXCL13 and CCL18 (Figure 4.9). Dendritic cells stimulated with CD40L, TNF or LPS did not show any significant change in expression of ADAMDEC1 compared to the unstimulated controls. On the other hand, dendritic cells showed a significant decrease in CXCL13 ($p < 0.001$) and CCL18 ($p < 0.001$) expression in response to stimulation with CD40L, TNF or LPS compared to the unstimulated controls. The decrease of expression for either CXCL13 or CCL18 was comparable between CD40L, TNF and LPS. CCL19 was the only transcript that showed a significant increase ($p < 0.001$) when stimulated with CD40L, but expression did not change in response to LPS and TNF stimulation. The above data shows unique regulation, distinct than macrophages, of CXCL13, CCL18 and CCL19 expression during dendritic cell activation causing significant decrease in CXCL13 and CCL18 by CD40L, TNF and LPS, and a moderate increase in CCL19 but only in response to CD40L, but not LPS or TNF.

Dendritic cell activation in response to different stimuli was confirmed by measuring IL-6 concentration in the supernatant of these cultures by ELISA (Figure 4.10). IL-6 levels increased in dendritic cells stimulated with CD40L, TNF and LPS compared to their unstimulated controls indicative of an activated phenotype.

Therefore ADAMDEC1, CXCL13 and CCL18 and CCL19 expression is differentially regulated between macrophages and dendritic cells and this may be the case for different populations of MMDC series in response to activation stimuli; CD40L, TNF and LPS. However, additional complexity is evident due to the individual differences between each transcript within the same cell type in response to each activation stimulus, likely suggesting that individual transcript expression is under the control of independent or multiple mechanisms. These data highlight the complicated yet finely tuned nature of the responses of MMDC populations to different activation stimuli and changes in microenvironment (43). These studies also demonstrate the difficulties that can be expected when studying individual parameters within these cell types.

4.8. EXPRESSION OF ADAMDEC1, CXCL13, CCL18 AND CCL19 IN M-CSF-DIFFERENTIATED MACROPHAGES

The accumulation of macrophages in an allograft during TCMR is largely mediated by macrophage differentiation from recently recruited monocytes with lesser contribution of local proliferation within the allograft (127). Local macrophage proliferation in tissues is mainly triggered by macrophage colony stimulating factor (M-CSF) that may be produced by T cells and parenchymal cells (128;129). Significant increase in serum levels of M-CSF during TCMR have been reported in humans (130), and blocking M-CSF receptor (c-fms) attenuates macrophage proliferation and accumulation by 80% and 50%, respectively in a mouse renal transplant rejection model (129). We attempted to model intragraft macrophage M-CSF driven proliferation by examining ADAMDEC1, CXCL13, CCL18 and CCL19 expression in macrophages cultured and expanded in the presence of M-CSF. Although we acknowledge that *in vitro* culture conditions will not completely capture the far more complex environmental condition to which macrophages are exposed to within an inflamed tissue, it will still give us an idea about the expression of individual transcript in M-CSF differentiated macrophages.

Monocytes isolated from whole blood of healthy volunteers were cultured in six-well plates in complete RPMI-10 in the presence of M-CSF. After six days incubation of cultures, cells were collected for total RNA extraction and RT-PCR. We also performed total RNA

extraction for RT-PCR from the freshly isolated monocytes. By RT-PCR, the expression of ADAMDEC1, CXCL13, CCL18 and CCL19 in M-CSF differentiated macrophages was compared to their respective expression in their monocyte precursors (Figure 4.11). Freshly isolated monocytes expressed low levels of ADAMDEC1 and CCL19, but did not express CXCL13 and CCL18. When monocytes were cultured in presence of M-CSF, we detected a marked increase in expression of ADAMDEC1 ($p < 0.0001$) and little but significant ($p < 0.0001$) increase of CCL19 when compared to their freshly isolated monocyte precursors. Also, CCL18 expression, which was below the threshold of detection by RT-PCR in monocytes, was markedly increased ($p < 0.001$) in a manner similar to that observed for ADAMDEC1 upon differentiation of monocytes to M-CSF macrophages. Despite the dramatic increases observed for ADAMDEC1 and CCL18, we failed to observe any changes in CXCL13 expression following M-CSF culture. This finding is noteworthy given that CXCL13 was so strongly increased upon 24 hours macrophage differentiation in absence of M-CSF as we showed earlier in this chapter.

Thus our data shows unique regulation of expression of ADAMDEC1, CCL18 and to a less degree CCL19 during monocyte differentiation to macrophages in presence of M-CSF; marked increase in ADAMDEC1 and CCL19 and induction of CCL18 that was initially absent in monocytes. The regulation of expression had a similar pattern in both macrophages (24 hours incubated monocytes) and M-CSF macrophages for all transcripts except CXCL13.

4.9. ADAMDEC1, CXCL13, CCL18 AND CCL19 EXPRESSION DURING M-CSF MACROPHAGE STIMULATION

Similar to what we have previously done with macrophages and dendritic cells, we wanted to examine the effect of activation of M-CSF-differentiated macrophages by different stimuli on expression of ADAMDEC1, CXCL13, CCL18 and CCL19. One of the advantages of working with M-CSF-differentiated macrophages (M-CSF macrophages) is the ability to start cultures with relatively low numbers of highly purified monocytes. Monocytes were purified and cultured in the presence of M-CSF as in the experiments above. M-CSF macrophages were stimulated with either CD40L TNF, or LPS as described

in materials and methods and compared to unstimulated cultures. Cultures were replenished with complete RPMI-10 and M-CSF on day 3 and day 5. After 6 days, cells were harvested for total RNA extraction and RT-PCR and supernatants were collected for cytokine measurements by ELISA. By RT-PCR (Figure 4.12), unstimulated M-CSF macrophages showed strong expression of ADAMDEC1 and CCL18, and weaker expression of CCL19. Expression of CXCL13 was not detectable in unstimulated M-CSF macrophages. Following stimulation, ADAMDEC1 did not show a significant change in expression in M-CSF macrophages stimulated by CD40L, TNF or LPS compared to unstimulated controls although there was a trend for increased expression following LPS stimulation. In contrast, CCL18 expression increased in M-CSF macrophages stimulated with CD40L ($p < 0.01$) but did not significantly change with TNF or LPS stimulation. We noticed a different pattern of expression with CXCL13 and CCL19. Similar to unstimulated controls, M-CSF macrophages did not express CXCL13 when stimulated by CD40L or TNF, but expression was induced ($p < 0.001$) only in response to LPS stimulation. Of note, although increased CXCL13 expression was statistically significant, it was considerably lower compared to values we had previously observed with macrophages differentiated through adherence to polystyrene. Similar to CXCL13, CCL19 did not show a significant change in expression in M-CSF macrophages stimulated with CD40L or TNF, but was only increased ($p < 0.001$) with LPS stimulation.

Activation of M-CSF macrophages in response to different stimuli was confirmed by IL-6 levels in culture supernatants (Figure 4.13). IL-6 levels were significantly higher ($p < 0.001$) in supernatants from M-CSF macrophage cultures stimulated with CD40L, TNF and LPS compared to their unstimulated controls. Thus despite the robust activation evidenced by high levels of IL-6 produced by each of the three stimuli, many of the stimuli were either not effective or only affected some, but not all of the transcripts examined.

4.10. TIME COURSE FOR ADAMDEC1, CXCL13, CCL18 AND CCL19 EXPRESSION IN M-CSF MACROPHAGES

Macrophage gene expression profile has been shown to change over time in culture and some macrophage transcripts undergo transient regulation during the first three days of *in*

vitro differentiation, then return to basal levels (42). Thus we studied the changes in mRNA expression for ADAMDEC1, CXCL13, CCL18 and CCL19 during differentiation of M-CSF macrophages along 7 days time course to examine whether the expression of these transcripts undergo transient regulation during differentiation. Monocytes isolated by negative selection from PBMCs from healthy donors were incubated in 6-well plates in complete RPMI-10 in presence of 50 ng/ml M-CSF for 1, 3, 5 and 7 days. Cultures were replenished with fresh medium and M-CSF on day 3 and day 5 as above. After incubation, cells were harvested for total RNA extraction and RT-PCR at each time point (day 1, 3, 5 and 7). M-CSF macrophages expressed high levels of ADAMDEC1 on day 1 (Figure 4.14), then expression subsequently stabilized with modest increase in ADAMDEC1 throughout day 3, day 5 and day 7. In contrast, CXCL13 expression showed a distinct expression pattern with peak expression on day 1, then markedly decreased expression on day 3 ($p < 0.01$), and no longer detectable on days 5 and 7. M-CSF macrophages expressed high levels of CCL18 on day 1, but there was no further increase in expression on day 3, 5 and 7. Finally, CCL19 did not show a significant change in expression from day 1 to 3, but expression increased ($p < 0.001$) and stabilized on day 5, a pattern most similar to that observed for ADAMDEC1. M-CSF macrophages demonstrated two distinct patterns of regulation of transcript expression throughout the 7 day time course culture; expression was either stable throughout the 7 day cultures (such as ADAMDEC1 and CCL18) or was transiently regulated during the first 3 days, but stabilized on day 5 and day 7 (such as CXCL13 and CCL19).

Thus expression of CXCL13 and CCL19 showed "transient" regulation (increased in ADAMDEC1 and decreased in CXCL13) during the first 3 days of M-CSF macrophage differentiation while ADAMDEC1 and CCL18 expression was stable throughout the M-CSF differentiation and did not show such transient regulation.

EXPRESSION OF ADAMDEC1, CXCL13, CCL18 AND CCL19 DURING MACROPHAGE – T CELL INTERACTION

4.11. OVERVIEW

In TCMR, activated effector T cells infiltrating the graft encounter donor antigens on antigen presenting cells such as macrophages, and secrete cytokines that induce the recruitment of inflammatory cells into the graft augmenting the inflammatory response. Thus the cognate interaction between infiltrating host effector T cells and macrophages may contribute to graft injury during TCMR (parenchymal injury and tubulitis) through effector mechanisms similar to DTH response. Effector T cell - macrophage interaction could be mediated via contact-dependent mechanisms requiring direct cell-cell contact or via contact-independent mechanisms through release of soluble factors such as cytokines and enzymes. Both contact-dependent and contact-independent (soluble factors) mechanisms of interaction between macrophages and effector T cells could play a role in regulation of expression of the top transcripts most highly expressed in TCMR.

We examined effector T cell- macrophage interactions *in vitro* and explored the regulation of ADAMDEC1, CXCL13, CCL18 and CCL19 expression. We sought to determine the extent by which expression of individual transcripts was increased in response to effector T cell soluble mediators alone versus in response to direct cell to cell contact between activated effector T cell interaction with macrophages.

4.12. EFFECT OF SOLUBLE FACTORS RELEASED FROM ACTIVATED T CELLS

Effector T cells release multiple cytokines following activation which have potent activation properties on macrophages. Macrophages can produce their own cytokines in response which further enhance production of T cell effector cytokines thus generating a positive feedback loop. To evaluate the effect of soluble factors released from effector T cells on expression of the four transcripts in macrophages we designed a co-culture system

that would allow for separation of macrophages from T cells, T cell activation, and passage of soluble factors (but not cells) between the two cell types. We used a multi-well plate setup that allowed for anti-CD3 antibodies to be coated on the bottom of the well and tissue culture inserts that the macrophages could rest upon. Following isolation of PBMCs from healthy volunteers, T cells were enriched by negative selection using immunomagnetic beads. T cells were cultured for 5 days in 6-well plates coated with anti-CD3 (5 μg/ml) and anti-CD28 (1 μg/ml) in complete RPMI-10 medium in the presence of recombinant human IL-2 (50 U/ml). The stimulation with anti-CD3/anti-CD28 antibodies was performed to mimic T cell priming (TCR complex signal 1 and CD28 costimulatory signal 2) and ensure an activated/ effector phenotype. After 5 days of anti-CD3/28 stimulation, primed/activated T cells were cultured in a new anti-CD3 (10 μg/ml) coated 6- well plates along with autologous freshly isolated monocytes (ratio monocytes : T cells = 2 : 1) on the inserts (transwell co-culture) for 24 hours. Gene expression changes were compared between activated T cell-macrophage co-cultures and cultures of activated T cells only without macrophages (in anti-CD3 bound well) or compared to $CD14^+$ monocytes only incubated on the inserts .

Using RT-PCR, we compared the expression of ADAMDEC1, CXCL13, CCL18 and CCL19 in co-cultured activated T cells and macrophages (24h incubated monocytes) to their respective controls, i.e. activated T cells only and macrophages only, respectively (Figure 4.15). High levels of ADAMDEC1 expression were observed in control macrophages but no expression in control activated T cells. Upon co-culture, co-cultured macrophages showed significant ($p < 0.0001$) increase in the expression of ADAMDEC1 compared to already high levels observed in control macrophages. In contrast, expression of ADAMDEC1 in co-cultured activated T cells remained negative. The expression pattern of CCL18 and CCL19 was similar to ADAMDEC1 expression. Macrophages cultured alone (control) expressed both CCL18 and CCL19, and their expression was further increased (CCL18 $p <0.0001$ and CCL19 $p<0.001$) when exposed to soluble mediators from activated T cells. In contrast to macrophages, activated T cells cultured in the absence of macrophages did not express CCL18 or CCL19, and co-culture with macrophages still failed to induce their expression in co-cultured activated T cells. A distinct expression

pattern was observed with CXCL13. Of the four transcripts examined only CXCL13 showed basal levels of CXCL13 expression in activated T cells cultured alone (control), at levels comparable to those observed in control macrophages. T cells co-cultured with macrophages did not show a significant change in CXCL13 expression when compared to control activated T cells. In contrast, basal CXCL13 expression in macrophages cultured alone, was sharply increased ($p < 0.0001$) in macrophages co-cultured with activated T cells.

As an additional confirmation of stimulation in our model, we measured cytokine production in cell culture supernatants collected from different culture conditions at the end of incubation period. Concentration of the key T cell effector cytokine IFNG, the macrophage cytokine IL-6, and the effector cytokine produced by both macrophages and T cells, TNF, were measured using commercially available ELISA kits for individual cytokine and shown in (Figure 4.16). As expected, high IFNG levels were detected in stimulated T cells alone but not in macrophages alone. Although high levels of IFNG were still detected in macrophage-T cell co-cultures, the levels were lower when compared to control T cells. This may reflect the high degree of IFNG uptake by macrophages in the inserts. Basal levels of TNF were detected with stimulated T cells alone with limited basal expression in macrophages alone. However, TNF dramatically increased in macrophage-T cell co-culture compared to control macrophages ($p < 0.0001$) and controls T cells ($p < 0.0001$). IL-6 production followed an expected pattern of expression being undetectable in stimulated T cells alone, low basal expression in macrophages alone, and strongly increased in macrophage-T cell co-culture compared to control macrophages ($p < 0.0001$).

Thus soluble factors released from activated T cells during contact independent interaction with macrophages stimulate the expression of ADAMDEC1, CXCL13, CCL18 and CCL19 in macrophages to levels higher than any of the other stimulations tested. The high increase in transcript expression in response to soluble factors released during activated T cell-macrophage contact independent interactions was restricted to macrophages, whereas the majority remained undetectable in co-cultured T cells.

4.13. EFFECT OF CONTACT INTERACTION BETWEEN ACTIVATED T CELLS AND MACROPHAGES

A second co-culture setup was also examined where activated T cells were allowed to be in contact with autologous macrophages. In this setup, T cells undergo the same initial stimulation with anti-CD3/28 for five days before being added to new multi-well plates pre-coated with anti-CD3 alone in the same manner as described above. The difference from the experiments described above is that in this set of experiments the macrophages were not added to a tissue culture insert but rather simply added on top of the stimulated T cells thus allowing for direct cell-to-cell contact. The expression of each transcript in contact macrophage-T cell co-culture was assessed by RT-PCR again compared to the its expression in control macrophages cultured alone and control activated T cell cultured alone (Figure 4.17). Similarly to our findings described above, the same patterns of expression in control activated T cell (cultured alone) and control macrophages (cultured alone) were observed for all four transcripts. ADAMDEC1, CCL18, and CCL19 were all absent in control activated T cell (cultured alone), strong basal expression for ADAMDEC1, CCL18, and modest expression for CCL19 in control macrophages (cultured alone). Basal expression in activated T cells was again limited to CXCL13. The co-culture results varied from those observed when activated T cells and macrophages were physically separated. Contact co-culture of macrophages and activated T cells surprisingly showed decreased ADAMDEC1 expression ($p < 0.01$) and unchanged CCL18 expression when compared to control macrophages. In contrast, CXCL13 and CCL19 expression were both significantly increased in contact co-cultures of macrophages and activated T cells compared to control macrophages ($p<0.0001$).

As was performed for the non-contact co-culture experiments described above, cytokine levels were measured in cell culture supernatants for IFNG, TNF, and IL-6 . Cytokine level for different culture conditions were expressed in pg/ml and shown in Figure 4.18. IFNG production highly increased in co-culture compared to control T cells ($p < 0.0001$), while TNF production increased in co-culture compared to control macrophages ($p < 0.0001$) and control T cells ($p < 0.0001$). Also, higher IL-6 production was detected in co-culture

compared to control macrophages ($p < 0.0001$). The increase in cytokine concentrations in co-culture is likely due to the combined activation of macrophages and T cells during their contact interactions.

Thus our data suggests that contact dependent mechanisms during activated T cell-macrophage interaction contribute to regulation of expression of ADAMDEC1, CXCL13 and CCL19, but in distinct patterns. While contact mechanisms attenuated the expression ADAMDEC1, they enhanced the expression of CXCL13 and CCL19.

4.14. CYTOKINE PROFILING

In the macrophage-activated T cell co-culture under no contact condition, we demonstrated that soluble mediators (contact-independent) released from activated T cells triggered a robust increase in expression of ADAMDEC1, CXCL13, CCL18 and CCL19. To identify soluble mediators that may be potential candidates contributing to such effect on expression, we performed a pilot assay using a protein microarray to screen for a number of cytokines and proinflammatory mediators. Cytokine profiling was performed on cell culture supernatants from different culture conditions were harvested at the end of the 24 hour incubation. Supernatants were analyzed using a Meso Scale Discovery® V-PLEX ™ Human Cytokine Panel 1 and Proinflammatory Panel 1 (Rockville, MD) that measured IFNG, IL-1α, IL-1β, IL-2, IL-4, IL-5, IL-6, IL-7, IL-8, IL-10, IL-12/IL-23p40, IL-12p-70, IL-13, IL-15, IL-16, IL-17-A, TNF-α, TNF-β, CSF-2, and VEGF. As this cytokine profile assay was done only once, and the cytokine concentration exceeded the maximum value on the standard curve for certain cytokines, we will only report on the profile of these cytokines (in co-culture) without quantifying the exact concentration, i.e. it will be reported as "exceeded the maximum detection limit" with providing this maximum limit (demonstrated on figure) according to manufacturer's instructions.

High levels of IFNG, IL-17, IL-6, TNF-α, TNF-β, IL-1α,, GM-CSF, were detected in supernatants from activated T cell-macrophage co-cultures compared to supernatant from control macrophages cultured alone (Figure 4.19). The higher concentration of these cytokines in co-culture could account for the increased expression of one or more of the

four transcripts of interest in our study. These soluble factors could act individually or in synergy to regulate macrophage expression of the four transcripts. As we previously mentioned, this pilot assay was performed only once for a single experiment/donor, and concentrations for many cytokines exceeded the maximum levels of detection. Thus further study and titration is required to examine the effect of individual cytokine on expression of each transcript in macrophages.

4.15. FIGURES

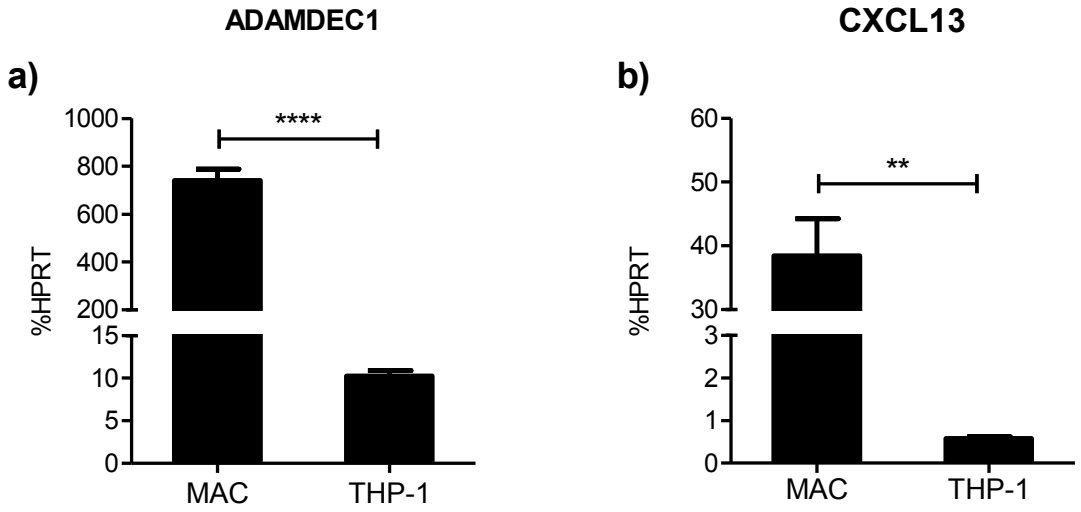

Figure 4.1. ADAMDEC1 and CXCL13 expression in THP-1 cell line and in primary monocytes/macrophages (RT-PCR). Monocytic THP-1 cells and primary CD14+ monocytes isolated from PBMCs from healthy volunteers were incubated separately in six-well plates in complete RPMI-10 medium. After 24 hours, cells were harvested for total RNA extraction and RT-PCR. mRNA values are %HPRT mean ± SE of three experiments. MAC; macrophages (24 hours incubated monocytes), THP-1; THP-1 cells. mRNA values for ADAMDEC1 (a) and CXCL13 (b) were compared between MAC and THP-1 cells by unpaired t test. $^{**}p < 0.01$, $^{****}p < 0.0001$

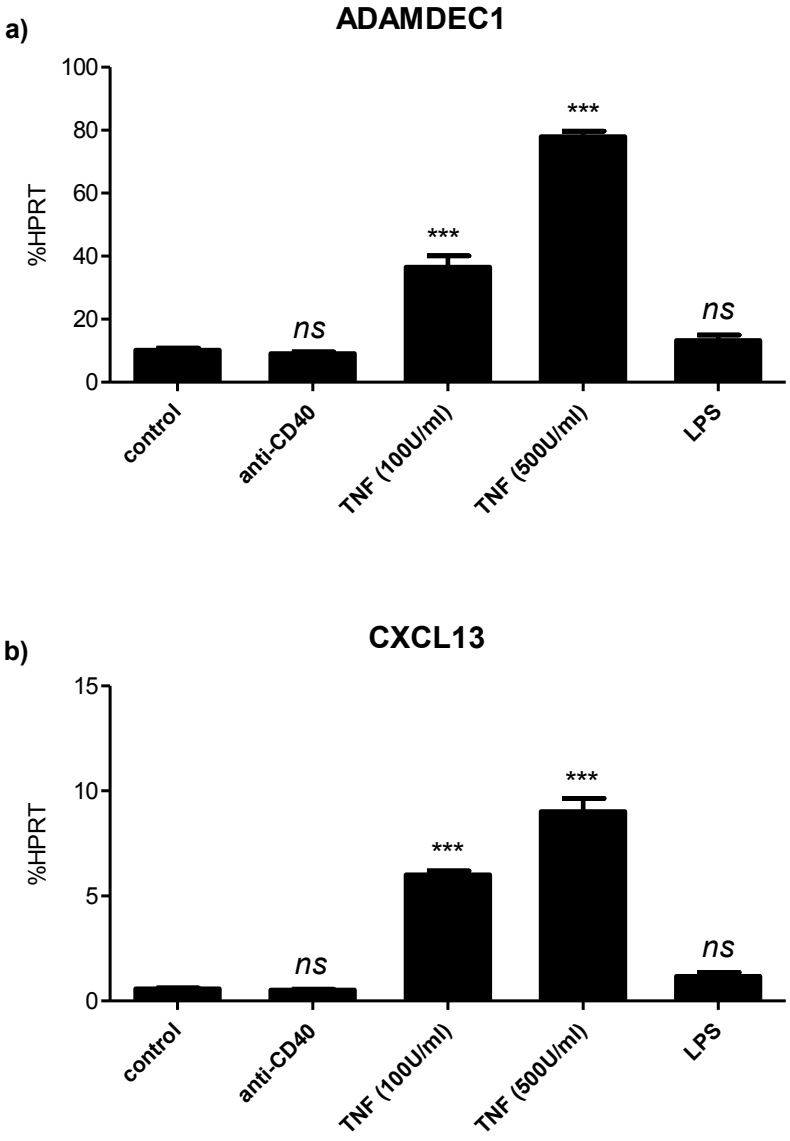

Figure 4.2. ADAMDEC1 and CXCL13 expression during stimulation of THP-1 cells (RT-PCR). THP-1 cells were incubated in in six-well plates in complete RPMI-10 medium only or with either anti CD40, LPS, or TNF (100 U/ml and 500 U/ml) as described in materials and methods. After 24h, cells were harvested for total RNA extraction and RT-PCR. ADAMDEC1 and CXCL13 mRNA levels in stimulated THP-1 cells was compared to their levels in unstimulated THP-1 controls by one-way ANOVA with Dunnett's Multiple Comparison Test. mRNA values are %HPRT mean ± SE of three experiments.

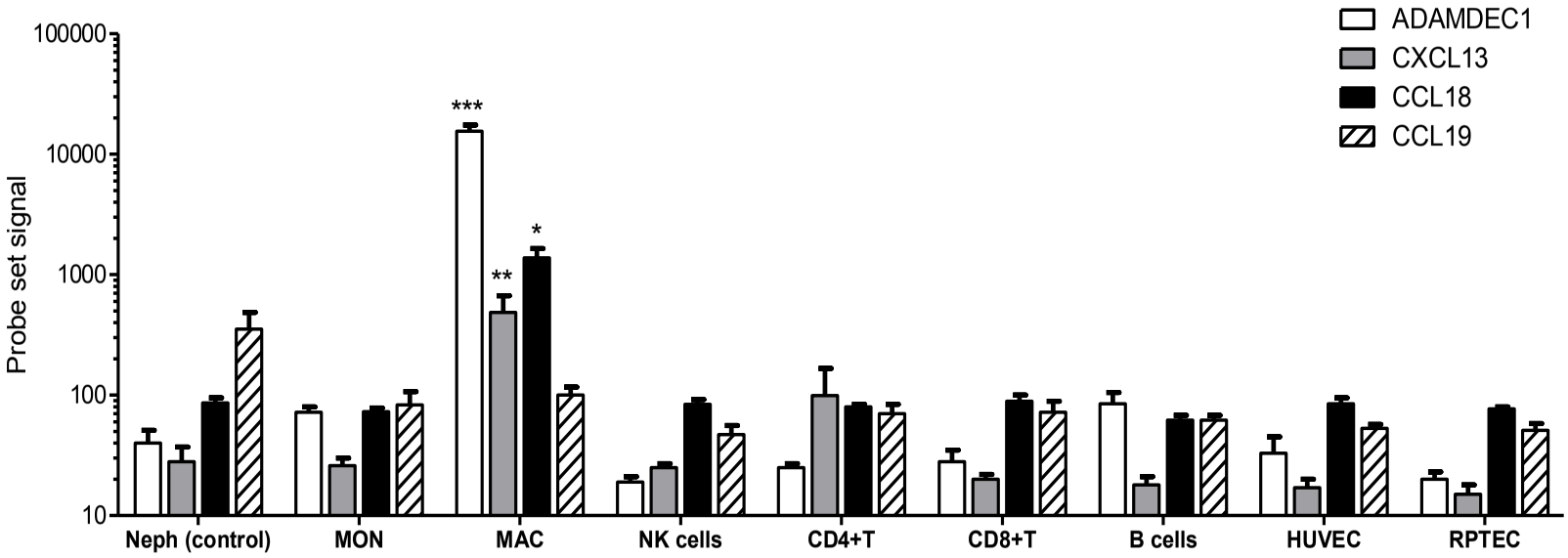

Figure 4.3. ADAMDEC1, CXCL13, CCL18 and CCL19 expression in Human cell panel (microarrays). Human cell panel was generated as described in material and methods. ERPTEC; renal proximal tubule epithelial cells, HUVEC; human umbilical vein endothelial cells; CD8+T: CD8+T cells, CD4+T: CD4+T cells, NK: natural killer cells, MAC; macrophages, MON: monocytes and Neph: nephrectomy. For individual transcript, probe set signal in each cell type was compared to signal in control nephrectomies by One-way ANOVA with Dunnett's Multiple Comparison Test. *$p<0.05$, **$p<0.01$, ***$p<0.001$

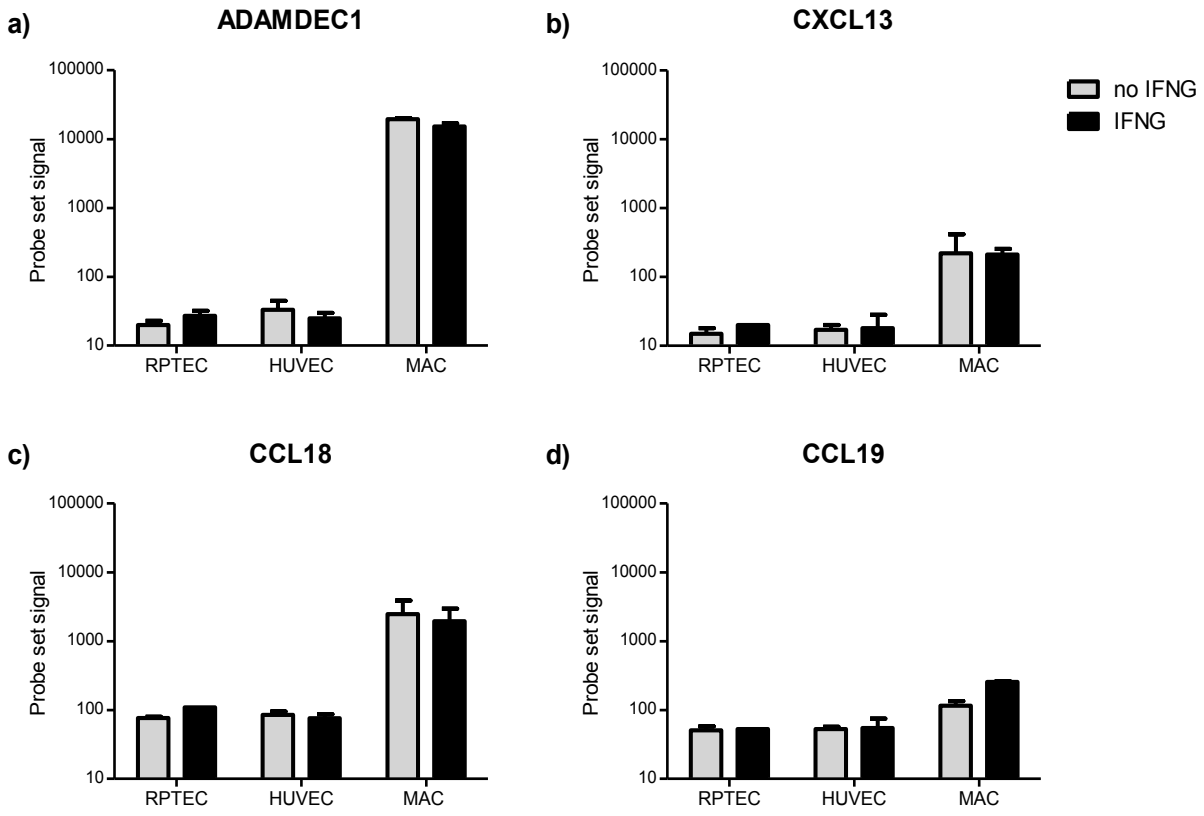

Figure 4.4. Effect of IFNG on expression of ADAMDEC1, CXCL13, CCL18 and CCL19 in macrophages, HUVEC and RPTEC (microarrays). RPTEC; renal proximal tubule epithelial cells, HUVEC; human umbilical vein endothelial cells, MAC; macrophages (24h incubated monocytes), IFNG; interferon gamma. Cultures of macrophages, RPTEC and HUVEC were incubated in culture media only or with 500 U/ml recombinant human IFNG for 24h. Cells were harvested for total RNA extraction and microarrays. Probe set signal for ADAMDEC1 (a), CXCL13 (b), CCL18 (c) and CCL19 (d) in MAC, HUVEC, and RPTEC treated with IFNG was compared to signal in its respective untreated controls by unpaired t test , and the change in expression in individual transcript in response to IFNG treatment was not significant. P-value <0.05 was considered significant. Probe set signals are mean ± SE of three experiments.

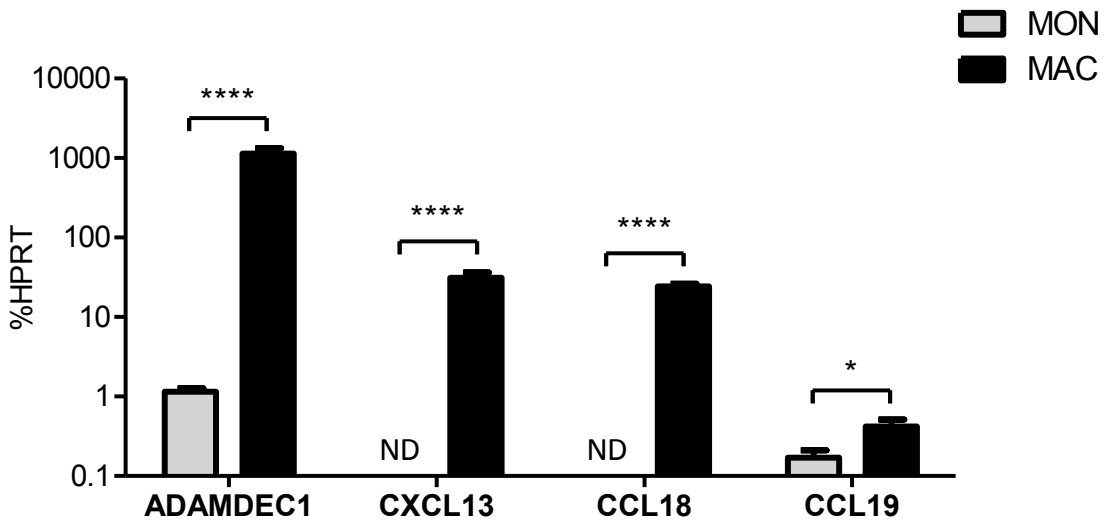

Figure 4.5. ADAMDEC1, CXCL13, CCL18 and CCL19 expression during macrophage differentiation (RT-PCR). Macrophages were generated from CD14+ monocytes incubated in six-well plates in complete RPMI-10 medium for 24h, then harvested for total RNA extraction and RT-PCR. Total RNA extraction and RT-PCR was also performed on part of the CD14+monocytes that were earlier isolated for macrophage culture. mRNA value are %HPRT mean ± SE of three experiments. For individual transcript, mRNA level in macrophages was compared to its level in their monocyte precursors by unpaired t test. *$p < 0.05$, ****$p < 0.0001$. Mon; monocytes, MAC; macrophages, DC; monocyte-derived dendritic cells, ND; not detectable.

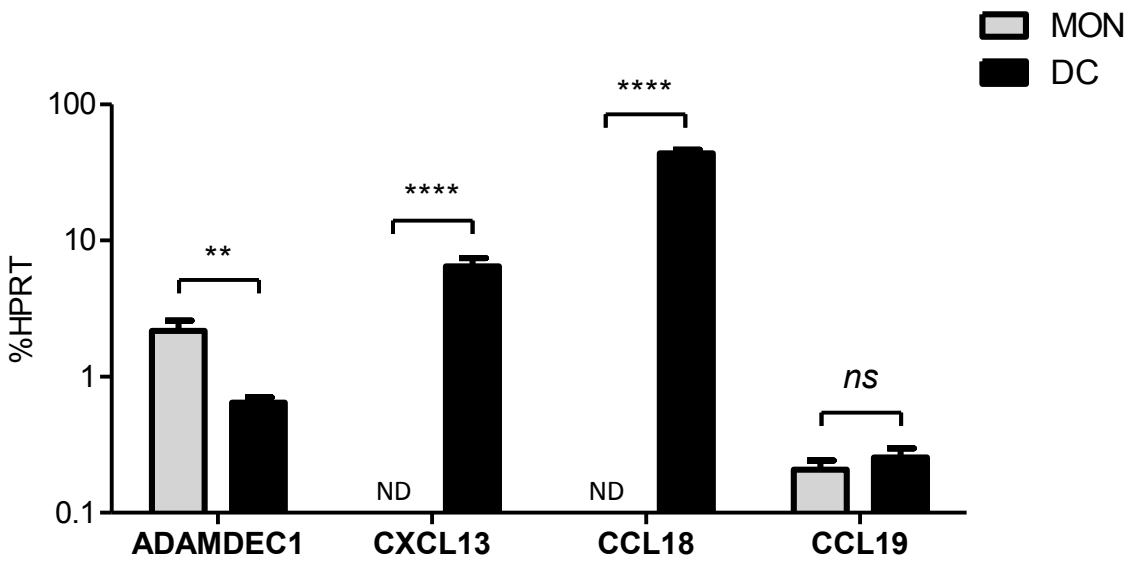

Figure 4.6. ADAMDEC1, CXCL13, CCL18 and CCL19 expression during dendritic cell differentiation (RT-PCR). Dendritic cells were generated from monocytes cultured in six-well plates in complete RPMI-10 medium in presence of GM-CSF and IL-4 as described in materials and methods. After 7 days, cells harvested for total RNA extraction and RT-PCR. Total RNA extraction and RT-PCR was also performed on part of the CD14+monocytes that were earlier isolated for dendritic cell culture. mRNA value are %HPRT mean ± SE of 3 experiments. For individual transcript, mRNA level in dendritic cells was compared to its level in their monocyte precursors by unpaired t test. **$p < 0.01$, ****$p < 0.0001$, ns; not significant $p > 0.05$. Mon; monocytes, DC; monocyte-derived dendritic cells, ND; not detectable.

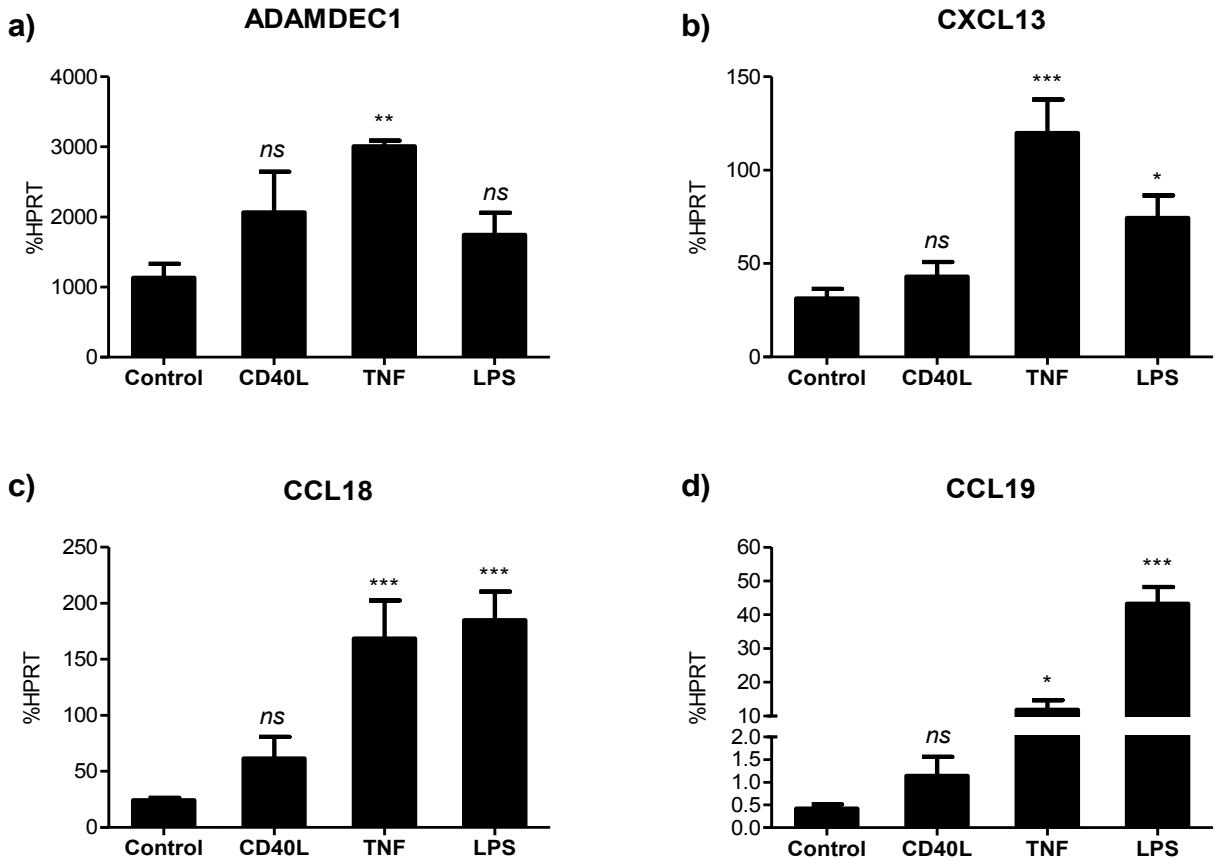

Figure 4.7. ADAMDEC1, CXCL13 , CCL18 and CCL19 expression during macrophage activation (RT-PCR). Monocytes were incubated in six-well plates in complete RPMI-10 medium only (unstimul43ated controls) or with CD40L, TNF or LPS as described in materials and methods. After 24h, cells were harvested for total RNA extraction and RT-PCR. mRNA values are %HPRT mean ± SE of three experiments. Expression of ADAMDEC1 (a), CXCL13 (b), CCL18 (c) and CCL19 (d) in macrophages stimulated with CD40L, TNF, or LPS was compared to its level in unstimulated macrophage controls by one-way ANOVA with Dunnett's Multiple Comparison Test. *$p < 0.05$, **$p < 0.01$, ***$p < 0.001$, ns; not significant $p > 0.05$.

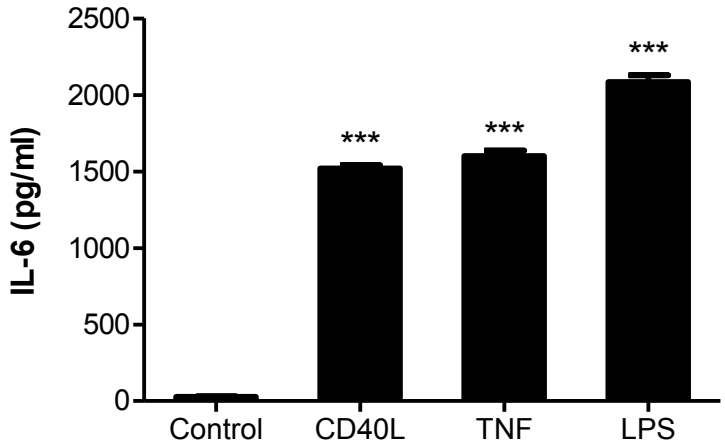

Figure 4.8. IL-6 production during macrophage activation (ELISA). Monocytes isolated from PBMCs of whole blood from healthy volunteers were incubated in complete RPMI-10 medium only or with CD40L, TNF or LPS as described in materials and methods. After 24h incubation, cell free culture supernatants were collected for IL-6 assay by ELISA. IL-6 level (pg/ml) in supernatants from macrophages stimulated with CD40L, TNF or LPS was compared to its level from unstimulated macrophage controls by one-way ANOVA with Dunnett's Multiple Comparison Test. ***$p < 0.001$

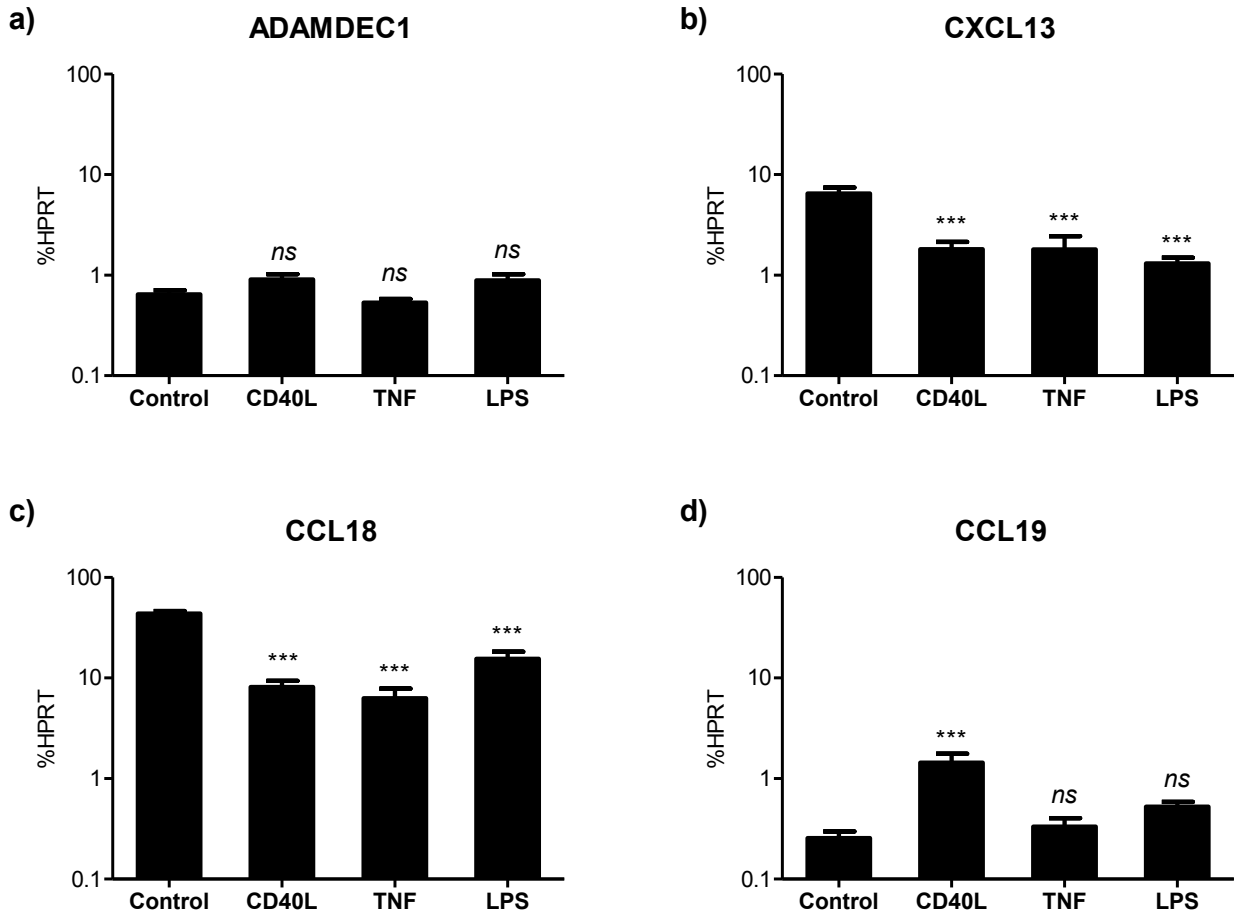

Figure 4.9. ADAMDEC1, CXCL13 , CCL18 and CCL19 expression during dendritic cell activation (RT-PCR). Dendritic cells were generated from monocytes cultured in six-well plates in presence of GM-CSF and IL-4 as described in materials and methods. Cultures were incubated with GM-CSF/IL-4 cocktail in complete RPMI-1640 medium only (unstimulated controls) or with either CD40L, TNF or LPS as described in materials and methods. After 7 days, cells were harvested for total RNA extraction and RT-PCR. mRNA values are %HPRT mean ± SE of three experiments. Expression of ADAMDEC1 (a), CXCL13 (b), CCL18 (c) and CCL19 (d) in dendritic cells stimulated with CD40L, TNF or LPS was compared to its level in unstimulated dendritic cell controls by one-way ANOVA with Dunnett's Multiple Comparison Test. ***$p < 0.001$, ns; not significant $p > 0.05$.

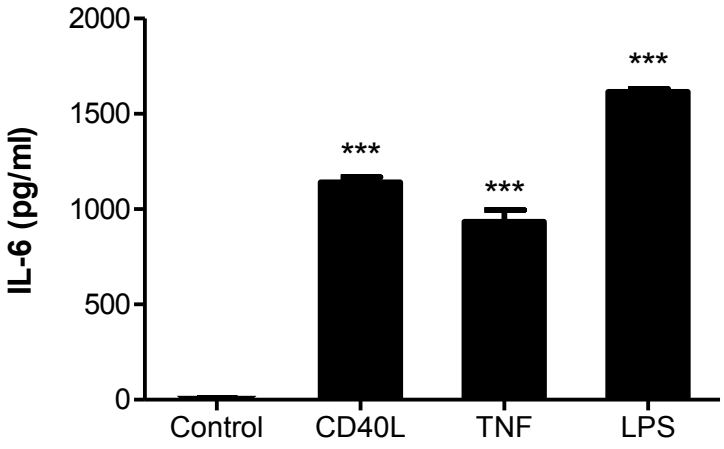

Figure 4.10. IL-6 production during dendritic cell activation (ELISA). Dendritic cells were generated from monocytes cultured in six-well plates in presence of GM-CSF and IL-4 for 7 days. Cultures were incubated in complete RPMI-10 medium only (unstimulated controls) or with CD40L, TNF or LPS as described in materials and methods. After incubation, cell free culture supernatants were collected for IL-6 assay by ELISA. IL-6 level (pg/ml) in supernatants from dendritic cells stimulated with CD40L, TNF or LPS was compared to its level from unstimulated dendritic cell controls by one-way ANOVA with Dunnett's Multiple Comparison Test. ***$p < 0.001$

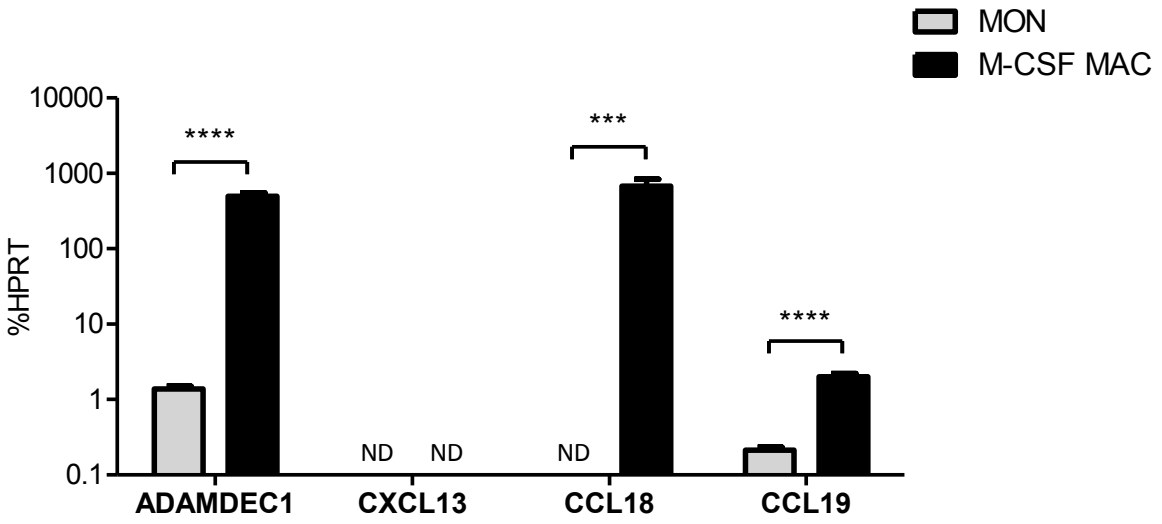

Figure 4.11. ADAMDEC1, CXCL13, CCL18 and CCL19 expression during M-CSF – macrophage differentiation (RT-PCR). M-CSF differentiated macrophages were generated from monocytes cultured in six-well plates in complete RPMI-10 medium in presence of M-CSF. After 6 days, cells were harvested for total RNA extraction and RT-PCR. Total RNA extraction and RT-PCR was also performed on part of the CD14+monocytes that were earlier isolated for dendritic cell culture. mRNA value are %HPRT mean ± SE of 3 experiments. For individual transcript, mRNA level in dendritic cells was compared to its level in their monocyte precursors by unpaired t test. ***p < 0.001, ****p < 0.0001. Mon; monocytes, M-CSF MAC; M-CSF - differentiated macrophages , ND; not detectable.

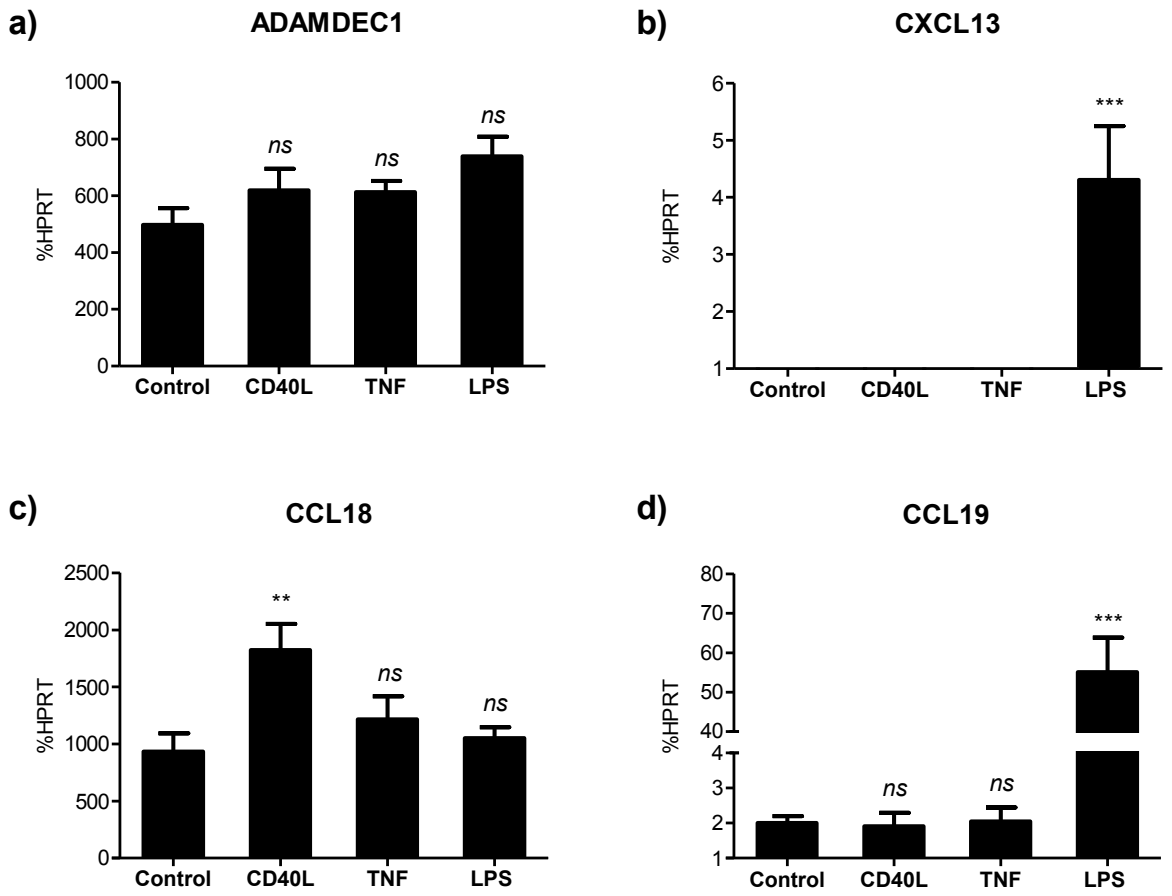

Figure 4.12. ADAMDEC1, CXCL13 , CCL18 and CCL19 expression during M-CSF macrophage activation (RT-PCR). M-CSF differentiated macrophages were generated from monocytes cultured with M-CSF in six-well plates for 6 days. Cultures were incubated in complete RPMI-10 medium only (unstimulated controls) or with CD40L, TNF or LPS as described in materials and methods. After incubation, cells were harvested for total RNA extraction and RT-PCR. mRNA values are %HPRT mean ± SE of three experiments. Expression of ADAMDEC1 (a), CXCL13 (b), CCL18 (c) and CCL19 (d) in M-CSF macrophages stimulated with CD40L, TNF, or LPS was compared to its level in unstimulated controls by one-way ANOVA with Dunnett's Multiple Comparison Test. **p < 0.1, ***p < 0.001, ns; not significant (p > 0.05).

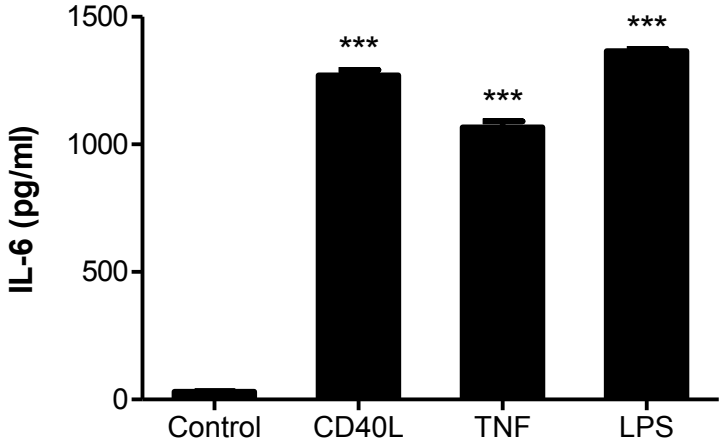

Figure 4.13. IL-6 production during M-CSF macrophage activation (ELISA). M-CSF macrophages were generated from monocytes cultured in six-well plates in presence of M-CSF for 6 days. Cultures were incubated in complete RPMI-10 medium only (unstimulated controls) or with CD40L, TNF or LPS as described in materials and methods. After incubation, cell free culture supernatants were collected for IL-6 assay by ELISA. IL-6 level (pg/ml) in supernatants from M-CSF macrophages stimulated with CD40L, TNF or LPS was compared to its level from unstimulated M-CSF macrophage controls by one-way ANOVA with Dunnett's Multiple Comparison Test. ***$p < 0.001$

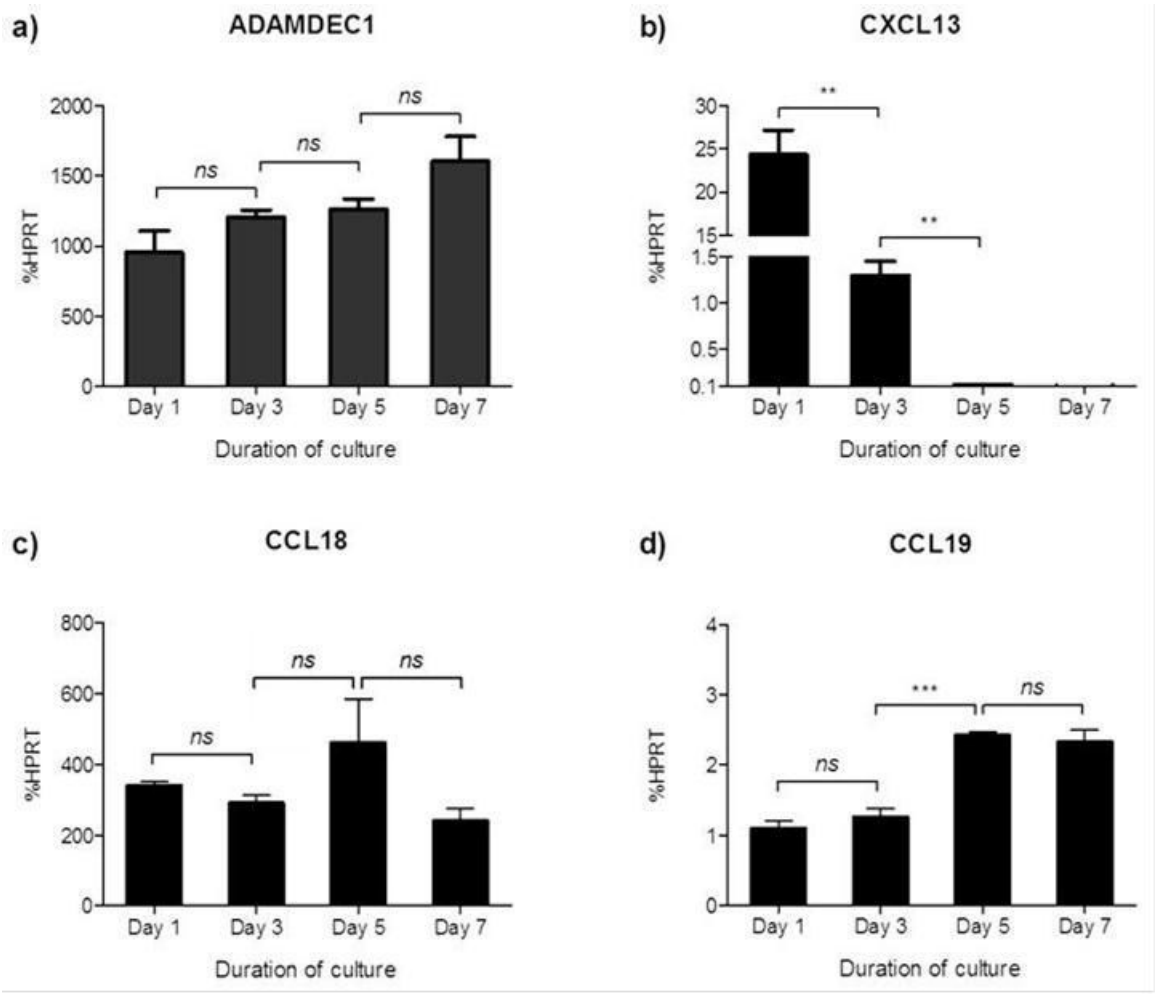

Figure 4.14. Time course for expression of ADAMDEC1, CXCL13, CCL18 and CCL19 in M-CSF macrophages (RT-PCR). Monocytes isolated from PBMCs from whole blood of healthy donors were cultured with M-CSF in complete RPMI-10 in six-well plates to induce monocyte differentiation into M-CSF macrophages. Cells were harvested for total RNA extraction and RT-PCR on day 1, day 3, day 5 and day 7 to examine the expression of ADAMDEC1 (a), CXCL13 (b), CCL18 (c) and CCL19 (d) during 7 days time course differentiation of M-CSF macrophages. mRNA value are %HPRT mean ± SE of 3 experiments Significance between two time points was assessed by unpaired t test. **p < 0.01, ***p < 0.001.

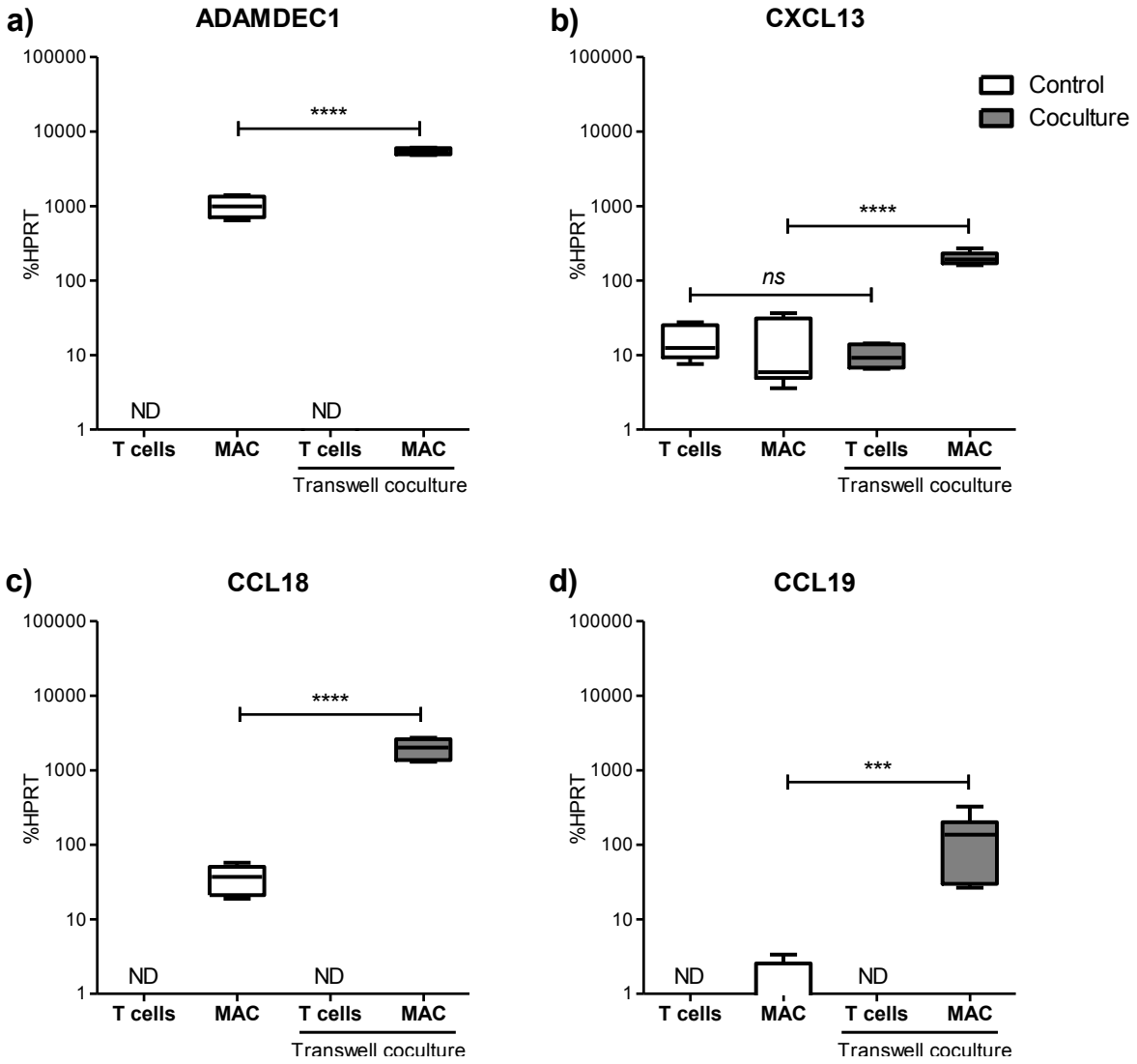

Figure 4.15. ADAMDEC1, CXCL13, CCL18 and CCL19 expression in macrophage – T cell transwell co-culture (RT-PCR). Expression of ADAMDEC1 (a), CXCL13 (b), CCL18 (c), and CCL19 (d) were examined in T cell – macrophage transwell co-cultures (i.e. under no contact conditions using culture inserts). mRNA values are %HPRT mean ± SE (n=3). MAC; macrophages, T cells; anti-CD3 stimulated T cells, ND; not detectable. Expression of ADAMDEC1 (a), CXCL13 (b), CCL18 (c) and CCL19 (d) in co-culture macrophages and co-culture T cells was compared to its expression in control macrophages (cultured alone) and control T cells (cultured alone) by unpaired t test. ***$p < 0.001$, ****$p < 0.0001$, ns; not significant ($p > 0.05$).

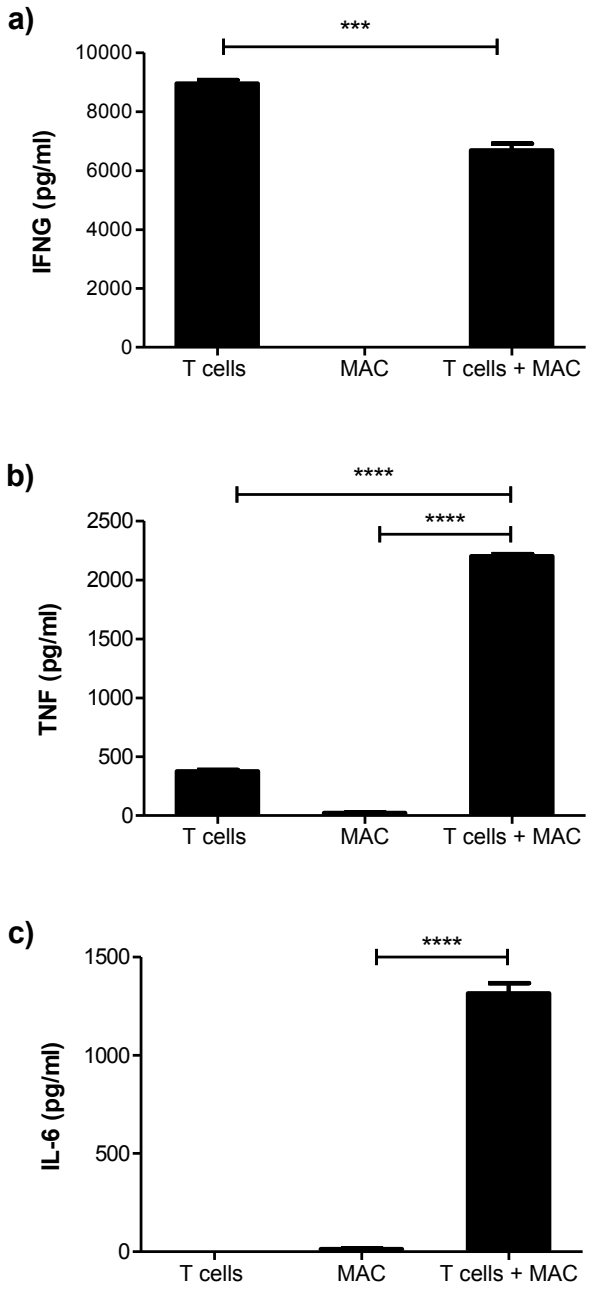

Figure 4.16. IFNG, TNF, and IL-6 production in macrophage – T cell transwell co-culture (ELISA). Macrophages were incubated with anti-CD3 activated T cells for 24h in transwell co-culture under no contact conditions using culture inserts. Cultures of macrophages alone, and anti-CD3 activated T cells alone were included as controls. After incubation, cell free culture supernatants were collected for assay of IFNG (a), TNF (b) and IL-6 (c) by ELISA. Concentration of individual cytokine (pg/ml) in supernatants from co-cultures was compared to its concentration in each control by unpaired t test. ***$p < 0.001$, ****$p<0.0001$.

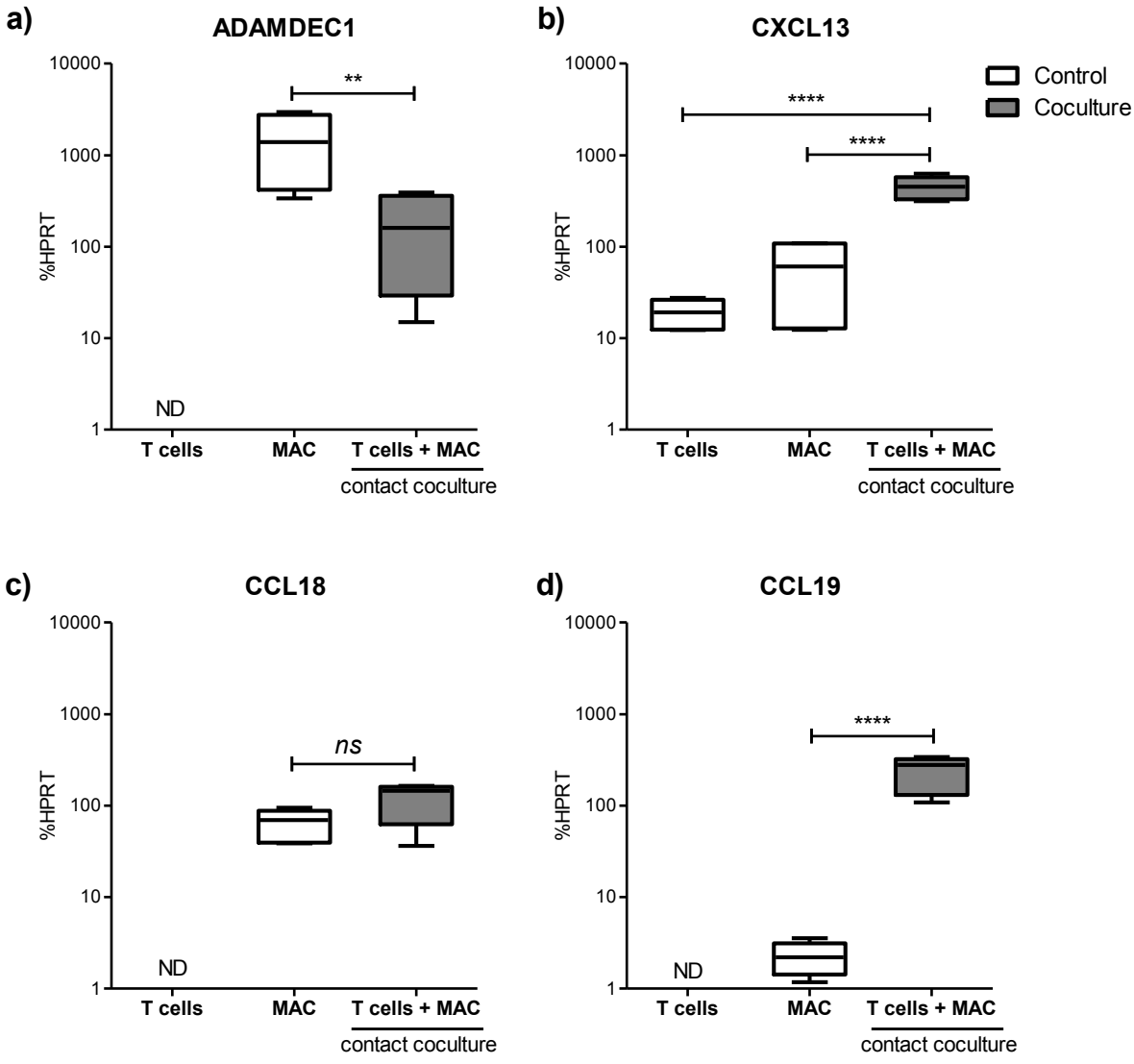

Figure 4.17. ADAMDEC1, CXCL13, CCL18 and CCL19 expression in macrophage – T cell contact co-culture (RT-PCR). ADAMDEC1 mRNA (a), CXCL13 mRNA (b), CCL18 mRNA (c), and CCL19 mRNA (d) were examined in T cell – macrophage contact co-cultures by RT-PCR. mRNA values are %HPRT mean ± SE (n=3). MAC; macrophages, T cells; anti-CD3 stimulated T cells, ND; not detectable. Expression of ADAMDEC1 (a), CXCL13 (b), CCL18 (c) and CCL19 (d) in macrophages + T cells co-culture was compared to its expression in control macrophages (cultured alone) and control T cells (cultured alone) by unpaired t test . **$p < 0.001$, ****$p < 0.0001$, ns; not significant ($p > 0.05$).

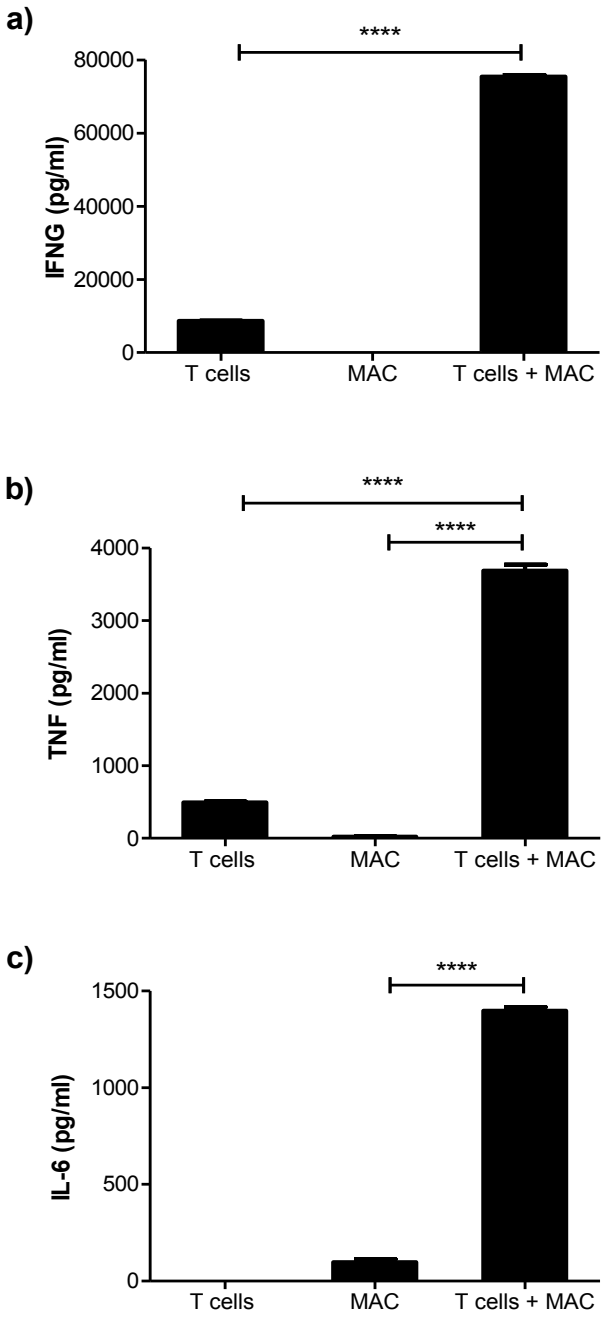

Figure 4.18. IFNG, TNF, and IL-6 production in macrophage – T cell contact co-culture (ELISA). Macrophages were incubated with anti-CD3 activated T cells for 24h in contact co-culture. Cultures of macrophages alone, and anti-CD3 activated T cells alone were included as controls. After incubation, supernatants were collected for assay of IFNG (a), TNF (b) and IL-6 (c) by ELISA. Concentration of individual cytokine (pg/ml) in supernatants from co-cultures was compared to its concentration in each control by unpaired t test. ***$p < 0.001$, ****$p<0.0001$.

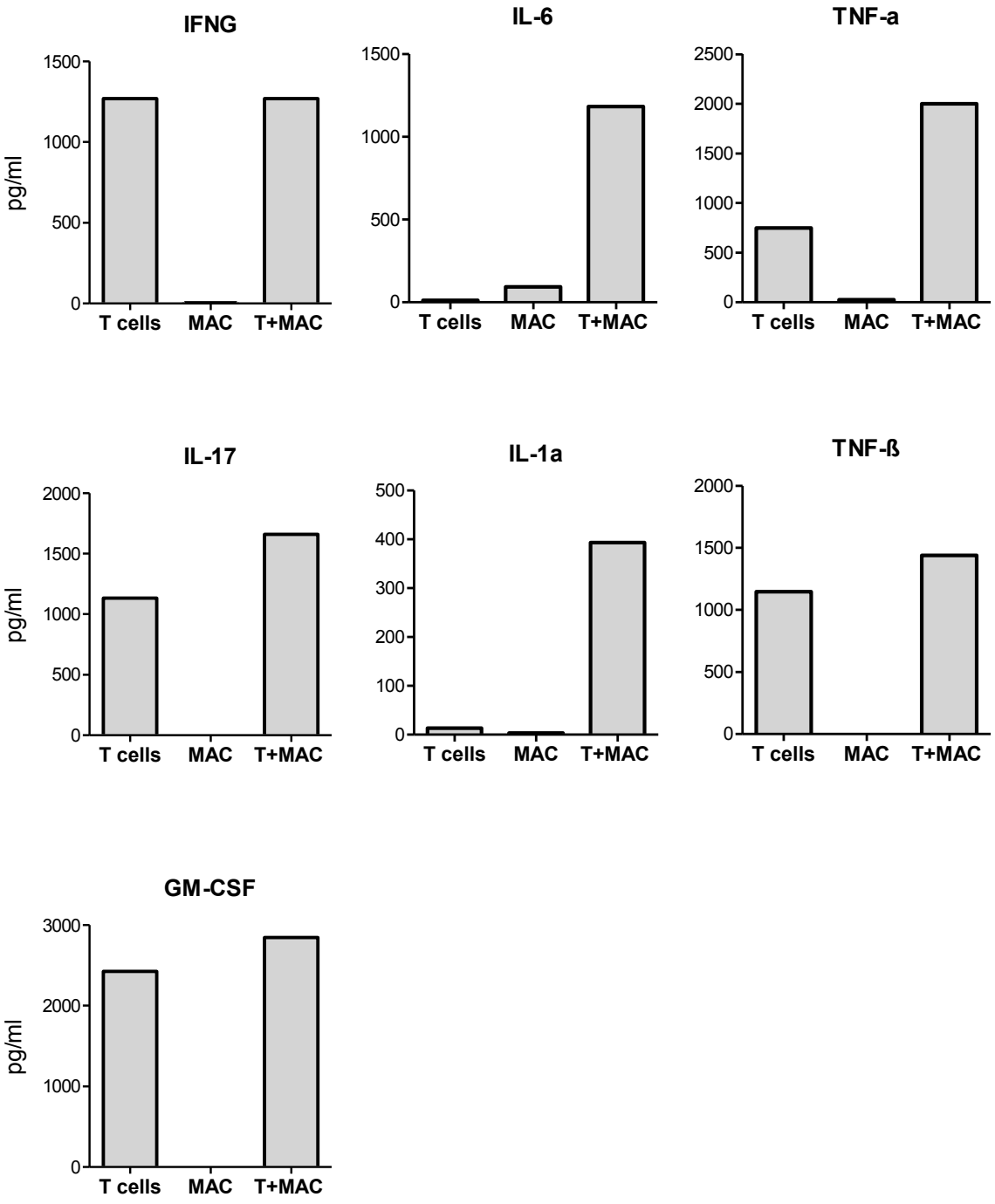

Figure 4.19. Cytokine profiling in macrophage – T cell transwell co-culture supernatants. Cytokine profiling was performed on supernatants from different culture conditions were harvested at the end of the 24 hour incubation. Supernatants were analyzed using a Meso Scale Discovery® V-PLEX ™ Human Cytokine Panel 1 and Proinflammatory Panel 1.

CHAPTER 5

ADAMDEC1, CXCL13 AND CCL19 IN MOUSE ALLOGRAFTS

ADAMDEC1, CXCL13 AND CCL19

IN MOUSE ALLOGRAFTS

5.1. OVERVIEW

Our group previously established a mouse kidney transplant model that parallels the events observed in human transplants undergoing rejection to allow us to study the mechanisms of T cell mediated rejection (30;103;131;132). This model is performed by leaving one host kidney in place thus allowing us to follow the rejecting kidneys for longer periods without compromising the health of the host (104). In this model, the transplanted kidney develops the characteristic histologic lesions seen in human biopsies with T cell mediated rejection. We have previously defined the changes in T cell-associated transcripts (103), IFNG-inducible transcripts (116), and MMDC transcripts (133) and characterized the inflammatory infiltrate during the early course of rejection in mouse kidney allografts and isografts (132). The IFNG effects and T cell response developed in allografts by day 1, and were associated with the presence of perivascular then interstitial T cell infiltration. At this time point, MMDC transcripts increased equally in both isografts and allografts. Thus the early trigger for MMDC response was non-specific injury. Later, progressive high macrophage burden developed in allografts due to recruitment by T cell-mediated inflammatory response and/or caused by alloimmune injury. Thus while IFNG effects and T cell response developed rapidly and plateaued by day 7, MMDC transcripts progressively increased as tubulitis and parenchymal deterioration developed at day 21 and later, despite persistent IFNG response (118).

We explored whether the mouse model would allow for assessment of ADAMDEC1, CXCL13, and CCL19 transcripts in a controlled in vivo model. We examined the time course (days 1-21 post transplant) of expression of Adamdec1, Cxcl13 and Ccl19 and related these findings to our aforementioned (previously established/published) time course

for changes in transcriptome in mouse allografts during rejection. Expression of Ccl18 could not be examined in mouse as human CCL18 does not have mouse homolog.

5.2 ADAMDEC1, CXCL13 AND CCL19 ARE NOT THE TOP TRANSCRIPTS EXPRESSED IN MOUSE ALLOGRAFTS

We used gene expression microarrays to assess transcript changes in allografts; CBA kidneys transplanted into B6 hosts, and compared these to isografts; CBA kidneys transplanted into CBA hosts, on day 7 and day 21 post transplant. Table 1 shows the top 20 (fold change) transcripts with significant higher expression in CBA allografts compared to CBA isografts on day 7 (Table 1) and day 21 post transplant (Table 2). Expression was expressed as fold change increase versus normal CBA kidneys. On day 7 (Table 5.1), the top transcripts with significant increase in expression included Ifng, and Ifng - inducible transcripts (Cxcl9, Cxcl10, Cxcl11, Ubd, and Gbp2b). Expression of CTL-associated transcripts (Fam26f, Gzmb, Cd8b1, Cd8a, Cd8a, Cd3d and Ifi209) was also increased in allografts on day 7 compared to isografts. On day 21 (Table 5.2), the top transcripts with higher expression in allografts compared to isografts included Ifng -induced transcripts (Gbp2b, Ubd, Cxcl9, Cxcl10, Cxcl11), and (T cell) CTL -associated transcripts (Fgl2, Fam26f), and immunoglobulin transcript (Ighm). Expression of Adamdec1, Cxcl13 and Ccl19 did not show significant increase in CBA allografts compared to CBA isografts on day 7 and day 21. Thus the transcriptome changes observed in mouse allografts recapitulate the general immunologic changes observed in rejecting human kidney transplants with high expression of transcripts reflecting IFNG effects and CTL-associated transcripts. However, the expression of individual transcripts that best differentiates TCMR from ABMR in human transplants failed to show significant changes in mouse allografts.

5.3. TIME COURSE FOR EXPRESSION OF ADAMDEC1, CXCL13 AND CCL19 IN MOUSE ALLOGRAFT REJECTION

We analyzed expression of Adamdec1, Cxcl13 and Ccl19 during the course of allograft rejection. Gene expression in isografts was also examined to distinguish the alloimmune response from the non-specific injury response. Expression of individual transcripts in

allografts and isografts at each time point from days 1 - 21 post-transplant expressed as fold increase versus normal CBA kidneys is shown in Figure 5.1. Expression of Adamdec1 was similar in isografts and allografts through to day 5. On day 7 Adamdec1 expression in allografts started increase up to day 21 but the increased expression was never significant when compared to isografts. Expression of Cxcl13 increased in both isografts and allografts on day 1 reflecting the nonspecific tissue response to injury. Expression decreased on isografts on day 3, then showed an unexpected progressive second increase on day 4 till day 7, decreased on day 21 but remained higher than normal kidney. In allografts, Cxcl13 expression increase on day 1 and 2, slightly dropped on day 3 and 4, but were significantly higher than isografts. Ccl19 expression decreased in both isografts and allografts on day 1 post transplant, then increased progressively up to day 4, then dropped in both isografts and allografts through to day 7, before showing another unexpected increase in both isografts and allografts. Ccl19 expression did not show significant difference in allografts compared to isografts except on day 3.

This course of expression of Adamdec1, Cxcl13 and Ccl19 in isografts and allografts was not related to the time course of expression of our previously defined pathogenesis-based transcript sets that reflect the major biological events in the allografts during rejection, particularly IFNG effects and T cell-associated transcripts and MMDC transcripts. We therefore concluded that the mouse kidney transplant model would not be suitable for the *in vivo* study of Adamdec1, Cxcl13 and Ccl19.

5.4. TABLES

Table 5.1. The top 20 transcripts increased on day 7 post transplant in mouse allografts

Day 7 post transplant				
Probe Set ID	Gene Symbol	Fold change	p- value	FDR
1426906_at	unannotated	121.2	1.44E-12	4.02E-08
1420549_at	Gbp2b	110.1	1.08E-10	1.32E-07
1436576_at	Fam26f	88.2	3.96E-11	9.67E-08
1418652_at	Cxcl9	83.7	1.68E-10	1.65E-07
1452205_x_at	unannotated	81.1	1.56E-11	8.48E-08
1418776_at	Gbp8	79.5	1.08E-09	3.87E-07
1419762_at	Ubd	78.5	3.57E-12	4.02E-08
1419060_at	Gzmb	66.5	4.07E-11	9.67E-08
1452231_x_at	unannotated	60.8	7.86E-12	5.91E-08
1423467_at	Ms4a4b	59.9	3.01E-10	1.97E-07
1419178_at	Cd3g	59.8	1.11E-11	7.17E-08
1419697_at	Cxcl11	57.9	4.82E-12	4.35E-08
1425947_at	Ifng	52.1	1.43E-10	1.50E-07
1426170_a_at	Cd8b1	46.4	1.19E-10	1.37E-07
1418536_at	unannotated	46.1	3.39E-11	9.67E-08
1435331_at	Ifi209	43.4	6.10E-10	2.87E-07
1418930_at	Cxcl10	41.9	3.19E-12	4.02E-08
1425294_at	Slamf8	41.8	2.07E-11	8.48E-08
1452349_x_at	unannotated	41.5	7.04E-10	3.05E-07
1426772_x_at	Tcrb-J	41.5	2.99E-11	9.67E-08

Table 5.2. The top 20 transcripts increased on day 21 post transplant in mouse allografts

Day 21 post transplant				
Probe Set ID	Gene Symbol	Fold change	p- value	FDR
1425385_a_at	Ighm	158.4	5.05E-08	3.73E-04
1420549_at	Gbp2b	121.4	1.63E-06	8.05E-04
1419762_at	Ubd	116.0	1.41E-07	4.28E-04
1426906_at	unannotated	94.9	6.57E-07	5.42E-04
1419697_at	Cxcl11	75.8	3.89E-07	5.06E-04
1418776_at	Gbp8	73.4	4.49E-07	5.06E-04
1436576_at	Fam26f	73.2	1.40E-06	7.42E-04
1443783_x_at	H2-Aa	67.0	1.15E-08	2.71E-04
1418536_at	unannotated	63.2	1.75E-07	4.28E-04
1452231_x_at	unannotated	53.8	4.22E-07	5.06E-04
1418652_at	Cxcl9	51.6	3.35E-07	5.06E-04
1424931_s_at	unannotated	51.2	3.57E-06	1.12E-03
1425294_at	Slamf8	43.5	8.80E-07	6.21E-04
1452348_s_at	unannotated	43.1	5.89E-06	1.46E-03
1439831_at	Gm4951	42.1	6.73E-07	5.42E-04
1423467_at	Ms4a4b	40.6	1.95E-06	8.47E-04
1418240_at	Gbp2	40.3	5.82E-07	5.42E-04
1421854_at	Fgl2	37.2	4.11E-07	5.06E-04
1418930_at	Cxcl10	37.1	4.38E-07	5.06E-04
1419042_at	Iigp1	31.3	1.38E-06	7.42E-04

5.5. FIGURES

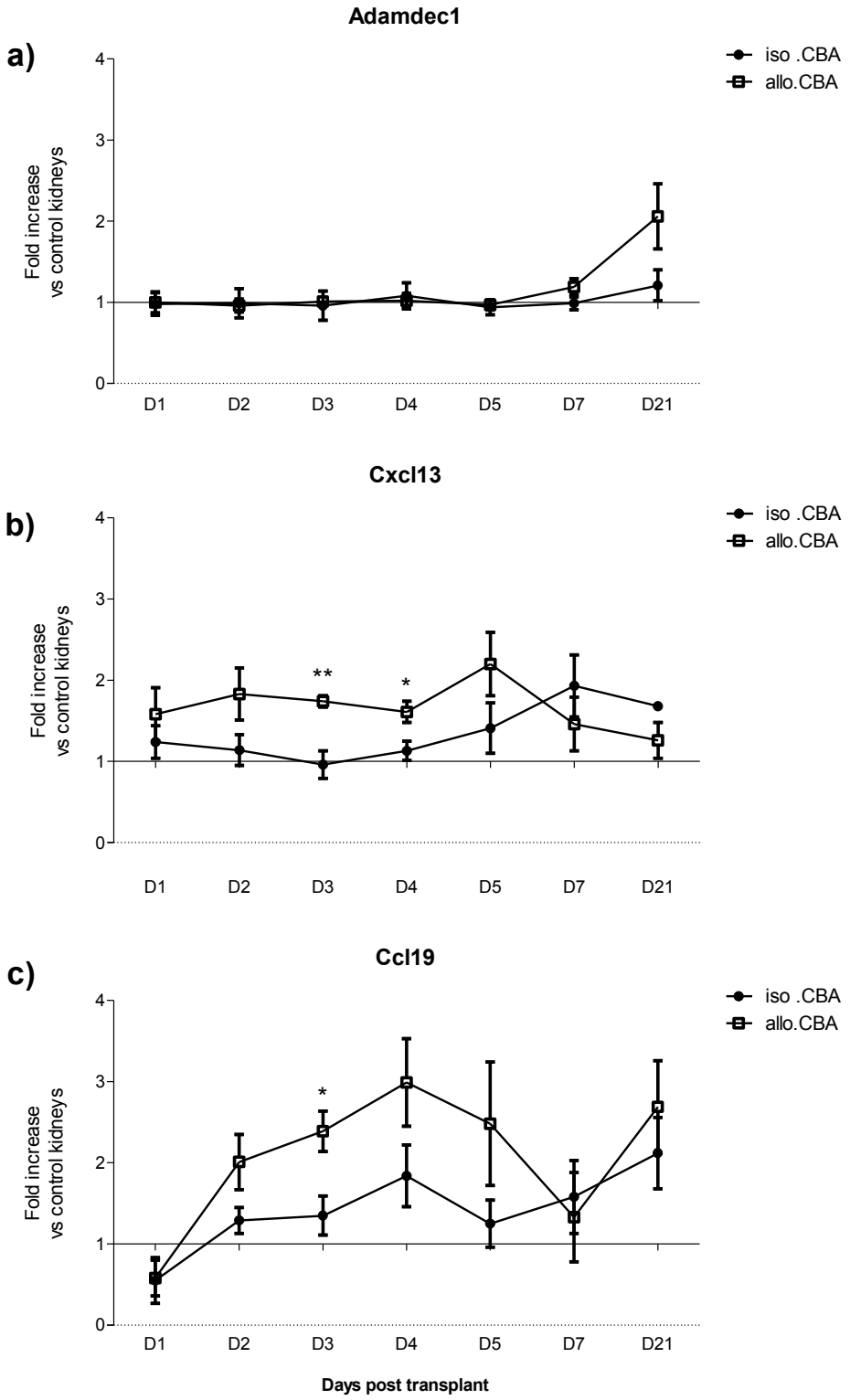

Figure 5.1. Time course for expression of Adamdec1, Cxcl13 and Ccl19 in mouse allografts and isografts (microarrays). Expression of Adamdec1 (a), Cxcl13 (b) and

Ccl19 (c) was assessed in allografts (CBA into B6) and isografts (CBA into CBA) at days 1-21 post transplant using Affymetrix microarrays. Expression of each transcript is shown for each time point in allografts, and isografts as fold increase versus normal CBA kidneys. Values represent mean ± SEM of 3 biological replicates. Individual transcript expression in allografts and isografts was compared at each time point by unpaired t test, *$p < 0.05$, **$p < 0.01$

CHAPTER 6

DISCUSSION

DISCUSSION

6.1. SUMMARY

To better understand the effector mechanisms in TCMR, we sought to define the transcripts preferentially increased in TCMR compared to ABMR using gene expression analysis and study their relationship to histologic lesions, inflammatory burden in human kidney transplant biopsies, and attempt to attribute their expression to specific cells. We also studied expression of the transcripts defined above in primary human cells, in response to stimulation, and during interactions between effector T cells and macrophages. We hypothesized that the transcripts preferentially increased in kidney allografts with TCMR when compared to ABMR will reflect MMDC interaction with cognate effector T cells. The top transcripts (by fold change) showing higher expression in TCMR versus normal kidneys were transcripts related to the intense IFNG response (IFNG inducible transcripts), the inflammatory cell recruitment and the tissue response to injury. The top three transcripts preferentially increased in TCMR versus ABMR were the metalloprotease ADAMDEC1 and the chemokines CXCL13 and CCL18, and their expression was significantly higher in TCMR versus both non specific acute kidney injury and non TCMR biopsies. Expression of ADAMDEC1, CXCL13 and CCL18 correlated with the histologic lesions diagnostic for TCMR. Also, their expression correlated with the inflammatory cell burden including macrophage transcript burden/MACtb (with no preference to either classic or alternative macrophage activation phenotypes) and T cell transcript burden/TCtb in all 703 kidney transplant biopsies as well as in TCMR biopsies. The increased expression of ADAMDEC1, CXCL13 and CCL18 was strongly associated and selective for TCMR and could differentiate it not only from ABMR, but also from AKI and non TCMR biopsies. The homeostatic chemokine CCL19 transcript was preferentially increased in TCMR versus ABMR, AKI and non TCMR but to a lesser degree than the top three transcripts, and its correlation to histopathologic lesions and MACtb/Ttb was weaker than the top three transcripts. *In vitro*, ADAMDEC1, CXCL13, CCL18 were primarily

expressed in human macrophages, and were not induced by IFNG. Increased ADAMDEC1 expression was a characteristic feature for macrophage differentiation, with CXCL13 and CCL18 expression common to both macrophages and dendritic cells. The expression of these transcripts further increased in response to macrophage activation, but not dendritic cell activation, including interaction with activated effector T cells. Soluble mediators from activated effector T cells increased expression of ADAMDEC1, CXCL13, CCL18 and CCL19 in macrophages in transwell (no contact co-culture). Expression of these transcripts showed marked heterogeneity between different MMDCs and in response to different stimuli. The MMDC transcripts ADAMDEC1, CXCL13, CCL18 are selective for TCMR and differentiate it from ABMR, AKI and non TCMR in human kidney transplants. The preferential increase in expression of these transcripts in TCMR likely reflects active events in TCMR including macrophage differentiation, activation and macrophage interaction with activated effector T cells. The interaction between these molecules (chemokines and metalloproteases) and their action on target cells and a wide array of substrates (e.g. cytokines, chemokines, adhesion molecules, cell surface molecules, and matrix components) may play role in active control of leukocyte influx, migration and interaction as well as tissue remodeling in response to injury within the inflamed graft during TCMR. Further study of these transcripts may help better understanding of effector mechanisms and active immunologic events selective for TCMR, and may provide potential diagnostic markers and novel therapeutic target.

6.2. TRANSCRIPTS DIFFERENTIATING TCMR FROM NORMAL KIDNEY ARE MOSTLY THOSE TRANSCRIPTS COMMON TO ALL REJECTION

The top transcripts that best differentiate rejection from non rejection are IFNG-induced transcripts (116) and transcripts with high expression in effector T cells (117). There is extensive sharing of molecular features between TCMR and ABMR, despite their differences in histologic lesions. Such extensive molecular sharing is due to the fact that both TCMR and ABMR create an inflammatory compartment largely driven by IFNG production but from different cell types (82;134). In ABMR, NK cells engage donor-specific antibodies bound to HLA on the endothelial surface via Fc receptors leading to the

production of the same set of effector cytokines as antigen-engaged T cells. In TCMR, effector/ effector memory T cells are activated by donor HLA (directly and indirectly) on antigen-presenting cells. Although antigen recognition differs between T cells and NK cells, both produce the same set of effector cytokines and chemokines, thus accounting for the extensive molecular sharing between ABMR and TCMR (135). Additional sharing of transcripts with high expression in both effector T cells and NK cells also contributes to the similarities in gene expression between ABMR and TCMR (96).

Therefore studies comparing rejection biopsies of any type (107;108) (TCMR, ABMR or mixed, individually or combined as one category) to non rejection biopsies, will primarily yield molecular features related to IFNG effects (116) (IFNG-induced transcripts such as the chemokines CXCL9, CXCL10, CXCL11) and effector T cells (CTL-associated transcripts) (117).

6.3. TRANSCRIPTS PREFERENTIALLY INCREASED IN TCMR VERSUS ABMR REFLECT AN IMPORTANT ROLE FOR MMDC IN TCMR

Cells of MMDC series are a major component of the inflammatory infiltrate in allografts undergoing TCMR (27). Some MMDC of donor origin may appear in early transplants but the majority in rejecting allografts are host MMDC that were recruited and activated in response to tissue injury or rejection (40). Although CD68+ macrophages are the most common MMDC population described in inflammatory infiltrate in allografts undergoing TCMR, dendritic cell markers are also detected (136).

Definitive proof of the important role of MMDC in TCMR is to examine how TCMR progresses in the absence of MMDC. This however is not easily achieved as there are multiple defects in cases where a genetic deletion leads to loss of function within MMDC. Alternatively, the depletion of MMDCs from an animal model would work but this approach has several limitations including incomplete depletion. Despite these limitations there is evidence from animal models that MMDCs, particularly macrophages are important players in TCMR. Macrophage depletion provided protection from acute rejection in a rat kidney allograft model. Protection was associated with a reduction in

inducible nitric oxide synthase (iNOS) expression and nitric oxide (NO) generation, but no change in T cell infiltration or activation, suggesting that macrophages themselves may act as effectors of allograft damage (33;137).

Clinical correlations stemming from studies in kidney transplant in kidney transplant patients receiving alemtuzumab (anti-CD52) depletion therapy where lymphocytes including T cells are profoundly depleted. Early clinical rejection in these patients receiving alemtuzumab-based induction therapy displayed significant graft dysfunction despite the presence of minimal lymphocytic infiltrate that did not fulfill the diagnostic threshold for Banff scores (138) Further studies from the same group (35) reported that renal allograft dysfunction and the clinical scenario of TCMR were most closely related to the CD68+ macrophage component of the inflammatory infiltrate, while T cell component showed weaker association with function. This type of rejection was labeled as "monocyte-rich" rejection and strongly argues for an effector role for macrophages in TCMR.

We would predict that the size of the inflammatory compartment will dictate the degree of expression of these macrophage transcripts in grafts. The much larger inflammatory compartment available in TCMR includes the extensive interstitial space. In contrast, the inflammatory compartment in ABMR is limited to the less extended microvascular compartment. In TCMR, cognate effector T cells are recruited to the interstitium where their T cell receptor complex engage MHC antigen complex on APCs leading to T cell activation and effector cytokine release that can act on multiple APCs in close proximity. In ABMR, donor specific antibodies binds to donor HLA on donor endothelial cells and engage the Fc receptors on NK cells leading to their activation within the microvascular lumen but fail to extravasate once engaged. and consequently manifested as microcirculation lesions. This difference in cognate recognition units operating in each type of rejection results in distinct targets and lesions in TCMR and ABMR. In TCMR, effector T cells cross the vascular endothelium, enter the interstitium and target the antigen-rich tubular epithelium, causing the interstitial inflammation and tubulitis diagnostic for TCMR. This is in contrast to ABMR where NK cells are restricted to the microvascular lumen, causing the microvascular inflammation and lesions diagnostic for ABMR. Thus although

there are MMDCs present in both TCMR and ABMR, the number of MMDCs activated by active T cells is simply greater in TCMR than the numbers activated by NK cells in ABMR.

6.4. COMMON PRESENCE OF CLASSICAL AND ALTERNATIVE MACROPHAGE ACTIVATION PHENOTYPES IN TCMR - HETEROGENEITY WITHIN THE MMDC INFILTRATE

Differences between the immune mechanisms active in TCMR and those in ABMR point towards distinct types of macrophage activation. In TCMR, macrophages and effector/ effector memory T cells are recruited into the rejecting allograft, and together form the majority of mononuclear interstitial infiltrate. Macrophages display at least two separate phenotypes in TCMR: 1) classically activated macrophages whose secreted cytokines can damage renal epithelium (82), and 2) alternatively activated macrophages that support tissue repair e.g. via collagen production and features of alternative macrophage activation (139;140). The latter being a phenotype commonly observed in AKI. In ABMR, macrophages are activated in at least two different ways. Following NK cell activation by DSA, the effector cytokines produced by NK cells strongly activate monocytes likely in a manner not unlike what we observed in our co-culture experiments with activated T cells. Monocytes also recognize DSA directly on the endothelial surface and the concurrent complement activation commonly observed. Importantly, the macrophage transcripts prominent in TCMR are not selective for ABMR or AKI (141). The top transcripts with preferentially increased in TCMR compared to ABMR included transcripts associated with alternative macrophage activation such as the chemokine CCL18 and the scavenger receptor CD163 (53). This occurs despite the intense IFNG production, which is a potent inducer of classical macrophage activation phenotype. This finding contradicts the strict dichotomous classic-alternative macrophage (or M1-M2) designation, and the concept that alternative macrophage inducers (e.g. IL-4) and IFNG production (classic macrophage inducer) are mutually exclusive. In mouse kidney transplants, both classical and alternative macrophage phenotypes are also observed despite intense IFNG production during allograft rejection and suggested that they are under independent control in the inflammatory

compartment (118;133). Also, macrophages exhibit a high degree of plasticity that enables them to continuously change their phenotype. An increasing body of evidence suggests that macrophages do not remain committed to a single activation phenotype. They may regress to a resting state and can subsequently be reactivated towards a distinct phenotype. For example, after phagocytosis of apoptotic cells, classically activated macrophages may revert to an alternatively activated macrophage phenotype (55). Also, bidirectional transformation between anti-inflammatory and immunosuppressive phenotypes has been demonstrated in tumor-associated macrophages (55;142;143).

6.5. ROLE FOR CHEMOKINES AND METALLOPROTEASES IN TCMR

It is interesting that the transcripts that differentiate TCMR from ABMR belong to two families of molecules: chemokines (and chemokine receptors) and metalloproteases (ADAM, ADAMTS, MMPs). The presence of such molecules in biopsies with TCMR likely reflects local mechanisms playing key roles in the formation of the inflammatory compartment, control of inflammatory cell recruitment, and traffic within the rejecting allograft . Chemokines are induced in the allograft by the non specific tissue response to injury as well as the alloimmune injury induced by TCMR (144).

Leukocytes recruited to the inflamed allograft during TCMR enter the interstitial tissue following extravasation from circulation following the general process of rolling, tight adhesion, diapedesis and transendothelial migration (26). Leukocyte rolling on selectins on vascular endothelium allows exposure to inflammatory chemokines that may mediate different actions depending on their mode of presentation and differential receptor targeting. For example, CXCL1 immobilized to endothelial proteoglycan matrix binds CXCR2 to mediate firm adhesion by activating monocyte integrins. In contrast, soluble CCL2 binds CCR2 to mediate chemotaxis by inducing monocyte shape changes, spreading and subsequent transendothelial migration (145). Other chemokines may be involved in both adhesion and chemotaxis depending on the differential binding to different receptors. For example, CCL5 immobilized to endothelial proteoglycan binds to CCR1 to mediate firm adhesion, and binds to CCR5 to induce shape changes, and spreading. Then, CCL5 in soluble form mediates subsequent transendothelial migration by binding both CCR1 and

CCR5 (146). Previous studies suggested a role for ADAMs in regulating leukocyte adhesion, and subsequent infiltration to the inflamed tissue. Shedding of adhesion molecules by ADAMs proteolytic activity could decrease adhesiveness of leukocytes or endothelial cells. Moreover, ADAM proteases could generate an excess of a soluble ligand that could antagonize the adhesion receptors on target cells and prevent adhesion (67;69). The movement of macrophages across the endothelial basement membrane is mediated by the action of matrix degradative enzymes produced by macrophages that help to break down the extracellular matrix proteins of the basement membrane, thus facilitating macrophage penetration through the basement membrane (26;73).

While many studies have focused on the mechanisms of transendothelial migration of leukocytes and their recruitment into the graft, little is known about the events that facilitate subsequent migration within the graft. Leukocyte migration within the interstitium depends largely on secretion of chemokines within the inflamed graft by inflammatory cells and renal epithelium, which in turn upregulate expression of chemokine receptors on specific leukocyte populations and promote migration (26;69). The affinity of chemokines for extracellular matrix components may play a role in creating the chemokine gradient required for guiding leukocyte migration within the tissue following transendothelial migration. The creation of such chemokine gradient may be facilitated by the action of matrix degradative enzymes, such as MMPs and ADAMs. Chemokines such as CCL2 and CCL5 can induce production of these enzymes, and thus amplify the potential for further recruitment of additional waves of leukocytes to the inflammatory compartment within the graft (147).

Also, MMPs and ADAMs produced by macrophages may play a role in modulating the inflammatory and immune responses by processing chemokines and extracellular matrix proteins (67;68). Thus they may control the cellular composition and organization of inflammatory compartment within the graft during rejection. For example, macrophages play a role in terminating the initial neutrophil influx to the interstitial tissue at the start of inflammation via action of macrophage metalloproteases on neutrophil attracting chemokines (148;149). In addition, chemokines may play a role in inducing phenotypic

changes in infiltrating macrophages. Murine studies demonstrated that monocytes may be phenotypically polarized by microenvironmental cues to perform specific functional programs (43).

Thus although chemokines and metalloproteases may at first appear as two unrelated set of proteins, it is easy to envision how they may play complementary roles in the orchestration and enhancement of the inflammatory compartment in TCMR.

6.6. MMDC ARE IMPORTANT PLAYERS IN TCMR BUT TCMR REMAINS A T CELL-DEPENDENT PROCESS

The necessity of T cells for development of TCMR is well established, and was confirmed by the fact that allograft rejection does not occur in allografts transplanted into T cell deficient mice (28). Allografts in T cell deficient mice fail to develop histologic lesions of TCMR and their morphology was similar to that of isografts (28). Also, studies demonstrating that the histologic lesions diagnostic for TCMR are caused by T-cell dependent alloimmune response have further underscored the role of T cells in TCMR. T cells recruited to the inflamed tissue during TCMR infiltrate the tubulointerstitium and produce proinflammatory cytokines that activates the renal tubular epithelium to express macrophage-attracting chemokines, such as CCL2 and CCL5, to promote macrophage recruitment and interstitial infiltration (26).

In TCMR, cognate effector T cells are recruited to the interstitium where their T cell receptor complex engage MHC on APCs, initiating the response that leads to the generation of histologic lesions associated with TCMR. Effector T cells cross the vascular endothelium and are trapped in the interstitium and targeting the tubular epithelium, causing the interstitial inflammation and tubulitis diagnostic for TCMR.

Interactions between alloantigen-specific effector T cells and APCs of the MMDC lineage in the interstitium activate effector functions analogous to the mechanism of DTH, where T cell activation is initiated when antigens are presented by APCs to sensitized memory T cells. Antigen presentation and subsequent T-cell activation trigger an influx of macrophages and lymphocytes at the site of antigen exposure, resulting in enhanced

production of inflammatory cytokines including TNF and IFNG. These cytokines mediate multiple proinflammatory actions, including activation of monocytes and macrophages, which are a prominent component of the mononuclear cell infiltrate in allograft rejection and could play a role as mediators of tissue damage (137). This activation causes further amplification of cytokine and chemokine production, along with generation of proteolytic enzymes, nitric oxide, and other soluble factors that help sustain and shape the local inflammatory response in the allograft. Soluble mediators of the DTH response act in an antigen-independent manner to promote chemotaxis and further activation of immune cells (36;37). This was observed in our in vitro transwell co-culture where soluble mediators produced by activated T cells diffused into co-culture medium and stimulated a marked increase of expression of ADAMDEC1, CXCL13, CCL18 and CCL19 in co-cultured macrophages. We also observed increased expression of these transcripts in monocyte-derived macrophages in direct response to TNF stimulation.

6.7. RELATIONSHIP TO TRANSCRIPTS USED BY THE TCMR MOLECULAR CLASSIFIER

The published TCMR molecular classifier for diagnosis of TCMR identified the 30 transcripts most strongly associated with TCMR in 403 kidney transplant biopsies for clinical indications (80). Our data shows that five of top 30 transcripts most frequently used in the TCMR classifier were among the top transcripts preferentially expressed in TCMR compared to ABMR. The top transcripts in the TCMR classifier were defined by the number of times they were selected to distinguish TCMR from other diseases in 1000 tests of random subsets of the 403 biopsies. In agreement with TCMR classifier, the five transcripts (CXCL13, ADAMDEC1, CD8A, BTLA, CD28, and MIR155) not only differentiated TCMR from ABMR in our analyses, but were also highly significant in differentiating TCMR from AKI and non TCMR biopsies. These transcripts reflect the interstitial interaction of cognate effector T cells and APCs (84) and correlates with the histologic lesions of TCMR (80). The molecular TCMR landscape study (84) also confirmed these findings and characterized additional changes that are associated with TCMR compared to other diseases including ABMR.

The differences in the top transcripts in our TCMR versus ABMR class comparison and the TCMR classifier study likely reflect differences in algorithms and filtering strategies used. The TCMR versus ABMR class comparison included all transcripts whereas the TCMR classifier used IQR filter that eliminated transcripts with minimal variability across the data set analyzed. Of note, analyses used to depict the TCMR landscape stopped using an IQR filter once it was noticed that some transcripts with small signal changes showed some of the strongest associations with TCMR e.g. CTLA-4 (84). Other differences are also expected given the differences in the categories of biopsies being compared in each. Our TCMR versus ABMR analysis is a comparison between two rejection classifications where any transcripts common to either type of rejection would be eliminated. The TCMR classifier compared biopsies with TCMR to all other diagnoses where the association strengths would be affected by the number of non-rejection biopsies.

Related to the points discussed above, it also makes sense that any transcripts capable of differentiating TCMR from ABMR should also display a high degree of usage by the TCMR classifier. The ability of ADAMDEC1 and CXCL13 to distinguish TCMR from ABMR, AKI and non TCMR agrees with the fact that these transcripts are among the top 30 transcripts most frequently used in TCMR molecular classifier. Also, the strength of CCL18 to differentiate TCMR from ABMR and non TCMR has also been displayed through other algorithms comparing TCMR and other diagnoses (134). However, the strength of CCL18 in differentiating TCMR from AKI was less than TCMR versus ABMR or non TCMR can be explained by a possible relationship between CCL18 and deposition of collagen and matrix components as part of tissue response to injury that we would expect to be active in AKI and other non rejection diagnoses. Previous studies reported the ability of CCL18 to stimulate collagen formation by fibroblasts (150).

6.8. ADAMDEC1, CXCL13, CCL18, AND CCL19

The ADAM-like decysin 1 (ADAMDEC1) is a secreted protein that belongs to the ADAM (a disintegrin and metalloprotease) family of zinc-binding proteins. Members of the ADAM family are involved in diverse biological processes, including adhesion, migration, proteolysis, fertilization, neurogenesis, muscle development, and the immune response

(70). Unlike all other members of the ADAM family of metalloproteases, ADAMDEC1 is characterized by the following unique features: 1) it possesses a partial disintegrin domain (only half of the disintegrin domain) and lacks the cysteine-rich domain, the transmembrane domain and the cytoplasmic domain. 2) A conserved histidine residue in the zinc-binding region is replaced by aspartate. Despite of these differences, ADAMDEC1 shares important homology with ADAM family members, particularly two closely related members ADAM7 and ADAM28 that share important homology at the amino acid and nucleotide levels. Therefore ADAMDEC1 has been designated as the first member of a novel subclass of the ADAM family (151).

ADAMDEC1 has been reported in association with many human disease processes. Expression of ADAMDEC1 was increased in pulmonary sarcoidosis (111), atherosclerotic plaques (152), intestinal inflammation (153), and intracranial tumors (craniopharyngioma) (110) but decreased expression in colorectal cancer (153).

The cellular source of ADAMDEC1 is unclear but ADAMDEC1 expression was demonstrated in germinal centre dendritic cells in secondary lymphoid organs and, in agreement with our studies, in monocyte-derived macrophages and dendritic cells (122) The substrate for the metalloprotease ADAMDEC1 is still unknown, although TNF/TNFR family members can be potential candidates (151;154). ADAM17/TACE is another member of ADAM family and is active on the membrane-bound pro-TNF, causing its cleavage and release of the active secreted TNF. ADAM17 cleavage of pro-TNF is the principle mechanism for release of TNF from the cell membrane. The fact that ADAMDEC1, unlike other related ADAM proteases, is exclusively secreted, suggests that ADAMDEC1 would be able to act on substrates that are soluble and/or produced at distant sites (151). For example, ADAMDEC1 produced by macrophages may play a role in the shedding of membrane- or matrix- bound substrates within the inflammatory site.

The chemokine CXCL13, B lymphocyte chemoattractant -1 (BLC-1), is a homeostatic chemokine constitutively expressed in secondary lymphoid organs. CXCL13 selectively attracts mature B cells and follicular helper T cells by binding its receptor, CXCR5 thus maximizing the opportunity for a successful antibody response. The role of CXCL13 in

lymphoid tissue has been extensively studied, however its role in peripheral tissues is unclear. The prominence of CXCL13 as one the top transcripts preferentially expressed in TCMR may be partially explained by the well established role for CXCL13/CXCR5 chemokine ligand/receptor pair in recruitment of B cells (155). It also suggests a possible role for myeloid cells of the MMDC lineage, by expression of CXCL13, in B cell recruitment to inflammatory compartment in TCMR. Indeed, CXCL13 receptor (CXCR5) is upregulated on antigen-specific CD4 T cells (156), and it is reasonable for MMDCs in an inflamed compartment to increase the number of encounters between effector T cells and antigen-specific B cells as this would increase the degree of antigen presentation by B cells (157). Previous studies demonstrated an increase in CXCL13 expression in peripheral blood mononuclear cells from kidney transplant recipients during acute rejection (92), and an association between CXCL13 expression and B cell cluster formation in TCMR in humans (158). CXCL13 was also reported to act directly on fibroblasts to increase collagen production (139), suggesting a role in matrix repair and remodeling following tissue injury. The role of B cell infiltration in TCMR is undefined but does not imply ABMR (159). Other B cell-related transcripts such as CD72, a B cell ligand for CD100 and CD5 on T cells were reported as one of the top 30 transcripts prominent in kidney transplant biopsies with TCMR versus other diseases, which support a role for B cells as antigen-specific APCs in sustaining cognate recognition within allograft. In this respect, B cells differ from other APCs in being antigen-specific, capable of undergoing clonal expansion and maturation and help sustaining T cell immune response (84).

The chemokine CCL18 is an orphan chemokine with unknown receptor and no rodent homolog. Little is known about CCL18 and its biological significance. In 1997, three different research groups reported the identification of genes encoding for novel chemokines; Adema et al. identified a chemokine termed dendritic cell chemokine 1 (DC-CK1) (160), Hieshima et al. identified a chemokine termed pulmonary and activation-regulated chemokine (PARC) (161) and Wells and Peitsch (162) identified a chemokine termed macrophage inflammatory protein 4 (MIP-4). Later, it was known that DC-CK1, PARC and MIP-4 were all describing C-C chemokine ligand CCL18. Early in vitro studies reported that CCL18 act as chemoattractant for naive T cells. Adema et al. reported that

CCL18 expression was not detected in freshly isolated monocytes and human dendritic cells expressed high levels of CCL18 that preferentially attracts naive T cells, and suggested an important role for CCL18 in induction of immune responses (160). Also, CCL18 expression was demonstrated in germinal centre dendritic cells and was suggested to attract CD38 negative mantle zone B cells play a role in inducing the primary immune response. In addition, CCL18 mRNA and protein expression was demonstrated in T cell areas and germinal centre of secondary lymphoid tissues, consistent with dendritic cell distribution (163). Little is known about CCL18 in non lymphoid tissues and there are discrepancies within the literature. For example, while a study reported CCL18 expression in CD11c+ dendritic cells (160), another study reported that CCL18 expression was not detected in CD11c blood dendritic cells (164). Also, expression of CCL18 mRNA was demonstrated in immature and mature monocyte-derived dendritic cells, and decreased in response to stimulation with CD40L (165). CCL18 has been reported in association with other pathological conditions including gastric, hepatocellular and breast tumors. CCL18 produced by tumor-associated macrophages was suggested to play a role in promoting angiogenesis and tumor progression and metastasis (154). Also, CCL18 may play a role in matrix repair and remodeling after tissue injury through direct action on fibroblasts to increase collagen production (140;150).

The chemokine CCL19/ macrophage inflammatory protein-3β (MIP-3β) is a homeostatic chemokine, constitutively produced in secondary lymphoid organs. CCL19 plays a critical role in initiation of the primary immune response through interaction with its chemokine receptor CCR7. Both CCL19 and another homeostatic chemokine CCL21 are involved in mediating the encounter between mature antigen-bearing dendritic cells and the rare antigen-specific T cells (166;166). While chemokines are commonly known to induce directional cell migration, CCL19 secreted by mature dendritic cells has the ability to induce random motility of naive T cells. This ability is unique to CCL19 and was not demonstrated with other chemokines including CCL21. This random motility increases naive T cell scanning of mature dendritic cells and naive T cell response to rare cognate antigen (167-169). Although the role of CCL19/CCR7 chemokine ligand/receptor pair in lymphoid tissue has been extensively studied, their role in peripheral tissues is unclear.

Expression of CCL19 was demonstrated in mature dendritic cells in human lymph nodes, and mature *in vitro* differentiated dendritic cells (170; 171). Mature dendritic cells also express CCR7, the receptor for CCL19. CCR7 signaling has been reported to increase the avidity of integrins (e.g LFA-1) for their ligands (172). Thus CCL19 may promote the formation of more stable contact encounter between APC and T cells by inducing conformational change of LFA-1. Thus the role for the expression of this homeostatic chemokine in rejecting allografts may be to guide the motility of APCs, to enhance its encounter with effector T cells and continue promoting the alloimmune response.

6.9. HERETEROGENEITY IN MMDC EXPRESSION OF ADAMDEC1, CXCL13, CCL18, AND CCL19

a) Role for differentiation

We sought to expand our understanding of TCMR immunobiology based on changes in gene expression in biopsies by cross-referencing them with gene expression in *in vitro* cultured primary human cells. In the human cell panel, ADAMDEC1, CXCL13 and CCL18 were mainly expressed in myeloid-derived cells (macrophages). Further study of expression of these three transcripts in different myeloid cell types, including monocytes, macrophages, and dendritic cells, demonstrated heterogeneity in the expression pattern of these three transcripts among cell types, with strong expression mainly in differentiated macrophages. We showed that ADAMDEC1 was weakly expressed in freshly isolated monocytes, but expression markedly increased upon monocyte differentiation into macrophages (24 hours macrophages and M-CSF macrophages), but not into dendritic cells. Our data demonstrates that ADAMDEC1 is a characteristic feature for macrophage differentiation, and agrees with previous studies showing marked expression of ADAMDEC1 in monocyte-derived macrophages but not in monocyte-derived dendritic cells (122). The association between ADAMDEC1 expression and macrophage differentiation may be related to acquiring a specific functional phenotype along the broad spectrum of macrophage phenotypes. Indeed, the ADAMDEC1 promoter region contains the binding sites for the transcription factors PU.1 and NF-Y. PU.1 is important for myeloid cell differentiation and is a critical transcription factor for macrophage differentiation,

survival, and proliferation through its regulation of M-CSF receptor expression (173). NF-Y controls transcription of human macrophage-specific genes involved in the acquisition of a functional macrophage phenotype e.g. ferritin heavy-chain and MHC class II genes (174). Differentiation of macrophages or dendritic cells also induced expression of CXCL13 and CCL18. In agreement with our findings, $CD68^{+}$ CXCL13-expressing macrophages are found in inflammatory areas devoid of follicular dendritic cells (known to express CXCL13) (175).

b) <u>Role for soluble mediators and macrophage activation</u>

In vitro gene expression of ADAMDEC1, CXCL13, CCL18 and CCL19 is most strongly regulated by macrophage activation and by soluble factors released from activated T cells suggestive of the immunological process active in TCMR. We showed that macrophages activated with TNF or LPS increased expression of ADAMDEC1, CXCL13, CCL18 and CCL19. This increase was strongest in 24 hours monocyte-derived macrophages. The selection of these different activation factors aimed at modeling the cell-cell interaction e.g. CD40L, the proinflammatory cytokine environment in rejecting grafts (e.g. TNF) and the most well-characterized and robust activation stimulus, LPS. Also, our *in vitro* data showed that expression of ADAMDEC1, CXCL13, CCL18 and CCL19 was most strongly regulated by the soluble factors released from activated T cells during contact-independent interaction with macrophages in transwell co-culture. This could explain the strong correlation between expression of ADAMDEC1, CXCL13, CCL18 and CCL19 and macrophage- and T cell- transcript burdens in kidney biopsies. The stronger correlation of CXCL13 and CCL19 expression to the T cell transcript burden than to macrophage transcript burden in biopsies may result from multiple direct and indirect contributions from T cells to expression of expression of these transcripts. For example, direct contribution via CXCL13 expression in activated T cells as we demonstrate in the current study and corroborated by other studies (176), and indirect contribution by increasing CXCL13 and CCL19 expression in macrophages through soluble mediators and/or perhaps cell-cell contact.

Surprisingly, not all transcripts showed increased expression in cultures where macrophages were in direct contact with activated T cells. Despite the increase in expression of ADAMDEC1, CXCL13, CCL18, and CCL19 in macrophages in response to soluble mediators released from activated T cells during their contact-independent interaction in transwell co-culture, expression of ADAMDEC1 decreased and CCL18 did not significantly change in macrophages during contact co-culture with activated T cells. As we do not know the ADAMDEC1 substrate or the CCL18 receptor, we cannot fully explain this finding, but we can only speculate that there may be a negative feedback mechanism involved in regulation of expression of ADAMDEC1 and/or CCL18. For example, if ADAMDEC1 acts on cellular surface molecules involved in cell-cell contact interactions, it is likely that contact interaction between T cells and macrophages may initiate a negative feedback to downregulate ADAMDEC1 expression upon cellular contact.

The degree of expression for all four transcripts was much higher in macrophages compared to dendritic cells. Nevertheless, we cannot exclude a role for dendritic cells in molecular features of TCMR particularly due to lack of precise definition of dendritic cell population and origin in allografts and phenotypic heterogeneity in dendritic cells. For example, follicular dendritic cells, a known source for CXCL13 in lymphoid follicles, were reported to have the ability to differentiate from precursor pericytes in inflamed tissue (177), which can be encountered in rejecting allografts. Also, dendritic cells resident in secondary lymphoid tissues are distinct from those in peripheral tissues, and dendritic cells continuously alter their chemokine production at different time points of their maturation stages (178).

6.10. CHALLENGES IN STUDYING MMDC IN INFLAMED ALLOGRAFTS

Myeloid cells are characterized by a high degree of heterogeneity and plasticity, which poses a challenge to studying MMDC in inflamed allografts. While most studies consider macrophages and dendritic cells as entirely distinct cells with respect to cellular function, in practice these cells occupy overlapping anatomical sites in peripheral tissues. Also, there is growing body of evidence that demonstrates a marked degree of plasticity of cell surface

markers and functions within myeloid cells of the MMDC population (41). It is difficult to firmly associate single markers with specific subsets of MMDCs, since markers are largely shared between different MMDC populations. A number of key markers previously thought to be specific for a distinct MMDC phenotype are now known to be non specific or shared between macrophages and dendritic cells. Segerer et al. (59) examined an array of commonly used macrophage and dendritic cell markers in 55 human kidney biopsies and reported abundant tubulointerstitial dendritic cells expressing the myeloid dendritic cell marker DC-SIGN (dendritic cell-specific ICAM-3 grabbing nonintegrin) coexpress the macrophage marker CD68. Moreover, the macrophage marker CD68 is expressed by other non-myeloid cells including fibroblasts and endothelial cells (61). Thus the assignment of MMDC markers to functional groups is problematic because the markers derived in other tissue compartments need to be re-evaluated in the rejecting kidneys.

MMDCs can also reversibly change their functional phenotype depending on their microenvironment (43). The origin and differentiation cues for myeloid cells of the MMDC series in vivo are unclear and in vitro culture systems may not fully recapitulate the complexities of their in vivo differentiation. Moreover, the marked plasticity of MMDCs further complicates interpretation of data. Indeed, murine studies suggest that microenvironmental signals can trigger monocyte differentiation towards distinct macrophage phenotypes required to perform specific functions. Also, the ability of cells of MMDC to respond to microenvironment cues by changing their phenotypes was suggested by previous studies demonstrating the ability of myeloid dendritic cells to revert to macrophage phenotypes (179-181) or to display functional and phenotypic characteristics of multinucleated osteoclasts (182).

Although human MMDC differentiation cues in vivo are incompletely understood, it is sensible to assume that the extremely tailored in vitro culture environment using individual or combined cocktail of limited mediators will be able to recapture the complex dynamics of the in vivo microenvironment driving the inflammatory events that are continuously changing in response to changes in the composition and cellular infiltrate. This poses a challenge for translating in vitro findings and applying them to the more complex in vivo

setting. Even the functional distinction between dendritic cells and macrophages have been challenged by studies suggesting the ability of macrophages (CD11c –) to effectively present antigen and stimulate naive CD8 T cells in vivo (62) and subcapsular splenic macrophages to effectively present antigen to B cells (183). Moreover, macrophages are known to change their cell surface antigen expression depending on their tissue site in human and mouse. For example, in the kidney, expression of peroxisome proliferator-activated receptor-gamma (PPARγ) was expressed in interstitial, but not glomerular macrophages in diabetic nephropathy, while CCR5 was expressed in glomerulonephritis (184-186). Thus the concept of using cell markers as surrogates for macrophages and myeloid dendritic cells and their function within the kidney is increasingly questioned. It is more sensible to consider these cells as cells that exist along a spectrum where they can express variable overlapping sets of markers (60).

As implied above, our in vitro models also suffer from several limitations. The main limitation is that it is not possible to emulate the puzzling broad spectrum of macrophage populations and activation states that are likely to be present in highly inflamed tissues such as rejecting allografts (40). One key differentiation effect that is difficult to model *in vitro* is the effect of vascular extravasation which recruited monocytes must undergo as they enter the inflamed allograft. Further, macrophage activation stemming from the dynamic interaction of macrophages with the extracellular matrix (187) is also difficult to model in vitro. Despite these limitations, the primary human cells used in our in vitro model have many advantages over human cell lines (e.g. THP-1) in terms of heterogeneity and cell behavior which are more representative of the in vivo population. Also, the primary cells' differentiation and activation phenotypes are all derived from the original, primary precursor - monocytes, in contrast to the cell lines derived from transformed cells at different maturation and differentiation stages. Monocytic cell line characteristics may also change with repeated passages, and their differentiation to macrophages is difficult to attain, requiring strong chemical stimuli as in PMA/ ionomycin used for THP-1 cells.

The human kidney transplant biopsies and *in vitro* primary cell cultures were the best available approach to study ADAMDEC1, CXCL13 and CCL18. Murine models cannot be

used to study these molecules; ADAMDEC1, CXCL13 and CCL19 were not strongly unregulated in mouse kidney transplant rejection and CCL18 lacks a murine homolog (154). In this study we extended our work in defining the molecular features of human TCMR, and characterized macrophage-associated transcripts preferentially increased in TCMR with respect to macrophage differentiation and activation states. Further characterization of such molecules will advance our understanding of the immune mechanisms active in TCMR and perhaps provide potential diagnostic markers or future therapeutic targets.

6.11. PROPOSED MODEL FOR ROLE OF MMDC TOP TRANSCRIPTS IN TCMR

The recently published model of TCMR suggests that cognate interactions between effector T cells and APCs of the MMDC series activate effector functions analogous to DTH. Soluble factors released from effector T cells and/or macrophages can promote chemotaxis, immune cell infiltration and activation (36;37;189), and can contribute to epithelial deterioration and tissue damage (36;37;189). In alignment with this TCMR model, we propose that the MMDC transcripts preferentially increased in allografts with TCMR versus ABMR reflect the immunologic events active in TCMR including continuous differentiation of recruited monocytes to macrophages and additional activation of recruited macrophages by effector T cells activated in the parenchyma. The top transcripts preferentially increased in TCMR versus ABMR are also increased following *in vitro* differentiation of monocytes to macrophages, and by activation of macrophages. Contact independent macrophage activation occurs in response to soluble factors, such as the inflammatory cytokine TNF, released during effector T cell activation and interactions between activated effector T cells and APC of the MMDC series (Figure 6.1). The responding activated macrophages will increase expression of MMDC transcripts, such as ADAMDEC1, CXCL13 and CCL18, among others. These macrophage products can mediate many actions that are likely involved in TCMR. For example, ADAMDEC1 may function as a metalloprotease on soluble or membrane/matrix bound substrates (e.g. cytokines, chemokines, or matrix components) in a manner similar to the related ADAM

family protease, ADAM 17, that acts on the membrane-anchored TNF precursor to release soluble TNF (151).

The chemokines preferentially associated with TCMR may play dual roles in aggravating the rejection process while at the same time aiding with the repair processes activated following the immune mediated injury in TCMR. CXCL13 may promote immune cell recruitment and localization within the allograft including B cells, further adding to the degree of antigen presentation (84;157). CXCL13 may also contribute to tissue repair and matrix remodeling by stimulating collagen production in fibroblasts . CCL18 may enhance inflammation, by attracting lymphocytes and immature dendritic cells, and aid with tissue repair and remodeling by promoting the maturation of IL-10 producing macrophages (191). The chemokine CCL19 may also be involved in guiding leukocyte migration out of the graft and thus enhancing the generation of effector T cells as well as contributing to tissue repair response and matrix remodeling by stimulating collagen production in fibroblasts.

Overall, the preferential high expression of all three chemokines and the metalloprotease in TCMR may possibly play a role in guiding migration of infiltrating leukocytes, control localization of interacting immune cells (e.g effector T cells and APCs) in the graft and direct leukocyte exit from peripheral tissues (graft) to secondary lymphoid organs. They can also act on many substrates and target cells causing the release and/or activation of soluble mediators involved in inflammation. Further study of the biology of these molecules will help unveil more details about the cause-effect relationship between expression of these molecules and the cellular infiltration and histologic lesions observed in TCMR.

6.12. FIGURES

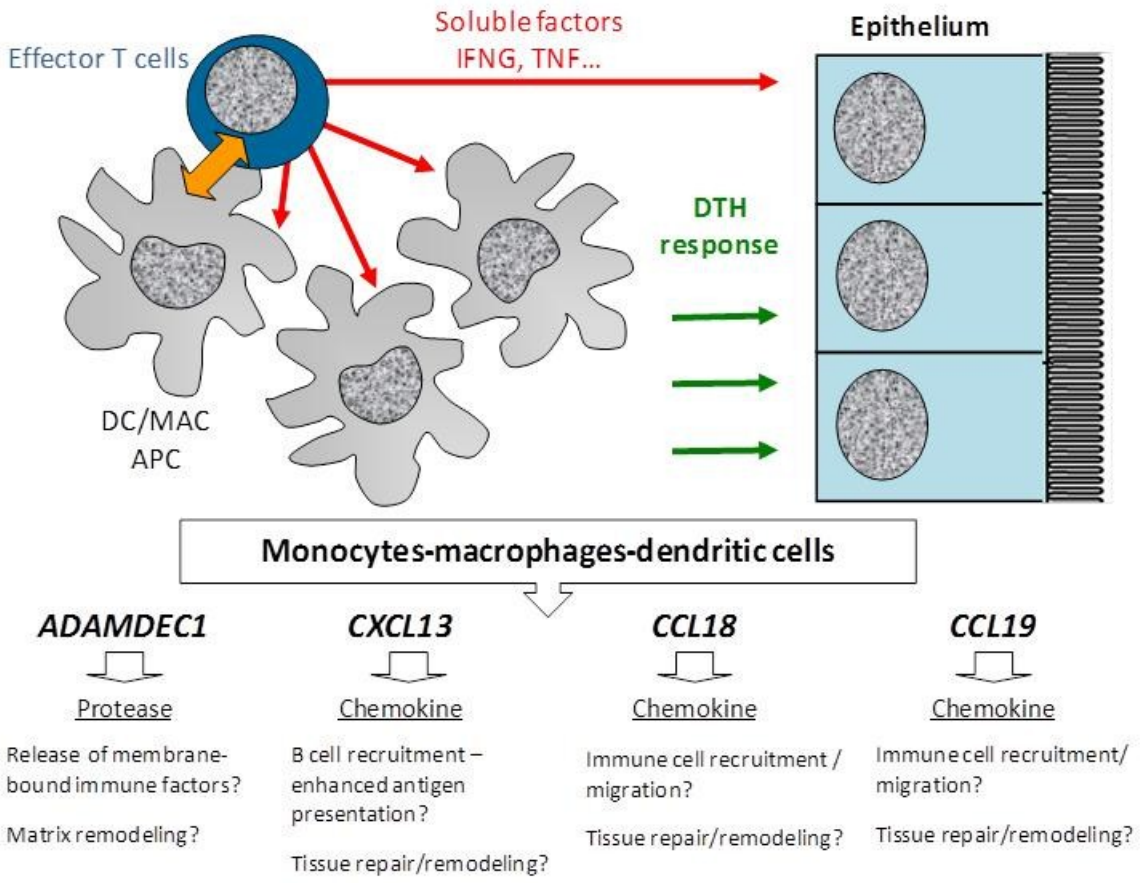

Figure 6.1. Proposed model for role of MMDC top transcripts in TCMR

BIBLIOGRAPHY

(1) Heeger PS. T-cell allorecognition and transplant rejection: a summary and update. Am J Transplant 2003 May;3(5):525-33.

(2) Lakkis FG, Arakelov A, Konieczny BT, Inoue Y. Immunologic 'ignorance' of vascularized organ transplants in the absence of secondary lymphoid tissue. Nature Medicine 2000;6:686-8.

(3) Zhou P, Hwang KW, Palucki D, Kim O, Newell KA, Fu YX, et al. Secondary lymphoid organs are important but not absolutely required for allograft responses. Am J Transplant 2003 Mar;3(3):259-66.

(4) Rogers NJ, Lechler RI. Allorecognition. Am J Transplant 2001 Jul;1(2):97-102.

(5) Zand MS, Bose A, Vo T, Coppage M, Pellegrin T, Arend L, et al. A renewable source of donor cells for repetitive monitoring of T- and B-cell alloreactivity. Am J Transplant 2005 Jan;5(1):76-86.

(6) Biedermann BC, Pober JS. Human endothelial cells induce and regulate cytolytic T cell differentiation. Journal of Immunology 1998 Nov 1;161(9):4679-87.

(7) Adams AB, Williams MA, Jones TR, Shirasugi N, Durham MM, Kaech SM, et al. Heterologous immunity provides a potent barrier to transplantation tolerance. J Clin Invest 2003 Jun;111(12):1887-95.

(8) von Andrian UH, MacKay CR. T-cell function and migration. Two sides of the same coin. N Engl J Med 2000 Oct 5;343(14):1020-34.

(9) Magee CN, Boenisch O, Najafian N. The role of costimulatory molecules in directing the functional differentiation of alloreactive T helper cells. Am J Transplant 2012 Oct;12(10):2588-600.

(10) Reis e Sousa. Dendritic cells in a mature age. Nat Rev Immunol 2006 Jun;6(6):476-83.

(11) Larsen CP, Elwood ET, Alexander DZ, Ritchie SC, Hendrix R, Tucker-Burden C, et al. Long-term acceptance of skin and cardiac allografts after blocking CD40 and CD28 pathways. Nature 1996;381:434-8.

(12) Curtsinger JM, Schmidt CS, Mondino A, Lins DC, Kedl RM, Jenkins MK, et al. Inflammatory cytokines provide a third signal for activation of naive CD4+ and CD8+ T cells. Journal of Immunology 1999 Mar 15;162(6):3256-62.

(13) Racusen LC, Solez K, Colvin RB, Bonsib SM, Castro MC, Cavallo T, et al. The Banff 97 working classification of renal allograft pathology. Kidney Int 1999 Feb;55(2):713-23.

(14) Einecke G, Sis B, Reeve J, Mengel M, Campbell PM, Hidalgo LG, et al. Antibody-Mediated Microcirculation Injury Is the Major Cause of Late Kidney Transplant Failure. Am J Transplant 2009;9(11):2520-31.

(15) Loupy A, Hill GS, Jordan SC. The impact of donor-specific anti-HLA antibodies on late kidney allograft failure. Nat Rev Nephrol 2012;8(6):348-57.

(16) Sellares J, De Freitas D, Mengel M, Reeve J, Einecke G, Sis B, et al. Understanding the causes of kidney transplant failure: the dominant role of antibody-mediated rejection and non-adherence. Am J Transplant 2012 Feb;12(2):388-99.

(17) Van Kooten C, Banchereau J. CD40-CD40 Ligand. J Leuk Biol 2000;67:2-17.

(18) Terasaki PI. Humoral theory of transplantation. Am J Transplant 2003 Jun;3(6):665-73.

(19) Zhang X, Reed EF. Effect of antibodies on endothelium. Am J Transplant 2009 Nov;9(11):2459-65.

(20) Hidalgo LG, Sis B, Sellares J, Campbell PM, Mengel M, Einecke G, et al. NK cell transcripts and NK cells in kidney biopsies from patients with donor-specific antibodies: evidence for NK cell involvement in antibody-mediated rejection. Am J Transplant 2010;10(8):1812-22.

(21) Akiyoshi T, Hirohashi T, Alessandrini A, Chase CM, Farkash EA, Neal SR, et al. Role of complement and NK cells in antibody mediated rejection. Hum Immunol 2012 Jul 28;73(12):1226-32.

(22) Feucht HE. Complement C4d in graft capillaries -- the missing link in the recognition of humoral alloreactivity. Am J Transplant 2003 Jun;3(6):646-52.

(23) Racusen LC, Colvin RB, Solez K, Mihatsch MJ, Halloran PF, Campbell PM, et al. Antibody-mediated rejection criteria - an addition to the Banff 97 classification of renal allograft rejection. Am J Transplant 2003 Jun;3(6):708-14.

(24) Colvin RB. Antibody-mediated renal allograft rejection: diagnosis and pathogenesis. J Am Soc Nephrol 2007 Apr;18(4):1046-56.

(25) Solez K, Colvin RB, Racusen LC, Haas M, Sis B, Mengel M, et al. Banff 07 classification of renal allograft pathology: updates and future directions. Am J Transplant 2008 Apr;8(4):753-60.

(26) Sean Eardley K, Cockwell P. Macrophages and progressive tubulointerstitial disease. Kidney Int 2005 Aug;68(2):437-55.

(27) Hancock WW, Thomson NM, Atkins RC. Composition of Interstitial Cellular Infiltrate Identified by Monoclonal-Antibodies in Renal Biopsies of Rejecting Human Renal-Allografts. Transplant 1983;35(5):458-63.

(28) Jabs WJ, Sedlmeyer A, Ramassar V, Hidalgo LG, Urmson J, Afrouzian M, et al. Heterogeneity in the evolution and mechanisms of the lesions of kidney allograft rejection in mice. Am J Transplant 2003 Dec;3(12):1501-9.

(29) Halloran PF, Urmson J, Ramassar V, Melk A, Zhu LF, Halloran BP, et al. Lesions of T-cell-mediated kidney allograft rejection in mice do not require perforin or granzymes A and B. Am J Transplant 2004 May;4(5):705-12.

(30) Einecke G, Fairhead T, Hidalgo LG, Sis B, Turner P, Zhu LF, et al. Tubulitis and Epithelial Cell Alterations in Mouse Kidney Transplant Rejection Are Independent of CD103, Perforin or Granzymes A/B. Am J Transplant 2006;6(9):2109-20.

(31) Kayser D, Einecke G, Famulski KS, Mengel M, Sis B, Zhu LF, et al. Donor Fas is not necessary for T-cell-mediated rejection of mouse kidney allografts. Am J Transplant 2008 Oct;8(10):2049-55.

(32) Kobayashi K, Kaneda K, Kasama T. Immunopathogenesis of delayed-type hypersensitivity. Microsc Res Tech 2001 May 15;53(4):241-5.

(33) Wyburn KR, Jose MD, Wu H, Atkins RC, Chadban SJ. The role of macrophages in allograft rejection. Transplant 2005 Dec 27;80(12):1641-7.

(34) Rowshani AT, Vereyken EJ. The role of macrophage lineage cells in kidney graft rejection and survival. Transplant 2012 Aug 27;94(4):309-18.

(35) Girlanda R, Kleiner DE, Duan Z, Ford EAS, Wright EC, Mannon RB, et al. Monocyte infiltration and kidney allograft dysfunction during acute rejection. Am J Transplant 2008 Mar;8(3):600-7.

(36) Miura M, Morita K, Kobayashi H, Hamilton TA, Burdick MD, Strieter RM, et al. Monokine induced by IFN-gamma is a dominant factor directing T cells into murine cardiac allografts during acute rejection. Journal of Immunology 2001 Sep 15;167(6):3494-504.

(37) Kapoor A, Morita K, Engeman TM, Koga S, Vapnek EM, Hobart MG, et al. Early expression of interferon-gamma inducible protein 10 and monokine induced by interferon-gamma in cardiac allografts is mediated by CD8+ T cells. Transplant 2000 Mar 27;69(6):1147-55.

(38) Ricardo SD, van GH, Eddy AA. Macrophage diversity in renal injury and repair. J Clin Invest 2008 Nov;118(11):3522-30.

(39) Hume DA, Ross IL, Himes SR, Sasmono RT, Wells CA, Ravasi T. The mononuclear phagocyte system revisited. J Leuk Biol 2002 Oct;72(4):621-7.

(40) Gordon S, Taylor PR. Monocyte and macrophage heterogeneity. Nat Rev Immunol 2005 Dec;5(12):953-64.

(41) Geissmann F, Gordon S, Hume DA, Mowat AM, Randolph GJ. Unravelling mononuclear phagocyte heterogeneity. Nat Rev Immunol 2010 Jun;10(6):453-U92.

(42) Martinez FO, Gordon S, Locati M, Mantovani A. Transcriptional profiling of the human monocyte-to-macrophage differentiation and polarization: New molecules and patterns of gene expression. Journal of Immunology 2006 Nov 15;177(10):7303-11.

(43) Stout RD, Jiang C, Matta B, Tietzel I, Watkins SK, Suttles J. Macrophages sequentially change their functional phenotype in response to changes in microenvironmental influences. J Immunol 2005 Jul 1;175(1):342-9.

(44) Gorgani NN, Ma Y, Clark HF. Gene signatures reflect the marked heterogeneity of tissue-resident macrophages. Immunol Cell Biol 2008 Mar;86(3):246-54.

(45) Geissmann F, Manz MG, Jung S, Sieweke MH, Merad M, Ley K. Development of monocytes, macrophages, and dendritic cells. Science 2010 Feb 5;327(5966):656-61.

(46) Taylor PR, Martinez-Pomares L, Stacey M, Lin HH, Brown GD, Gordon S. Macrophage receptors and immune recognition. Annual Review of Immunology 2005;23:901-44.

(47) Mosser DM, Edwards JP. Exploring the full spectrum of macrophage activation. Nat Rev Immunol 2008 Dec;8(12):958-69.

(48) Gordon S, Pluddemann A, Martinez EF. Macrophage heterogeneity in tissues: phenotypic diversity and functions. Immunol Rev 2014 Nov;262(1):36-55.

(49) Wang Y, Harris DC. Macrophages in renal disease. J Am Soc Nephrol 2011 Jan;22(1):21-7.

(50) Broichhausen C, Riquelme P, Geissler EK, Hutchinson JA. Regulatory macrophages as therapeutic targets and therapeutic agents in solid organ transplantation. Curr Opin Organ Transplant 2012 Aug;17(4):332-42.

(51) Murray PJ, Allen JE, Biswas SK, Fisher EA, Gilroy DW, Goerdt S, et al. Macrophage activation and polarization: nomenclature and experimental guidelines. Immunity 2014 Jul 17;41(1):14-20.

(52) Mosser DM. The many faces of macrophage activation. J Leuk Biol 2003 Feb;73(2):209-12.

(53) Gordon S, Martinez FO. Alternative Activation of Macrophages: Mechanism and Functions. Immunity 2007;32:593-604.

(54) Fleming BD, Mosser DM. Regulatory macrophages: setting the threshold for therapy. Eur J Immunol 2011 Sep;41(9):2498-502.

(55) Duffield JS. The inflammatory macrophage: a story of Jekyll and Hyde. Clin Sci 2003 Jan 1;104(1):27-38.

(56) Ziegler-Heitbrock L, Ancuta P, Crowe S, Dalod M, Grau V, Hart DN, et al. Nomenclature of monocytes and dendritic cells in blood. Blood 2010 Oct 21;116(16):e74-e80.

(57) Geissmann F. The origin of dendritic cells. Nat Immunol 2007 Jun;8(6):558-60.

(58) Epelman S, Lavine KJ, Randolph GJ. Origin and functions of tissue macrophages. Immunity 2014 Jul 17;41(1):21-35.

(59) Segerer S, Heller F, Lindenmeyer MT, Schmid H, Cohen CD, Draganovici D, et al. Compartment specific expression of dendritic cell markers in human glomerulonephritis. Kidney Int 2008 Jul;74(1):37-46.

(60) Ferenbach D, Hughes J. Macrophages and dendritic cells: what is the difference? Kidney Int 2008 Jul;74(1):5-7.

(61) Gottfried E, Kunz-Schughart LA, Weber A, Rehli M, Peuker A, Muller A, et al. Expression of CD68 in non-myeloid cell types. Scand J Immunol 2008 May;67(5):453-63.

(62) Pozzi LA, Maciaszek JW, Rock KL. Both dendritic cells and macrophages can stimulate naive CD8 T cells in vivo to proliferate, develop effector function, and differentiate into memory cells. J Immunol 2005 Aug 15;175(4):2071-81.

(63) Segerer S, Cui Y, Eitner F, Goodpaster T, Hudkins KL, Mack M, et al. Expression of chemokines and chemokine receptors during human renal transplant rejection. Am J Kidney Dis 2001 Mar;37(3):518-31.

(64) Mueller SN, Hosiawa-Meagher KA, Konieczny BT, Sullivan BM, Bachmann MF, Locksley RM, et al. Regulation of homeostatic chemokine expression and cell trafficking during immune responses. Science 2007 Aug 3;317(5838):670-4.

(65) Ebert LM, Schaerli P, Moser B. Chemokine-mediated control of T cell traffic in lymphoid and peripheral tissues. Mol Immunol 2005 May;42(7):799-809.

(66) Halloran PF. T Cell Mediated Rejection of Kidney Transplants: A Personal Viewpoint. Am J Transplant 2010;10(5):1126-34.

(67) Tan RJ, Liu Y. Matrix metalloproteinases in kidney homeostasis and diseases. Am J Physiol Renal Physiol 2012 Jun 1;302(11):F1351-F1361.

(68) Rodriguez D, Morrison CJ, Overall CM. Matrix metalloproteinases: What do they not do? New substrates and biological roles identified by murine models and proteomics. Biochim Biophys Acta 2009 Oct 1.

(69) Reiss K, Ludwig A, Saftig P. Breaking up the tie: disintegrin-like metalloproteinases as regulators of cell migration in inflammation and invasion. Pharmacol Ther 2006 Sep;111(3):985-1006.

(70) Primakoff P, Myles DG. The ADAM gene family: surface proteins with adhesion and protease activity. Trends Genet 2000 Feb;16(2):83-7.

(71) Racusen LC, Halloran PF, Solez K. Banff 2003 meeting report: new diagnostic insights and standards. Am J Transplant 2004 Oct;4(10):1562-6.

(72) Haas M. The Revised (2013) Banff Classification for Antibody-Mediated Rejection of Renal Allografts: Update, Difficulties, and Future Considerations. Am J Transplant 2016;16(5):1352-7.

(73) Haas M, Sis B, Racusen LC, Solez K, Glotz D, Colvin RB, et al. Banff 2013 Meeting Report: Inclusion of C4d-Negative Antibody-Mediated Rejection and Antibody-Associated Arterial Lesions. Am J Transplant 2014;14(2):272-83.

(74) Sis B, Halloran PF. Endothelial transcripts uncover a previously unknown phenotype: C4d-negative antibody-mediated rejection. Curr Opin Organ Transplant 2010 Feb;15(1):42-8.

(75) Sis B, Einecke G, Chang J, Hidalgo LG, Mengel M, Kaplan B, et al. Cluster analysis of lesions in kidney transplant biopsies: Microcirculation changes, tubulointerstitial inflammation, and scarring. Am J Transplant 2010;10(2):421-30.

(76) Salazar ID, Merino LM, Chang J, Halloran PF. Reassessing the Significance of Intimal Arteritis in Kidney Transplant Biopsy Specimens. J Am Soc Nephrol 2015 Dec;26(12):3190-8.

(77) Marcussen N, Olsen TS, Benediktsson H, Racusen L, Solez K. Reproducibility of the Banff classification of renal allograft pathology. Inter- and intraobserver variation. Transplant 1995;60:1083-9.

(78) Furness PN, Taub N, Assmann KJ, Banfi G, Cosyns JP, Dorman AM, et al. International variation in histologic grading is large, and persistent feedback does not improve reproducibility. Am J Surg Pathol 2003 Jun;27(6):805-10.

(79) Reeve J, Einecke G, Mengel M, Sis B, Kayser N, Kaplan B, et al. Diagnosing rejection in renal transplants: a comparison of molecular- and histopathology-based approaches. Am J Transplant 2009 Aug;9(8):1802-10.

(80) Reeve J, Sellares J, Mengel M, Sis B, Skene A, Hidalgo L, et al. Molecular diagnosis of T cell-mediated rejection in human kidney transplant biopsies. Am J Transplant 2013;13(3):645-55.

(81) Reeve J, Chang J, Salazar IDR, Lopez MM, Halloran PF. Using molecular phenotyping to guide improvements in the histologic diagnosis of T cell-mediated rejection. Am J Transplant 2016;16(4):1183-92.

(82) Mueller TF, Einecke G, Reeve J, Sis B, Mengel M, Jhangri.G., et al. Microarray analysis of rejection in human kidney transplants using pathogenesis-based transcript sets. Am J Transplant 2007;7(12):2712-22.

(83) Famulski KS, Einecke G, Sis B, Mengel M, Hidalgo LG, Kaplan B, et al. Defining the Canonical Form of T-Cell-Mediated Rejection in Human Kidney Transplants. Am J Transplant 2010;10(4):810-20.

(84) Venner JM, Famulski K, Badr D, Hidalgo LG, Chang J, Halloran PF. Molecular landscape of T cell-mediated rejection in human kidney transplants: Prominence of CTLA4 and PD ligands. Am J Transplant 2014;14(11):2565-76.

(85) Kaser A, Blumberg RS. Survive an innate immune response through XBP1. Cell Res 2010 May;20(5):506-7.

(86) Halloran PF, Pereira AB, Chang J, Matas A, Picton M, De Freitas D, et al. Microarray diagnosis of antibody-mediated rejection in kidney transplant biopsies: an international prospective study (INTERCOM). Am J Transplant 2013;13(11):2865-74.

(87) Venner JM, Hidalgo LG, Famulski KS, Chang J, Halloran PF. The molecular landscape of antibody-mediated kidney transplant rejection: Evidence for NK involvement through CD16a Fc receptors. Am J Transplant 2015;15(5):1336-48.

(88) Loupy A, Haas M, Solez K, Racusen L, Glotz D, Seron D, et al. The Banff 2015 Kidney Meeting Report: Current Challenges in Rejection Classification and Prospects for Adopting Molecular Pathology. Am J Transplant 2017 Jan;17(1): 28-41.

(89) Reeve J, Bohmig GA, Eskandary F, Einecke G, Lefaucheur C, Loupy A, et al. Assessing rejection-related disease in kidney transplant biopsies based on archetypal analysis of molecular phenotypes. JCI Insight 2017;2(12).

(90) Halloran PF, Reeve J, Pereira AB, Hidalgo LG, Famulski KS. Antibody-mediated rejection, T cell-mediated rejection, and the injury-repair response: new insights from the Genome Canada studies of kidney transplant biopsies. Kidney Int 2014;(85):258-64.

(91) Halloran PF, Famulski K, Reeve J. The molecular phenotypes of rejection in kidney transplant biopsies. Current Opinion In Organ Transplantation 2015;20(3):359-67.

(92) Mao Y, Wang M, Zhou Q, Jin J, Wang Y, Peng W, et al. CXCL10 and CXCL13 Expression were highly up-regulated in peripheral blood mononuclear cells in acute rejection and poor response to anti-rejection therapy. J Clin Immunol 2011 Jun;31(3):414-8.

(93) Hidalgo LG, Campbell PM, Sis B., Einecke G, Mengel M, Chang J, et al. De novo donor specific antibody at the time of kidney transplant biopsy associates with microvascular pathology and late graft failure. Am J Transplant 2009;9(11):2532-41.

(94) Sellares J, Reeve J, Loupy A, Mengel M, Sis B, Skene A, et al. Molecular diagnosis of antibody-mediated rejection in human kidney transplants. Am J Transplant 2013;13(4):971-83.

(95) Parkes MD, Halloran PF, Hidalgo LG. Direct evidence for CD16a-mediated NK cell stimulation in antibody-mediated kidney transplant rejection. Transplant 2016;101(4):e102-e111.

(96) Hidalgo LG, Einecke G, Allanach K, Halloran PF. The transcriptome of human cytotoxic T cells: similarities and disparities among allostimulated CD4(+) CTL, CD8(+) CTL and NK cells. Am J Transplant 2008 Mar;8(3):627-36.

(97) Hoves S, Krause SW, Schutz C, Halbritter D, Scholmerich J, Herfarth H, et al. Monocyte-derived human macrophages mediate anergy in allogeneic T cells and induce regulatory T cells. J Immunol 2006 Aug 15;177(4):2691-8.

(98) van Lieshout AW, van der Voort R, le Blanc LM, Roelofs MF, Schreurs BW, van Riel PL, et al. Novel insights in the regulation of CCL18 secretion by monocytes and dendritic cells via cytokines, toll-like receptors and rheumatoid synovial fluid. BMC Immunol 2006;7:23.

(99) Sallusto F, Lanzavecchia A. Efficient presentation of soluble antigen by cultured human dendritic cells is maintained by granulocyte/macrophage colony-stimulating factor plus interleukin 4 and downregulated by tumor necrosis factor a. J Exp Med 1994;179:1109-18.

(100) Zhou LJ, Tedder TF. CD14+ blood monocytes can differentiate into functionally mature CD83+ dendritic cells. Proc Natl Acad Sci U S A 1996 Mar 19;93 (6): 2588-92.

(101) Prehn JL, Thomas LS, Landers CJ, Yu QT, Michelsen KS, Targan SR. The T cell costimulator TL1A is induced by FcgammaR signaling in human monocytes and dendritic cells. J Immunol 2007 Apr 1;178(7):4033-8.

(102) Heid CA, Stevens J, Livak KJ, Williams PM. Real time quantitative PCR. Genome Research 1996 Oct;6(10):986-94.

(103) Einecke G, Melk A, Ramassar V, Zhu LF, Bleackley RC, Famulski KS, et al. Expression of CTL associated transcripts precedes the development of tubulitis in T-cell mediated kidney graft rejection. Am J Transplant 2005 Aug;5(8):1827-36.

(104) Halloran PF, Miller LW, Urmson J, Ramassar V, Zhu LF, Kneteman NM, et al. IFN-gamma alters the pathology of graft rejection: protection from early necrosis. Journal of Immunology 2001 Jun 15;166(12):7072-81.

(105) Famulski KS, Reeve J, de Freitas DG, Kreepala C, Chang J, Halloran PF. Kidney transplants with progressing chronic kidney diseases express high levels of acute kidney injury transcripts. Am J Transplant 2013;13(3):634-44.

(106) Masutani K, Shapiro R, Basu A, Tan H, Ninomiya T, Randhawa P. Putative Episodes of T-Cell-Mediated Rejection in Patients With Sustained BK Viruria but No Viremia. Transplant 2012 Jul 15;94(1):43-9.

(107) Sarwal M, Chua MS, Kambham N, Hsieh SC, Satterwhite T, Masek M, et al. Molecular heterogeneity in acute renal allograft rejection identified by DNA microarray profiling. N Engl J Med 2003 Jul 10;349(2):125-38.

(108) Flechner SM, Kurian SM, Head SR, Sharp SM, Whisenant TC, Zhang J, et al. Kidney transplant rejection and tissue injury by gene profiling of biopsies and peripheral blood lymphocytes. Am J Transplant 2004 Sep;4(9):1475-89.

(109) Schaub S, Nickerson P, Rush D, Mayr M, Hess C, Golian M, et al. Urinary CXCL9 and CXCL10 levels correlate with the extent of subclinical tubulitis. Am J Transplant 2009 Jun;9(6):1347-53.

(110) Xu J, Liu L, Zheng X, You C, Li Q. Expression and inhibition of ADAMDEC1 in craniopharyngioma cells. Neurol Res 2012 Sep;34(7):701-6.

(111) Crouser ED, Culver DA, Knox KS, Julian MW, Shao G, Abraham S, et al. Gene expression profiling identifies MMP-12 and ADAMDEC1 as potential pathogenic mediators of pulmonary sarcoidosis. Am J Respir Crit Care Med 2009 May 15;179(10):929-38.

(112) Rodder S, Scherer A, Korner M, Eisenberger U, Hertig A, Raulf F, et al. Meta-analyses qualify metzincins and related genes as acute rejection markers in renal transplant patients. Am J Transplant 2010 Feb;10(2):286-97.

(113) Lefaucheur C, Loupy A, Vernerey D, Duong-Van-Huyen JP, Suberbielle C, Anglicheau D, et al. Antibody-mediated vascular rejection of kidney allografts: a population-based study. Lancet 2013;381(9863):313-9.

(114) Sis B, Jhangri GS, Riopel J, Chang J, de Freitas DG, Hidalgo L, et al. A new diagnostic algorithm for antibody-mediated microcirculation inflammation in kidney transplants. Am J Transplant 2012 May;12(5):1168-79.

(115) Luther SA, Bidgol A, Hargreaves DC, Schmidt A, Xu Y, Paniyadi J, et al. Differing activities of homeostatic chemokines CCL19, CCL21, and CXCL12 in lymphocyte and dendritic cell recruitment and lymphoid neogenesis. J Immunol 2002 Jul 1;169(1):424-33.

(116) Famulski KS, Einecke G, Reeve J, Ramassar V, Allanach K, Mueller T, et al. Changes in the transcriptome in allograft rejection: IFN-g induced transcripts in mouse kidney allografts. Am J Transplant 2006;6(6):1342-54.

(117) Hidalgo LG, Einecke G, Allanach K, Mengel M, Sis B, Mueller TF, et al. The transcriptome of human cytotoxic T cells: measuring the burden of CTL-associated transcripts in human kidney transplants. Am J Transplant 2008 Mar;8(3):637-46.

(118) Famulski KS, Kayser D, Einecke G, Allanach K, Badr D, Venner J, et al. Alternative macrophage activation-associated transcripts in T-cell-mediated rejection of mouse kidney allografts. Am J Transplant 2010;10(3):490-7.

(119) Tsuchiya S, Yamabe M, Yamaguchi Y, Kobayashi Y, Konno T, Tada K. Establishment and characterization of a human acute monocytic leukemia cell line (THP-1). Int J Cancer 1980 Aug;26(2):171-6.

(120) Daigneault M, Preston JA, Marriott HM, Whyte MK, Dockrell DH. The identification of markers of macrophage differentiation in PMA-stimulated THP-1 cells and monocyte-derived macrophages. PLoS ONE 2010 Jan 13;5(1):e8668.

(121) Qin Z. The use of THP-1 cells as a model for mimicking the function and regulation of monocytes and macrophages in the vasculature. Atherosclerosis 2012 Mar;221(1):2-11.

(122) Fritsche J, Muller A, Hausmann M, Rogler G, Andreesen R, Kreutz M. Inverse regulation of the ADAM-family members, decysin and MADDAM/ADAM19 during monocyte differentiation. Immunology 2003 Dec;110(4):450-7.

(123) Boehm U, Klamp T, Groot M, Howard JC. Cellular responses to interferon-g. Ann Rev Immunol 1997;15:749-95.

(124) Gorczynski RM. Role of cytokines in allograft rejection. Curr Pharm Des 2001 Jul;7(11):1039-57.

(125) Gordon S. Pattern recognition receptors: doubling up for the innate immune response. Cell 2002 Dec 27;111(7):927-30.

(126) Larsen CP, Pearson TC. The CD40 pathway in allograft rejection, acceptance, and tolerance. Curr Opin Immunol 1997 Oct;9(5):641-7.

(127) Grau V, Herbst B, Steiniger B. Dynamics of monocytes/macrophages and T lymphocytes in acutely rejecting rat renal allografts. Cell Tissue Res 1998 Jan;291(1):117-26.

(128) Hallet MM, Praloran V, Vie H, Peyrat MA, Wong G, Witek-Giannotti J, et al. Macrophage colony-stimulating factor (CSF-1) gene expression in human T-lymphocyte clones. Blood 1991 Feb 15;77(4):780-6.

(129) Le MY, Jose MD, Mu W, Atkins RC, Chadban SJ. Macrophage colony-stimulating factor expression and macrophage accumulation in renal allograft rejection. Transplant 2002 Apr 27;73(8):1318-24.

(130) Le MY, Leprivey-Lorgeot V, Mons S, Jose M, Dantal J, LeMauff B, et al. Serum levels of macrophage-colony stimulating factor (M-CSF): a marker of kidney allograft rejection. Nephrol Dial Transplant 2004 Jul;19(7):1862-5.

(131) Einecke G, Broderick G, Sis B, Halloran PF. Early loss of renal transcripts in kidney allografts: relationship to the development of histologic lesions and alloimmune effector mechanisms. Am J Transplant 2007 May;7(5):1121-30.

(132) Einecke G, Mengel M, Hidalgo LG, Allanach K, Famulski KS, Halloran PF. The early course of renal allograft rejection: Defining the time when rejection begins. Am J Transplant 2009;9(3):483-93.

(133) Famulski KS, Sis B, Billesberger L, Halloran PF. Interferon-gamma and donor MHC class I control alternative macrophage activation and activin expression in rejecting kidney allografts: a shift in the Th1-Th2 paradigm. Am J Transplant 2008 Mar;8(3):547-56.

(134) Halloran PF, Venner JM, Famulski KS. Comprehensive analysis of transcript changes associated with allograft rejection: Combining universal and selective features. Am J Transplant 2017;17(7):1754-69.

(135) Parkes MD, Halloran PF, Hidalgo LG. Mechanistic sharing between NK cells in ABMR and effector T cells in TCMR. Am J Transplant 2017; http://onlinelibrary.wiley.com/doi/10.1111/ajt.14410/abstract.In press

(136) Neumayer HH, Kunzendorf U, Schrieber M. Protective effects of diltiazem and the prostazycline analogue iloprost in human renal transplantation. Ren Fail 1992;14:289-96.

(137) Jose MD, Ikezumi Y, van Rooijen N, Atkins RC, Chadban SJ. Macrophages act as effectors of tissue damage in acute renal allograft rejection. Transplant 2003 Oct 15;76(7):1015-22.

(138) Kirk AD, Hale DA, Mannon RB, Kleiner DE, Hoffmann SC, Kampen RL, et al. Results from a human renal allograft tolerance trial evaluating the humanized CD52-specific monoclonal antibody alemtuzumab (CAMPATH-1H). Transplant 2003 Jul 15;76(1):120-9.

(139) Lisignoli G, Toneguzzi S, Piacentini A, Cristino S, Grassi F, Cavallo C, et al. CXCL12 (SDF-1) and CXCL13 (BCA-1) chemokines significantly induce proliferation and collagen type I expression in osteoblasts from osteoarthritis patients. J Cell Physiol 2006 Jan;206(1):78-85.

(140) Atamas SP, Luzina IG, Choi J, Tsymbalyuk N, Carbonetti NH, Singh IS, et al. Pulmonary and activation-regulated chemokine stimulates collagen production in lung fibroblasts. Am J Respir Cell Mol Biol 2003 Dec;29(6):743-9.

(141) Famulski KS, de Freitas DG, Kreepala C, Chang J, Sellares J, Sis B, et al. Molecular phenotypes of acute kidney injury in human kidney transplants. JASN 2012 May;23(5):948-58.

(142) Mantovani A, Sozzani S, Locati M, Allavena P, Sica A. Macrophage polarization: tumor-associated macrophages as a paradigm for polarized M2 mononuclear phagocytes. Trends Immunol 2002 Nov;23(11):549-55.

(143) Watkins SK, Egilmez NK, Suttles J, Stout RD. IL-12 rapidly alters the functional profile of tumor-associated and tumor-infiltrating macrophages in vitro and in vivo. J Immunol 2007 Feb 1;178(3):1357-62.

(144) Anders HJ, Vielhauer V, Schlondorff D. Chemokines and chemokine receptors are involved in the resolution or progression of renal disease. Kidney Int 2003 Feb;63(2):401-15.

(145) Weber KS, von HP, Clark-Lewis I, Weber PC, Weber C. Differential immobilization and hierarchical involvement of chemokines in monocyte arrest and transmigration on inflamed endothelium in shear flow. Eur J Immunol 1999 Feb;29(2):700-12.

(146) Weber C, Weber KS, Klier C, Gu S, Wank R, Horuk R, et al. Specialized roles of the chemokine receptors CCR1 and CCR5 in the recruitment of monocytes and T(H)1-like/CD45RO(+) T cells. Blood 2001 Feb 15;97(4):1144-6.

(147) Robinson SC, Scott KA, Balkwill FR. Chemokine stimulation of monocyte matrix metalloproteinase-9 requires endogenous TNF-alpha. Eur J Immunol 2002 Feb;32(2):404-12.

(148) Dean RA, Cox JH, Bellac CL, Doucet A, Starr AE, Overall CM. Macrophage-specific metalloelastase (MMP-12) truncates and inactivates ELR+ CXC chemokines and generates CCL2, -7, -8, and -13 antagonists: potential role of the macrophage in terminating polymorphonuclear leukocyte influx. Blood 2008 Oct 15;112(8):3455-64.

(149) McQuibban GA, Gong JH, Wong JP, Wallace JL, Clark-Lewis I, Overall CM. Matrix metalloproteinase processing of monocyte chemoattractant proteins generates CC chemokine receptor antagonists with anti-inflammatory properties in vivo. Blood 2002 Aug 15;100(4):1160-7.

(150) Prasse A, Pechkovsky DV, Toews GB, Jungraithmayr W, Kollert F, Goldmann T, et al. A vicious circle of alveolar macrophages and fibroblasts perpetuates pulmonary fibrosis via CCL18. Am J Respir Crit Care Med 2006 Apr 1;173(7):781-92.

(151) Bates EE, Fridman WH, Mueller CG. The ADAMDEC1 (decysin) gene structure: evolution by duplication in a metalloprotease gene cluster on chromosome 8p12. Immunogenetics 2002 May;54(2):96-105.

(152) Papaspyridonos M, Smith A, Burnand KG, Taylor P, Padayachee S, Suckling KE, et al. Novel candidate genes in unstable areas of human atherosclerotic plaques. Arterioscler Thromb Vasc Biol 2006 Aug;26(8):1837-44.

(153) Galamb O, Gyorffy B, Sipos F, Spisak S, Nemeth AM, Miheller P, et al. Inflammation, adenoma and cancer: objective classification of colon biopsy specimens with gene expression signature. Dis Markers 2008;25(1):1-16.

(154) Schutyser E, Richmond A, Van DJ. Involvement of CC chemokine ligand 18 (CCL18) in normal and pathological processes. J Leukoc Biol 2005 Jul;78 (1): 14-26.

(155) Ansel KM, Harris RB, Cyster JG. CXCL13 is required for B1 cell homing, natural antibody production, and body cavity immunity. Immunity 2002 Jan;16(1):67-76.

(156) Vissers JL, Hartgers FC, Lindhout E, Figdor CG, Adema GJ. BLC (CXCL13) is expressed by different dendritic cell subsets in vitro and in vivo. Eur J Immunol 2001 May;31(5):1544-9.

(157) Malynn BA, Romeo DT, Wortis HH. Antigen-Specific B-Cells Efficiently Present Low-Doses of Antigen for Induction of T-Cell Proliferation. Journal of Immunology 1985;135(2):980-8.

(158) Steinmetz OM, Panzer U, Kneissler U, Harendza S, Lipp M, Helmchen U, et al. BCA-1/CXCL13 expression is associated with CXCR5-positive B-cell cluster formation in acute renal transplant rejection. Kidney Int 2005 Apr;67(4):1616-21.

(159) Halloran PF, Wadgymar A, Ritchie S, Falk J, Solez K, Srinivasa NS. The significance of the anti-class I antibody response. I. Clinical and pathologic features of anti-class I-mediated rejection. Transplant 1990 Jan;49(1):85-91.

(160) Adema GJ, Hartgers F, Verstraten R, de Vries E, Marland G, Menon S, et al. A dendritic-cell-derived C-C chemokine that preferentially attracts naive T cells. Nature 1997 Jun 12;387(6634):713-7.

(161) Hieshima K, Imai T, Baba M, Shoudai K, Ishizuka K, Nakagawa T, et al. A novel human CC chemokine PARC that is most homologous to macrophage-inflammatory protein-1 alpha/LD78 alpha and chemotactic for T lymphocytes, but not for monocytes. J Immunol 1997 Aug 1;159(3):1140-9.

(162) Wells TN, Peitsch MC. The chemokine information source: identification and characterization of novel chemokines using the WorldWideWeb and expressed sequence tag databases. J Leukoc Biol 1997 May;61(5):545-50.

(163) Lindhout E, Vissers JL, Hartgers FC, Huijbens RJ, Scharenborg NM, Figdor CG, et al. The dendritic cell-specific CC-chemokine DC-CK1 is expressed by germinal center dendritic cells and attracts CD38-negative mantle zone B lymphocytes. J Immunol 2001 Mar 1;166(5):3284-9.

(164) Penna G, Vulcano M, Sozzani S, Adorini L. Differential migration behavior and chemokine production by myeloid and plasmacytoid dendritic cells. Hum Immunol 2002 Dec;63(12):1164-71.

(165) Vulcano M, Struyf S, Scapini P, Cassatella M, Bernasconi S, Bonecchi R, et al. Unique regulation of CCL18 production by maturing dendritic cells. J Immunol 2003 Apr 1;170(7):3843-9.

(166) Forster R, Davalos-Misslitz AC, Rot A. CCR7 and its ligands: balancing immunity and tolerance. Nat Rev Immunol 2008 May;8(5):362-71.

(167) Mempel TR, Henrickson SE, von Andrian UH. T-cell priming by dendritic cells in lymph nodes occurs in three distinct phases. Nature 2004 Jan 8;427(6970):154-9.

(168) Miller MJ, Hejazi AS, Wei SH, Cahalan MD, Parker I. T cell repertoire scanning is promoted by dynamic dendritic cell behavior and random T cell motility in the lymph node. Proc Natl Acad Sci U S A 2004 Jan 27;101(4):998-1003.

(169) Benvenuti F, Lagaudriere-Gesbert C, Grandjean I, Jancic C, Hivroz C, Trautmann A, et al. Dendritic cell maturation controls adhesion, synapse formation, and the

duration of the interactions with naive T lymphocytes. J Immunol 2004 Jan 1;172(1):292-301.

(170) Kaiser A, Donnadieu E, Abastado JP, Trautmann A, Nardin A. CC chemokine ligand 19 secreted by mature dendritic cells increases naive T cell scanning behavior and their response to rare cognate antigen. J Immunol 2005 Aug 15;175(4):2349-56.

(171) Katou F, Ohtani H, Nakayama T, Nagura H, Yoshie O, Motegi K. Differential expression of CCL19 by DC-Lamp+ mature dendritic cells in human lymph node versus chronically inflamed skin. J Pathol 2003 Jan;199(1):98-106.

(172) Constantin G, Majeed M, Giagulli C, Piccio L, Kim JY, Butcher EC, et al. Chemokines trigger immediate beta2 integrin affinity and mobility changes: differential regulation and roles in lymphocyte arrest under flow. Immunity 2000 Dec;13(6):759-69.

(173) Valledor AF, Borras FE, Cullell-Young M, Celada A. Transcription factors that regulate monocyte/macrophage differentiation. J Leukoc Biol 1998 Apr;63(4):405-17.

(174) Marziali G, Perrotti E, Ilari R, Coccia EM, Mantovani R, Testa U, et al. The activity of the CCAAT-box binding factor NF-Y is modulated through the regulated expression of its A subunit during monocyte to macrophage differentiation: regulation of tissue-specific genes through a ubiquitous transcription factor. Blood 1999 Jan 15;93(2):519-26.

(175) Carlsen HS, Baekkevold ES, Morton HC, Haraldsen G, Brandtzaeg P. Monocyte-like and mature macrophages produce CXCL13 (B cell-attracting chemokine 1) in inflammatory lesions with lymphoid neogenesis. Blood 2004 Nov 15;104(10):3021-7.

(176) Takagi R, Higashi T, Hashimoto K, Nakano K, Mizuno Y, Okazaki Y, et al. B cell chemoattractant CXCL13 is preferentially expressed by human Th17 cell clones. J Immunol 2008 Jul 1;181(1):186-9.

(177) Krautler NJ, Kana V, Kranich J, Tian Y, Perera D, Lemm D, et al. Follicular dendritic cells emerge from ubiquitous perivascular precursors. Cell 2012 Jul 6;150(1):194-206.

(178) Sallusto F, Palermo B, Lenig D, Miettinen M, Matikainen S, Julkunen I, et al. Distinct patterns and kinetics of chemokine production regulate dendritic cell function. Eur J Immunol 1999 May;29(5):1617-25.

(179) Hausser G, Ludewig B, Gelderblom HR, Tsunetsugu-Yokota Y, Akagawa K, Meyerhans A. Monocyte-derived dendritic cells represent a transient stage of differentiation in the myeloid lineage. Immunobiology 1997 Nov;197(5):534-42.

(180) Zhang M, Tang H, Guo Z, An H, Zhu X, Song W, et al. Splenic stroma drives mature dendritic cells to differentiate into regulatory dendritic cells. Nat Immunol 2004 Nov;5(11):1124-33.

(181) Shortman K, Wu L. Are dendritic cells end cells? Nat Immunol 2004 Nov;5(11):1105-6.

(182) Rivollier A, Mazzorana M, Tebib J, Piperno M, Aitsiselmi T, Rabourdin-Combe C, et al. Immature dendritic cell transdifferentiation into osteoclasts: a novel pathway sustained by the rheumatoid arthritis microenvironment. Blood 2004 Dec 15;104(13):4029-37.

(183) Martinez-Pomares L, Gordon S. Antigen presentation the macrophage way. Cell 2007 Nov 16;131(4):641-3.

(184) Segerer S, Mack M, Regele H, Kerjaschki D, Schlondorff D. Expression of the C-C chemokine receptor 5 in human kidney diseases. Kidney Int 1999 Jul;56 (1):52-64.

(185) Paueksakon P, Revelo MP, Ma LJ, Marcantoni C, Fogo AB. Microangiopathic injury and augmented PAI-1 in human diabetic nephropathy. Kidney Int 2002 Jun;61(6):2142-8.

(186) McKnight AJ, Gordon S. Membrane molecules as differentiation antigens of murine macrophages. Adv Immunol 1998;68:271-314.

(187) Chana RS, Martin J, Rahman EU, Wheeler DC. Monocyte adhesion to mesangial matrix modulates cytokine and metalloproteinase production. Kidney Int 2003 Mar;63(3):889-98.

(188) Halloran PF, de Freitas DG, Einecke G, Famulski KS, Hidalgo LG, Mengel M, et al. The molecular phenotype of kidney transplants. Am J Transplant 2010;10(10):2215-22.

(189) Kapoor A, Fairchild RL. Early and Late Chemokine Cascades During Acute Allograft Rejection. Transplantation Reviews 2000; 14, 82-95.

(190) Rosenberg AS, Singer A. Cellular basis of skin allograft rejection: an in vivo model of immune-mediated tissue destruction. Ann Rev Immunol 1992;10:333-58.

(191) Schraufstatter IU, Zhao M, Khaldoyanidi SK, Discipio RG. The chemokine CCL18 causes maturation of cultured monocytes to macrophages in the M2 spectrum. Immunology 2012 Apr;135(4):287-98.